The University of Manitoba

Department of Mechanical Engineering

COUPLED THERMOELASTOPLASTIC FINITE ELEMENT ANALYSIS OF AXISYMMETRIC STRUCTURES

by

Andrzej Banas

A Thesis

Submitted to the Faculty of Graduate Studies

in Partial Fulfilment of the Requirements

for the Degree

Master of Science

August, 1984

COUPLED THERMOELASTOPLASTIC FINITE ELEMENT ANALYSIS OF AXISYMMETRIC STRUCTURES

BY

ANDRZEJ BANAS

A thesis submitted to the Faculty of Graduate Studies of the University of Manitoba in partial fulfillment of the requirements of the degree of

MASTER OF SCIENCE

ABSTRACT

A temperature-displacement formulation of the coupled theory of quasi-static isotropic thermoelastoplasticity has been proposed along with the finite element solution procedure. The unknowns in the finite element model are: nodal displacements, nodal temperatures, and sampling points' values of independent stress components and equivalent plastic strains. The theory was implemented in the form of the two-dimensional code 'TEPAP' designed to perform analyses in axisymmetric geometries. The preliminary assessment of the approach included three example cases.

ACKNOWLEDGEMENTS

I would like to thank my advisor Dr. Tai-Ran Hsu for his guidance, encouragement and support, without which this thesis could not have been written. I am also grateful to the other staff members and fellow graduate students of the Thermomechanics Laboratory of the University of Manitoba for providing a uniquely friendly and stimulating atmosphere of work. My special thanks are directed to Mr. Gordon Pizey for his generous assistance in coping with variety of problems and to Mr. Nan-Sheng Sun for his help in debugging and improving the TEPAP code. Support received under the University of Manitoba Fellowship is also gratefully acknowledged.

The very skillful typing of this thesis by Mrs. Debbie Harris deserves my great appreciation.

Last but not least, I wish to thank my family, my wife Teri, my daughter Krystyna and son Miklos, and my parents in Poland, for their great love, patience, support and constant encouragement during the long venture of this thesis work.

TABLE OF CONTENTS

LIST OF TABLES

LIST OF FIGURES

NOMENCLATURE

a_i, a_{ij}, a_{ijkl}	–	coefficients of a polynomial which defines the isoparametric transformation
$\bar{a}_{ij}$, $\bar{a}_i$	–	coefficients appearing in the displacement boundary condition
b_i	–	density of distributed forces per unit mass
B_{ij}	–	Cartesian components of the thermomechanical coupling tensor
c	–	correction factor used in numerical determination of stress state
c_ε	–	specific heat at constant elastic and plastic strains
$C^{(e)}_{ijkl}$	–	Cartesian components of the elastic stiffness tensor
$C^{(p)}_{ijkl}$	–	Cartesian components of the plastic stiffness (Yamada's) tensor
$C^{(ep)}_{ijkl}$	–	Cartesian components of the elastoplastic stiffness tensor
$C^{(e)}_{IJ}$	–	generalized thermal capacitance matrix of the e-th element
det	–	determinant operator
D	–	internal dissipation rate
$D^{(e)}_{ijkl}$	–	Cartesian components of elastic compliance tensor
e	–	internal energy per unit mass
$e^{(e)}$	–	thermoelastic component of specific internal energy
$e^{(p)}$	–	thermoinelastic component of specific internal energy

e_{ijk} - permutation tensor

E - Young's modulus

E' - asymptotic value of hardening modulus at a given temperature

$E^{(e)}_{iIJ}$ - thermal expansivity matrix of the e-th element

f - an arbitrary function of global coordinates x_i

$\bar{f}$ - function f transformed to local coordinates ξ_i

F - yield function

$F^{(e)}_{iI}$ - vector of rates of external forces in the e-th element

g - gravitational acceleration

G - shear (Kirchhoff's) modulus

h - hardening modulus

$\bar{h}$ - heat transfer coefficient prescribed on the boundary ∂R_q

H' - yield stress derivative with respect to the strain hardening parameter

H'' - yield stress derivative with respect to the temperature

j - parameter indicating whether given point attained plastic range

k - thermal conductivity

K - compressibility modulus

$K^{(e)}_{ijIJ}$ - tangent stiffness matrix of the e-th element

M - number of sampling points in an element

M' - number of sampling points on one face of an element's boundary (used in evaluation of boundary integrals)

n - number of components of the displacement vector
- exponent appearing in the continuous representation of the stress-strain curve

n_i - Cartesian components of the outward unit vector normal to the system boundary surface

N - number of nodes in an element

N_{el} - total number of elements

$N_I^{(e)}$ - interpolation (shape) function corresponding to the I-th node of the e-th element

p - pressure

$\dot{\bar{p}}$ - pressure rate prescribed on the boundary ∂R_σ

q - internal energy flow rate (or heat flow rate)

q_i - Cartesian components of the internal energy (or heat) flux vector

$\bar{q}$ - heat flux prescribed on the boundary ∂R_q

$Q_I^{(e)}$ - vector of heat generation rates in the e-th element

r - internal heat generation rate per unit mass
- radial coordinate

$R_{iIJ}^{(e)}$ - thermomechanical coupling matrix of the e-th element

R - region occupied by the body

$\hat{R}$ - approximation of region R in the finite element model

s - entropy per unit mass

S - auxiliary hardening modulus
- area of the system boundary surface ∂R

$S^{(e)}$ - area of the external surface of the e-th element

S_q - area of the surface ∂R_q

S_σ - area of the surface ∂R_σ

$S_{IJ}^{(e)}$ - thermal conductance of the e-th element

t - time

t_i - Cartesian components of the surface traction vector

T - excess temperature (temperature in excess of T_o)

T_o - reference absolute temperature

$T_I^{(e)}$ - excess temperature of the I-th node of the e-th element

T_∞ - bulk fluid temperature prescribed on the boundary ∂R_q

T - trial temperature solution

T^* - test function for the internal energy balance equation

u_i - Cartesian components of displacement vector

$u_{iI}^{(e)}$ - Cartesian components of displacement vector of the I-th node of the e-th element

u_i - trial displacement solution

u_i^* - test functions for the momentum balance equations

v_i - Cartesian components of the velocity vector

V - volume of the region R occupied by the body

x_i - Cartesian components of the position vector

x_{iI} - Cartesian components of the I-th node's position vector

z - axial coordinate

Greek Letters

α - coefficient of thermal expansion of isotropic material

$\alpha_{ij}^{(e)}, \alpha_{ij}^{(p)}, \alpha_{ij}^{(th)}, \alpha_{ij}^{(ep,th)}$ - Cartesian components of elastic, plastic, thermal, and generalized thermal moduli tensors

$\beta_{ij}^{(e,th)}, \beta_{ij}^{(p,th)}, \beta_{ij}^{(ep,th)}$ - Cartesian components of the thermoelastic, thermoplastic, and generalized thermal moduli tensors, respectively

γ - entropy production per unit mass

$\tilde{\gamma}$ - thermoplastic contribution to the heat capacity

δ - subincrementation operator

δ - dimensionless number expressing intensity of thermoelastic coupling

δ_{ij} - Kronecker's delta operator

Δ - finite increment operator

ε_y - equivalent plastic strain accumulated up to the last unloading

$\varepsilon_{ij}^{(e)}, \varepsilon_{ij}^{(p)}, \varepsilon_{ij}^{(th)}, \varepsilon_{ij}$ - Cartesian components of the elastic, plastic, thermal, and total strain tensors, respectively

$\varepsilon_{ij}^{(p)'}$ - Cartesian components of deviatoric part of plastic strain tensor

$\bar{\varepsilon}$ - equivalent total strain

$\bar{\varepsilon}^{(p)}$ - equivalent plastic strain (Odqvist's strain-hardening parameter)

θ - absolute temperature

κ - work-hardening parameter

λ - proportionality factor in normality rule

Λ - parameter appearing in Need-Batermann model of coupled thermoplasticity and expressing the ratio of the rate of energy stored on the microlevel to the plastic power during adiabatic process

ν - Poisson's ratio

ξ - parameter expressing the ratio of the internal dissipation to the energy stored on the microlevel

ξ_i - local (natural) coordinates associated with each element

π - 3.1415926535

- power-conjugate variable to the internal state variable κ

ρ - mass density

σ_y - yield stress

σ_{kink} - virgin yield stress for bilinear representation of uniaxial stress-strain relationship

σ_{ij} - Cartesian components of stress tensor

σ'_{ij} - Cartesian components of deviatoric part of stress tensor

$\bar{\sigma}$ - effective stress

$\bar{\sigma}^*$ - trial effective stress computed in state determination phase

σ_y - function assigning yield stress to given total equivalent strain

Σ - element assembly operator

$\psi, \psi^{(e)}, \psi^{(p)}$ - specific free energy (Helmholtz function) along with its elastic and plastic components

Matrices

$\{\ \}$ - column vector

$\{\ \}^T$ - transpose of the column vector (row vector)

$[\ ]$ - rectangular matrix

$\{B^{(ep)}\}, \{B^{(e)}\}, \{B^{(p)}\}$ - thermomechanical coupling matrix along with its elastic and plastic components

$\{B^{(ep,th)}\}, \{B^{(e,th)}\}, \{B^{(p,th)}\}$ - thermal moduli matrix along with its thermoelastic and thermoplastic components

$[C^{(e)}], [C]$ - elemental and assembled thermal capacitance matrices

$[C^{(ep)}], [C^{(e)}], [C^{(p)}]$ - elastoplastic matrix along with its elastic and plastic components

$[E^{(e)}], [E]$ - elemental and assembled thermal expansivity matrices

$\{\varepsilon\}$ - strain vector

$\{F^{(e)}\}, \{F\}$ - elemental and assembled vectors of the external forces rates

$[H_u^{(e)}], [H_T^{(e)}]$ - elemental strain and temperature gradient interpolation matrices

$[K^{(e)}], [K]$ - elemental and assembled tangent stiffness matrices

n_r
n_z - outward unit vector normal to the external boundary of an element

$\{N_u^{(e)}\}, \{N_T^{(e)}\}$ - elemental displacement and temperature interpolation matrices

$\{Q^{(e)}\}, \{Q\}$ - elemental and assembled vectors of the heat generation rates

$[R^{(e)}], [R]$ - elemental and assembled thermomechanical coupling matrices

$[S^{(e)}], [S]$ - elemental and assembled thermal conductance matrices

$\{\sigma\}, \{\sigma'\}$ - stress vector and stress deviator vector

$\{T^{(e)}\}, \{T\}$ - elemental and assembled vectors of nodal temperatures

$\{u\}$ - elemental displacement vector

$\{U^{(e)}\}, \{U\}$ - elemental and assembled vectors of nodal displacements

$\{\nabla_\varepsilon\}$	-	matrix differential operator transforming displacements into strains
$\{\nabla_q\}$	-	matrix gradient operator

Subscripts and Superscripts

(e)	-	superscript denoting elastic component of a quantity
	-	superscript referring to the e-th element
i,j,k,l,m,n,r,s	-	subscripts referring to the Cartesian components of vectors and tensors
(i)	-	superscript referring to the iteration number
I,J	-	subscripts referring to node numbers
K	-	subscript referring to sampling points numbers
m	-	subscript referring to the element's number
(p)	-	superscript denoting plastic component of a quantity
r	-	subscript referring to the local coordinate number
r,z	-	subscripts referring to the radial and axial coordinates, respectively

Special Symbols

$\varnothing$	-	empty set
$\cup$	-	logical sum
$\cap$	-	logical product

CHAPTER 1

MOTIVATION AND OBJECTIVES OF THIS WORK

During the past decade the research effort directed towards designing more comprehensive and more realistic models of the behaviour of engineering materials and structural components increased dramatically. Development in aerospace, nuclear, and other technologically advanced fields require new, more detailed, more accurate, and more reliable predictive tools for application in analysis and design. As a result the finite element method (FEM), introduced some twenty five years ago, witnessed further development. While serving both as a means for testing new modelling concepts and as a primary tool in computer aided design (CAD), it became the most established numerical technique in many engineering disciplines. The tendency to broaden the scope of applications opened the way to finite element codes capable of modelling various nonlinearities and couplings between distinct physical fields. Other developments included: trends to automation and robustness, increased sophistication in numerical approach to the solution of systems of simultaneous equations, and studies aimed at deeper understanding of the nature of discrete field approximation.

In the areas of solid and structural mechanics the potential and attractiveness of the finite element method have been especially

recognized after its successful applications to more complex problems, such as analyses of systems in which there is concurent interest in both thermal and mechanical behaviour. Stress analyses of structural and machine components designed to serve at elevated temperatures are nowadays routine procedures in industry. A typical application involves temperature analysis preceding the actual stress analysis which often includes a model for inelastic material behaviour. Variable material properties are assigned to various parts of the analysed structure on the basis of the previously found temperature field, and the entire analysis is usually performed with the help of a commercially available FE code.

The rationale of this approach is, that modelling complications are rarely rewarded with more meaningful predictions, identification procedures for complex models of material behaviour are difficult, and that realistic analytical representation of in-service boundary conditions calls for further models and/or experiments. As a result, the methodologies popular with many FEM practitioners put forward demands of modelling conservatism and stress the need for simplified but reliable models.

There exists, however, another noticeable trend in the ongoing development of FEM for solid and structural mechanics applications. It stems from the basic recognition that there is a growing number of problems of current interest in many technological disciplines which presently lack appropriate models for their analytical studies. Areas such as mechanics of metal forming and fabrication processes, micromechanics of flow and fracture processes in heterogenous media,

prediction methods of in-service life and deformation, and many others have recognized the need for and embarked on the development of new deformation models. As a rule, these new models aim at better representation of the role material flow plays in the overall response. Despite the fact that such nonelastic models do not yet offer completely satisfactory means for prediction of material behaviour in various possible environments, their use in finite element analyses of structural components, is increasing. However, while novel constitutive modelling concepts often emphasise the links between macroscopic deformation and the flow mechanisms responsible for it, the interdependence between mechanical aspects of deformation and thermal state of material is rarely paid the attention it deserves. Mechanistic models, which strive to fit the ample information from material science into the framework of phenomenological modelling, seem to neglect largely the evidence of passive thermomechanical coupling, i.e. the fact that changes in strain and/or stress fields might result in changes of thermodynamic state of material. This happens in defiance of increasing awareness that for many technological problems two way coupling between thermal and deformation states is of importance.

Stability analysis at metal forming, catastrophic shear at machining, and fatigue are only a few examples of such problems [55]. The existence of coupled thermomechanical phenomena in the field of solid fueled rockets was reported to be a motivating force for the development of new constitutive equations and innovative computation methods [20]. Possible relevance of coupled thermomechanical analysis

to a variety of other problems, such as fault analysis of nuclear reactors, damping of solid wave propagation, deformation localization after bifurcation, and generation of residual stresses, was also independently stated [20,50,36].

As seen from the above examples, the need for methods capable of simultaneously handling deformational and thermal aspects of material behaviour, is clear. In this context, a fully coupled thermomechanical analysis by the FE technique naturally appears as a viable alternative to traditional approaches. The idea of such a coupled analysis is not new, but various development efforts in this area did not yet result in a unified and systematic approach. Despite significant advances in understanding the physics of phenomena responsible for the passive thermomechanical coupling, a general and simple enough phenomenological model did not emerge. Consequently, the results obtained with various models are difficult to compare, and the relevance of particular forms of coupling terms included in analysis has not been systematically studied and is difficult to assess.

In view of these facts, the problem of coupling the traditional finite element heat conduction and elastoplastic stress analyses is approached in this thesis. The primary objective is to show how the occurence of passive thermomechanical coupling may be, at least in principle, taken into account. To achieve this objective a simple temperature-displacement formulation is proposed in the simplified setting of small deformation theory and rate independent isotropic hardening plasticity. The formulation is implemented in the

form of a code named TEPAP (Thermo-Elasto-Plastic Analysis Program), developed for the two-dimensional axisymmetric case, and employing quadrilateral four-to-nine-nodes isoparametric elements. The secondary objective is to gain some insight into the question of the proposed formulation feasibility for applications in the area of stress analysis at elevated temperatures. To achieve this secondary objective three test cases are studied with the aim of assessing the effects of coupling terms in the model.

As the final point, the research topic undertaken in this thesis ought to be considered an integral part of the long term effort of the Thermomechanics Laboratory of the University of Manitoba, to develop improved methodologies of Finite Element Analyses.

CHAPTER 2

LITERATURE SURVEY

The effects, broadly termed thermomechanical couplings in solids have been of interest to researchers from several disciplines for many years. Abundant literature exists on the topics relevant to the subject. Since the purely physical aspects of the said phenomena are not of main interest in this work, most of the reviewed publications come from the areas of continuum and computational mechanics. The current understanding of the physical basis of the coupled thermomechanical effects is only briefly discussed. Finally, the review of theoretical and numerical works is of necessity restricted to those publications which were studied by the author in the course of this thesis work.

2.1 Literature on Thermomechanical Coupling Theory and Modelling

The classical reference sources on the thermomechanics of solids, e.g. Boley and Weiner [6] or Fung [15], usually contain general discussions of the phenomenological origins of coupled thermomechanical effects. While laying ground for future developments in this area, they tend to concentrate on thermoelastic problems. Newer monographs on thermoelasticity, e.g. Nowinski [50], offer

extensive bibliographies on the subject of coupled thermoelastic phenomena, and allow to conclude that nowadays their basic features are fairly well understood. In fact, following an early paper by Danilovskaya [13], several analytical and many numerical solutions of specific initial/boundary value problems have been reported, and new solutions are appearing along with the indications of new possible applications.

As discussed by many authors [14,28,49], the first quantitative experimental results in support of the relevance of the thermomechanical coupling during inelastic deformation were obtained by Farren and Taylor (1925) and Taylor and Quinney (1934). Their measurements of heat evolution during plastic deformation have shown that for strains over 10% only about 10% of the work of deformation is stored in a metal, while about 90% of the work leaves it as heat [40]. These results were later used by many authors as important guidance in the construction of models of coupled thermoplastic behaviour [14,28,31,32], and are also employed in this work for this purpose. Later developments in material science offered more precise explanation of energy storage, concluding that "energy stored inside a crystal is almost completely made up of strain energy of the total length of dislocations introduced by strain-hardening, while the energy storage due to point defects produced by dislocation intersection makes up a small fraction of the total" [40]. Since that time, understanding of the microstructural mechanisms responsible for the coupled thermomechanical phenomena has advanced significantly, and a good tutorial review on the physical approach to their interpreta-

tion may be found for example in the work of Klepaczko [27]. It contains a general classification of the thermomechanical couplings in metals based on the microstructural interpretation of macroscopic effects. According to this classification, coupling effects should be divided into two groups. The first group involves the effects attributed to the movements of an ideal crystal lattice and/or to the presence of immobile lattice defects. These effects include both the active and the passive thermoelastic couplings (e.g. a possibility of inducing stresses by applied temperature field, and inducing temperature fields by applied stressing, respectively), and the thermoelastic energy dissipation, giving rise to the hysteresis effect during a cyclic loading/unloading process within the elastic range. The second group, corresponding to couplings known as thermoplastic in the phenomenological terminology, includes effects resulting from the movement of structural defects. The passive thermoplastic coupling effects belonging to this group may be of two types. The direct thermoplastic coupling, also known as adiabatic coupling in metal plasticity, is associated with heat generation in the vicinity of a slip band. This coupling results in adiabatic yield stress being lower than isothermal yield stress, and affects the hardening ability of metals at low temperatures. The indirect thermoplastic coupling reflects the experimentally observed sensitivity of yield stress in polycrystalline metals to the history of temperature changes during a deformation process.

The early attempts to consider the passive thermoplastic coupling effects within the continuum mechanics framework were

summarized by Naghdi [45]. These works were followed by the publications of Dillon [14], Kratochvil and Dillon [28], and others. While solutions of specific boundary problems were not attempted in any of these works, the observable trend was an increasing tendency to present the proposed theories using the new advances of thermodynamics of continuum media. In particular, the proposed general theory of thermodynamics with internal state variables [12] enabled reinterpretation of many previously obtained results within a new thermodynamic framework. Also, following the publication of the fundamental work by Green and Naghdi [18] on a general theory of elastic-plastic continuum, many researchers such as Lee [30], began presenting their theories within a general setting of continuum medium undergoing finite strains and rotations.

Later theoretical developments took many directions. Despite the lack of agreement on what should constitute the thermodynamic framework for new constitutive theories, many authors attempted to generalize the previously proposed models to consistently include the thermomechanical coupling effects. The series of works by Lehmann [31-37] may serve as examples of such serious undertakings. Other authors stressed a greater need for more comprehensive and realistic phenomenological models, built in such a way as to indicate experimental procedures leading to identification of material response parameters [29], or suggested maintaining microstructural interpretations of additional variables (e.g. internal state variables) introduced in the models [5,49].

The mathematical aspects of coupled thermoplasticity formulation based on the Ziegler's orthogonality principle [62] were investigated by Mróz and Raniecki [43,44], leading to the conclusion that the existence and uniqueness of the posed problem is assured in a wide range of material parameters. A review of the developments on theoretical and applied plasticity published in 1972 [54] reported a number of solutions to various thermoplastic boundary value problems including some coupled ones. The lack of a satisfactory thermodynamical theory of nonequilibrium processes, persisting even today, seems to be responsible for an active search for new ways of phenomenological macroscopic descriptions of the thermomechanical effects in solids. Some of the authors, e.g. Guelin and Boisserie [17] go as far as to question the origins hitherto assigned to coupling terms in the energy balance equation, and speculate on the need for major revisions.

2.2 Literature on the Finite Element Application to Coupled Thermoelastoplasticity

The ease of including the active thermoelastic coupling into finite element codes based on linear elasticity has been recognized almost at the start of the finite element method appearance [63]. Its ability to correctly predict both thermal distortions and thermal stresses in the statically loaded structural and machine components subjected to temperature gradients had to be appreciated. The early variational formulations of such problems, however, resisted straight-

forward extensions to include transient mechanical and thermal behaviours. The appropriate variational formulation of coupled linear thermoelasticity, proposed by Nickell and Sackmann [46], for the first time allowed a finite element solution of coupled transient problems. An alternative approach proposed later by Keramidas and Ting [26] claimed simplifications in the variational formulation. One of the first attempts to consider coupled thermoelasticity finite element formulation in a general non-linear setting was pursued by Oden [52]. Using integral energy balances, equivalent to what is now called the Galerkin approach, he considered thermoelastic behaviour involving both material and geometrical non-linearities.

With the introduction of the finite element inelastic stress analyses by Yamada et al. [61], various demands, mainly from nuclear industries, quickly stimulated extensions of the technique to include thermal effects. The success of these formulations [23,64] placed even stronger demands for more complex material constitutive models and improved numerics in order to handle larger structures and transient scenarios such as those considered in the studies of nuclear reactor core accidents. A new generation of finite element procedures evolved featuring fully non-linear kinematics, couplings introduced by temperature dependencies of material properties, and material rate effects [1,2,23,39,42,58,64]. Some of these procedures gained sufficient acceptance to be included as textbook material [3,53,63].

Along with this development of finite element techniques for non-linear structural analysis, the focus has shifted from the details of formulation (no longer variational) to the search for effective

numerical solution algorithms [38,40,51,59,60]. Successful usage of the technique in non-structural applications and availability of more and more powerful computers helped to renew the interest in the formulation and solution of problems involving coupled fields. Coupled thermomechanics of solids was not one of them, however. Published papers concerned with coupled thermomechanical analysis are scarce and evidently lack the common theoretical background on which their models are based. Chung and Yagawa [11] postulated the validity of Gibbs thermodynamics over short time intervals, and arrived at an incremental numerical scheme for the calculation of transient response of thermoplastic material. Rebello and Kobayashi [56] employed a thermodynamic process formalism combined with a constitutive equation postulated for dislocation density, in order to predict thermoviscoplastic behaviour during compression of bulk metal. Other authors also attempted coupled thermomechanical modelling employed in analyses of metalforming operations. Material flow effects were, however, most often modelled with the use of viscous non-Newtonian fluids, rather than elastoplasticity.

Finally, it should be mentioned that on several ocassions doubts were expressed by various authors with respect to the necessity of passive thermomechanical coupling being included into finite element models of inelastic behaviour of some materials at elevated to high temperatures. The reason quoted was suspected insignificance of such effects due to the distinctly different time scales of mechanical and thermal processes in such cases.

CHAPTER 3

PHYSICAL MODEL AND ITS SIMPLIFYING ASSUMPTIONS

The physical system under consideration consists of a structural component (or its part) made from a solid crystaline material, exposed to a thermal environment and to mechanical loading. The nature of the thermal environment is not explicitly stated, but it is assumed that it represents an energy source (or sink) whose interaction with the system has the net effect of energy transfer through a heat flux mechanism. Exposure to mechanical loading implies a mechanical power flux as another form of energy exchange between the system and the neighbouring media. Considering these two fluxes as the only possible means of energy exchange with surroundings covers quite a broad scope of situations of interest in engineering applications. They include structural components totally or partially submerged in fluids and simultaneously subjected to the action of pressure and convective/radiative heating or cooling. The model also addresses more idealized situations, such as those involving parts of the component external surface subjected to prescribed histories of temperature and motion, since they also may be interpreted in terms of energy being exchanged either as heat or as mechanical work.

In order to further focus the attention on the thermo-mechanical aspects of the behaviour of the system under consideration,

a purely thermomechanical approach to modelling interactions between the system and its surroundings is also adopted for modelling of all phenomena within the system. The following simplifying assumptions in regard to the physical model express this point of view in a general way:

(i) All non-thermal influences of environment on the thermomechanical response of component material are absent.

(ii) Non-thermomechanical phenomena taking place within the system and resulting in macroscopic deformation or termperature changes may be included in the model with the provision that they are represented by prescribed energy sources, explicitly dependent on time and/or position.

The first assumption excludes from consideration all non-thermal aging phenomena (such as corrosion or neutron radiation damage of material microstructure) that otherwise would be manifested by altered mechanical and/or thermophysical properties of the component material.

Assumption (ii) leads to a simplified pattern of energy flow within the system, as it is schematically depicted in FIGURE 1. The only types of energy stored within the system that need to be considered are the (macroscopic) kinetic and internal energies with

mechanical power flux and heat flux as their corresponding mechanisms of exchange with the environment. Of the two internal sources of energy supply, one (gravitational energy) may affect the kinetic energy balance only, while the other one (electromagnetic energy) is able to directly contribute to the creation (or destruction) of both kinetic and internal energies currently stored within the system. As a result, the physical model may encompass distributed forces of gravitational and electromagnetic origin, Joule's and inductance heating, etc. Implications of some further assumptions on the pattern of energy flow within the system will be discussed along with the details of the mathematical model in CHAPTER 4.

The following assumptions are put forward to simplify the description of events taking place during component material evolution in time, while subject to thermal environment and mechanical loading:

(iii) at the outset of the process the component material is in its virgin, stress- and strain-free state, and remains in thermal equilibrium,

(iv) during the evolution process the continuity of the component material is preserved, and the process itself is quasi-static,

(v) the temperature levels (thermal regimes) and the stress regimes attained during the process are such that phase transformations, phase migrations and material composition changes do not occur,

(vi) material thermomechanical response during the evolution process exhibits features of rate insensitivity and classical history dependence,

(vii) the (macroscopic) deformation of the component material remains small in the sense that displacements of individual material points and displacement gradients remain small during the evolution process.

These assumptions will be explained below in some detail, with an attempt to further identify the scenarios falling within the scope of the restricted physical model.

From the physical point of view, assumptions (iv) - (vii) restrict considerations to sufficiently homogeneous materials undergoing slow changes and justify modelling of processes occuring at room and elevated temperatures. Fracture and wave phenomena are explicitly excluded by virtue of assumption (iv), while assumption (v) renders solute phase migration and solid phase transformation processes absent or insignificant. Diffusion-like phenomena (such as moisture infiltration or solid diffusion under combined action of temperature and stress) which would imply both an additional energy transfer mechanism and deformation induced by the solute phase concentration gradient, are not modelled. Similarly, phase transformations and their influences on both deformation (transformation induced strains) and thermal state of the material (absorption or liberation of latent

heat energy in the phase transition zones) are excluded from consideration. In addition assumptions (i) and (v) indicate that all dimensional changes exhibited by the component material should be regarded as the combined effect of free thermal expansion and stress induced straining.

For most crystalline solids plastic deformation (i.e. yielding in the sense of permanent deformation) is attributed to a flow process of crystalline lattice defects, which are normally described in terms of development and propagation of dislocations [5], while the restorable lattice distortion is identified with reversible elastic straining. The total deformation may be interpreted as a composition of those two effects [5,31,32]. They may be, in the first approximation, considered as independent of each other [5,31,32] and the composition itself becomes additive when deformations and their gradients remain small. The plastic strain may then be defined to be that component of inelastic strain which occurs during "zero time" loading which denotes a loading input to be short enough to negate any time dependent strain, but long enough to eliminate rate dependent material properties [2]. Limiting consideration to such defined plastic straining is then equivalent to assuming that the mechanical response of the considered material is rate insensitive*. According to Lehmann [36], when both thermal and mechanical responses are

---

* The usual notion of rate sensitivity exhibited by the mechanical response of a given material is concerned with the relationship between the rate of applied loading and the rate of strain considered as mechanical response. The deformation process is said to be rate insensitive whenever different loading rates imply the same responses, with the possibility of variant response rates [29].

considered, the notion of material rate insensitivity should include (rate dependent) effects due to transient heat conduction. Material rate insensitivity understood in such an extended sense still excludes effects like creep, relaxation, aftereffect and defect annealing phenomena [29,37]. A classical case of history dependent material response is said to occur when the material memory for the past deformation is nonfading, i.e. when prior deformation permanently changes material response parameters [29]. The nonfading material memory is well represented by subsequent hardening (softening) of some metals at low homologous temperatures [29].

As one may surmise from the above discussion, assumptions (iii), (v) and (vi) impose quite restrictive measures on the general scenario of situations which can be represented in the developed mathematical model. In particular, without explicitly excluding crystalline non-metallic materials, they effectively restrict the applicability of the proposed model to representing the idealized behaviour of annealed metals at low homologous temperatures [37].

In the continuum approach to modelling a real material containing dislocations, voids and other microstructural features is replaced by a homogenized effective medium. The classical isotropic hardening plasticity theory offers the simplest mathematical model of inelastic behaviour which features both the material rate insensitivity and the classical case of response dependence on prior deformation history [29]. Such an approach, consistent with the other assumptions, still leaves room for various effects coupling mechanical and thermal behaviours to be included in the model. Since the physical

processes underlying these couplings are diversified, the problem of their modelling is approached from the purely phenomenological point of view in the next chapter. There, it is shown that the approach taken aids the interpretation of the energetics of thermoelastoplastic behaviour corresponding to the proposed physical model.

CHAPTER 4

MATHEMATICAL FORMULATION OF THE PROBLEM

4.1 Preliminary Considerations and Notation

The solid medium under consideration is assumed to occupy a closed region R of a three-dimensional Euclidean space, where a space-fixed Cartesian coordinate system x_i (i = 1,2,3) is defined. Relative to this coordinate system the positions of material particles are represented by their Cartesian coordinates x_i, and their displacement vectors by the Cartesian components $u_i = u_i(x_1,x_2,x_3,t)$. In accordance with the previous assumptions the medium is said to undergo (infinitesimally) small deformations. As a result, the linearized kinematics may be used in all considerations, obviating the need to distinguish positions in the initial (reference) and the current (deformed) configurations, and to differentiate between material (Lagrangean) and spatial (Eulerian) descriptions of motion. Adopting the indicial notation for Cartesian vectors and tensors, the basic kinematic relationship, i.e. the relation between strain and displacement vector components, may be written as:

$$\varepsilon_{ij} = \frac{1}{2}(u_{i,j} + u_{j,i}) \qquad (4.1.1)$$

where the indicies following commas denote partial differentiation with respect to the indicated coordinates. In addition, all indices repeated in monomial terms are to be summed over their admissible range according to the Einstein summation convention. Temporal differentiation is denoted by a dot placed over the differentiated quantity, and a typical rate expression becomes:

$$\dot{\varepsilon}_{ij} = \frac{1}{2}(\dot{u}_{i,j} + \dot{u}_{j,i}) = \frac{1}{2}(v_{i,j} + v_{j,i}) \tag{4.1.2}$$

where the particle's velocity is:

$$v_i = \dot{u}_i \tag{4.1.3}$$

Since convective effects cannot be accounted for within the assumed framework, one does not have to distinguish between material and local time differentiation.

The basic constitutive kinematic assumption, underlying the entire theoretical and numerical formulation presented in this thesis, is concerned with the additive decomposition of the total strain tensor into elastic and inelastic (plastic) parts:

$$\varepsilon_{ij} = \varepsilon_{ij}^{(e)} + \varepsilon_{ij}^{(e)} \tag{4.1.4}$$

As an immediate conclusion, the additive decomposition of the strain tensor rate (or strain rate tensor) $\dot{\varepsilon}_{ij}$ follows:

$$\dot{\varepsilon}_{ij} = \dot{\varepsilon}^{(e)}_{ij} + \dot{\varepsilon}^{(p)}_{ij} \tag{4.1.5}$$

The following sections are devoted to the presentation of the theoretical background necessary for the development of the coupled temperature-displacement formulation of the thermoelastoplastic analysis. Physical interpretations, which are helpful in understanding the phenomenological nature of the thermomechanical couplings, are attempted whenever possible. The derived equations are applicable to axisymmetrical analysis in the cylindrical coordinate system after replacing the Cartesian components of vectors and tensors with their contravariant cylindrical components, and replacing the partial differentiation with the covariant differentiation in that system [15]. The transition to the physical components, usually employed in practical finite element analyses, is then fairly straightforward to accomplish.

4.2 Balance Principles of Continuum Thermomechanics

The balance principles of interest in continuum thermomechanics are conservation of mass, balance of linear momentum, balance of angular momentum and balance of energy. Their global (integral) forms refer to any arbitrary portion of the body under consideration, and may be summarized as follows:

(i) Conservation of Mass:

$$\frac{d}{dt} \int_V \rho dV = 0 \tag{4.2.1}$$

(ii) Balance of Linear Momentum:

$$\frac{d}{dt}\int_V \rho v_i \, dV = \int_V \rho b_i \, dV + \int_S t_i dS \qquad (4.2.2)$$

(iii) Balance of Moment of Momentum:

$$\frac{d}{dt}\int_V e_{ijk} x_j \rho v_k dV = \int_V e_{ijk} x_j \rho b_k dV + \int_S e_{ijk} x_j t_k dS \qquad (4.2.3)$$

(iv) Balance of Energy (First Law of Thermodynamics):

$$\frac{d}{dt}\int_V \rho(e + \frac{1}{2}\rho v_i v_i)dV = \int_V \rho(r+b_i v_i)dV + \int_S (t_i v_i + q)dS \qquad (4.2.4)$$

In the above equations all integrations extend over the volume V or the boundary surface S of an arbitrary portion of the region R occupied by the body, and the symbols used denote:

ρ - mass density,

x_i - spatial coordinates of body particles,

$v_i = \dot{u}_i$ - velocity field of body particles,

b_i - distributed body forces per unit mass,

t_i - surface tractions (distributed surface forces per unit area),

e - internal energy density,

r - rate of internal energy generation per unit mass,

q - influx of internal energy through the surface S,

e_{ijk} - permutation tensor.

Equations (4.2.1-4) represent balance principles for the classical model of continuum and invoke a simple model for the production and the exchange of momenta and energy.

In thermomechanics, the energy stored in the system is assumed to be the sum of the (macroscopic) kinetic and internal energies. The net production of these energies can be accomplished through conversions with the gravitational and electromagnetic energies, represented in the energy balance equation (4.2.4) by the net production integral with volumetric density $\rho(b_i v_i + r))$*. Similar production integrals appear in the linear and the angular momentum balances, indicating possible contributions of gravitational and electromagnetic fields to momenta changes.

In addition to the net productions, the changes of energy and momenta stored within the material volume V, may take place through exchanges with surrounding media, represented by the boundary integrals in balance equations. The transfer mechanisms of linear momentum and internal energy require additional models to relate the surface densities t_i and q to quantities independent of the surface orientation. When the traction vector t_i is referred to a surface whose exterior normal has the components n_i, the Cauchy's stress principle defines the stress tensor through the relationship:

$$t_i = \sigma_{ij} n_j \qquad (4.2.5)$$

---

* Volumetric sources of kinetic energy $\rho b_i v_i$ may be of gravitational or electromagnetic origin, while the density of internal energy production ρr accounts for conversions between internal and electromagnetic energies (see FIGURE 1). By specifying b_i and r as functions of position and time, without regard to the presence of other bodies or their parts nearby, the effects of mutual gravitation and mutual radiation are excluded [57].

Similarly, the internal energy transported across a unit area of the same surface may be related to the internal energy flux vector q_i through the relationship:

$$q = -q_i n_i \tag{4.2.6}$$

Assuming further that internal energy transport involves mainly the transport of thermal energy (as a subclass of internal energy), vector q_i becomes the heat flux*.

The balance of energy in equation (4.2.4) may be transformed to the more convenient form [15]:

$$\frac{d}{dt}\int_V \rho e \, dV = \int_V \sigma_{ij} v_{i,j} dV + \int_V \rho r \, dV + \int_S q dS \tag{4.2.7}$$

representing balance of internal energy alone.

Substracting (4.2.7) from (4.2.4), a separate balance of kinetic energy is derived:

$$\frac{d}{dt}\int_V \rho(\frac{1}{2} v_i v_i)dV = -\int_V \sigma_{ij} v_{i,j} dV + \int_V \rho b_i v_i dV + \int_S t_i v_i dS \tag{4.2.8}$$

Equations (4.2.7-8) are obviously not independent of each other, but offer additional insight into the energy transfer processes within the

---

* Internal energy flux q_i may take the form of a heat flux and other types of fluxes. Migration of dislocations and diffusion of solute species are examples of internal energy fluxes that do not constitute heat flux [36].

system. Interpretation of these equations in terms of the transport of internal and kinetic energies indicates the manner in which mutual conversion between them takes place in the body. Clearly, the first integral on the right-hand-side of the equation (4.2.7), represents that part of the kinetic energy stored within the volume V which is being converted into the internal energy. The conversion process takes place locally, whenever stress power $\sigma_{ij}v_{i,j}$ becomes positive somewhere in the body. Negative value of $\sigma_{ij}v_{i,j}$ indicates the opposite process of local creation of kinetic energy at the cost of internal energy decrease.

The mutual conversion process described above lies at the bottom of what is termed the passive thermomechanical coupling. Since this conversion is known to be only partially reversible, giving rise to internal dissipation phenomena, the problem of how to determine which part of the converted kinetic energy is stored in the form of recoverable internal energy, arises. The difficulty of tackling internal dissipation exclusively on the basis of continuum approach may be in part attributed to the fact that no universal balances for internal energy subclasses (such as strain and thermal energies) are available and consequently, the forms of their mutual conversions have to be postulated.

The pattern of internal transfer of energy within the body is simplified in the case of a quasi-static process. By definition, a quasi-static thermomechanical process takes place whenever velocities of all the body particles vary slowly enough to justify disregarding their accelerations. This condition is, however, equivalent to the

assumption that kinetic energy density $\frac{1}{2} v_i v_i$ remains time-invariant during the process. Understandably, the kinetic energy is then conserved in the global sense:

$$\frac{d}{dt} \int_V (\frac{1}{2} \rho v_i v_i) \, dV = 0 \tag{4.2.9}$$

and the global balance of energy takes the form:

$$\frac{d}{dt} \int_V \rho e \, dV = \int_V \rho(b_i v_i + r) \, dV + \int_S (t_i v_i + q) \, dS \tag{4.2.10}$$

All the kinetic energy net production and net exchange with the surrounding is instantaneously converted into the net production and net exchange of the internal energy. The thermomechanical process is transient only with respect to internal energy changes, while the motion of the body is approximated as steady state.

The local (differential) forms of the balance principles are easily derived from the global statements (4.2.1-4) through subsequent transformations of all surface integrals into volume integrals (using relationships (4.2.5-6) and applying the divergence theorem), and taking advantage of the arbitrariness of material volume V and assumed continuity of all field variables [15].

The moment of momentum balance equation (4.2.3) may then be shown to lead to the requirement of stress tensor symmetry:

$$\sigma_{ij} = \sigma_{ji} \tag{4.2.11}$$

while, in the quasi-static case, equations (4.2.2) and (4.2.4) yield local equilibrium and internal energy balance equations:

$$\sigma_{ij,j} + \rho b_i = 0 \tag{4.2.12}$$

$$\rho \frac{de}{dt} = \sigma_{ij} v_{i,j} + \rho r - q_{i,i} \tag{4.2.13}*$$

Within the framework of small deformation theory and linearized kinematics, and under the previously stated assumptions, the mass of the body is always conserved both globaly and locally. The mass conservation equation (4.2.1) becomes an identity, and the density field must be prescribed, usually as a function of position only:

$$\rho = \rho(x_i) \tag{4.2.14}$$

Equation (4.2.14) is then used instead of the local mass conservation (local continuity) equation.

In general, the local balancing approach reduces the number of scalar functional balance equations from eight to four, adding four independent algebraic equations represented by (4.2.11) and (4.2.14).

---

* Using the symmetry property of the stress tensor (4.2.11) and the definition of the strain tensor rate (4.1.2) it may be easily verified that

$$\sigma_{ij} v_{i,j} = \sigma_{ij} \dot{\varepsilon}_{ij} \tag{4.2.15}$$

The simple forms of these equations allow the elimination of mass density ρ from further consideration, and the retention of only six independent components of the stress tensor, namely σ_{11}, σ_{22}, σ_{33}, σ_{12}, σ_{13} and σ_{23}.

4.3 Second Law of Thermodynamics and Balance of Entropy

The second law of thermodynamics is usually postulated in continuum mechanics in the form of the Clausius-Duhem inequality [15]:

$$\frac{d}{dt}\int_V \rho s \, dV \geq \int_V \frac{1}{\theta} \rho r \, dV + \int_S \frac{1}{\theta} q \, dS \qquad (4.3.1)$$

where s denotes the specific entropy (i.e. entropy per unit mass), θ is the absolute temperature, and $\theta = T + T_o$, with T_o and T being the reference temperature and temperature change, respectively.

The inequality (4.3.1) is often regarded as a form of general constraint imposed on every conceivable physical process that may involve both reversible and irreversible phenomena. Then, it may be utilized to derive restrictions which must be obeyed by any postulated constitutive relationships. Aside from this, inequality (4.3.1) may be considered as an "incomplete" balance of entropy. In view of the earlier stated assumptions, the heat flow q which represents the only mode of internal energy exchange between the material volume V and its surroundings is also considered to be the sole mechanism of entropy exchange. The entire net entropy supply across area S per unit time is represented by the surface integral in equation (4.3.1). Therefore

introducing the notion of internal (irreversible) entropy production density γ, the entropy of the body is balanced according to the equation:

$$\frac{d}{dt}\int_V \rho s \, dV = \int_V \gamma \, dV + \int_S \frac{1}{\theta} q \, dS \qquad (4.3.2)$$

Since any irreversible generation of entropy is always accompanied by some changes of internal energy (see FIGURE 1 and References [15] and [57]), it is convenient to relate the corresponding phenomena. The entropy production density may be represented as the sum of three terms:

$$\gamma = \frac{1}{\theta}(D - \frac{1}{\theta} q_i \theta_{,i} + \rho r) \qquad (4.3.3)$$

accounting for the irreversibility associated with:

- the conversion of kinetic energy into internal energy,
- internal energy (i.e. heat) propagation within the body,
- volumetric supply of internal energy from internal sources

The internal dissipation function D, introduced by Coleman and Gurtin [12], may be aimed at accounting for the irreversible mode of the conversion of kinetic energy into internal energy. It may therefore be expected to directly contribute to the passive thermomechanical coupling in the internal energy balance.

Introducing (4.3.3), (4.2.5) and (4.2.6) into (4.3.1) and (4.3.2), and applying the divergence theorem, the global forms of the Clausius-Duhem inequality and the entropy balance equation become:

$$\int_V \frac{1}{\theta} \left(D - \frac{1}{\theta} q_i \theta_{,i}\right) dV \geq 0 \tag{4.3.4}$$

$$\frac{d}{dt} \int_V \rho s \, dV = \int_V \frac{1}{\theta} \left(D + \rho r - q_{i,i}\right) dV \tag{4.3.5}$$

The local forms of (4.3.4) and (4.3.5) are:

$$D - \frac{1}{\theta} q_i \theta_{,i} \geq 0 \tag{4.3.6}$$

$$\rho\theta \frac{ds}{dt} = D + \rho r - q_{i,i} \tag{4.3.7}$$

Equation (4.3.7) will be later employed in the presentation of the constitutive theory of thermoelastoplastic behaviour.

4.4 Constitutive Relationships of Isotropic Thermoelastoplasticity

The irreversible nature of phenomena involving inelastic and nonisothermic deformations makes it expedient to employ a thermodynamic framework for constitutive modelling of real materials and processes. In particular, a thermodynamic formalism seems to be essential for formulation of the theory which pays special attention to the effects usually considered secondary, and therefore neglected, in order to systematize the development of the constitutive model(s).

The choice of such a thermodynamic formalism to be employed is not an easy task, for the thermodynamics of irreversible (non-equilibrium) phenomena continues to remain a controversial area, where "there are nearly as many approaches as authors in the field" [36].

An approach to the thermodynamic description of irreversible behaviour of materials, which allows it to remain within the phenomenological framework of continuum mechanics, but appears to be able to cover quite a wide range of physical phenomena, was developed in a series of recent works by Lehmann [31,32,33,34,35,36,37]. His approach combines two thermodynamic formalisms previously used in thermomechanics of solids. These are the state variable and thermodynamic process approaches. The theory is based on the fundamental assumption that each (infinitisemal) material element may be treated as a local thermodynamic system [36]. As a result, the postulated constitutive relations in general consist of both equations of state and relationships derived from the process description. Since Lehmann's approach clearly delineates the role which the thermomechanical couplings play in a constitutive model for a solid material, it will be used here for the presentation of the simplest case of isotropic thermoelastoplasticity. The development of equations of state, derived within the scope of the thermodynamic state variables approach, will be followed by the development of evolution equations originating from the thermodynamic process description. The discussion on the constitutive modelling of the passive thermomechanical coupling, which appears in the internal energy balance equation, could then be followed.

4.4.1 Equations of State

The thermodynamic state formalism was developed as an extension of the classical thermodynamics to the non-homogenous systems remaining close to the thermodynamic equilibrium, using the notions of thermodynamic state and state variables as primitive concepts of the theory [31,32]. The assumption regarding the treatment of material elements as local thermodynamic systems leads to the description of state by instantaneous values of a finite number of independent field variables. When other state variables are introduced, they are always related to the set of independent state variables through algebraic equations known as equations of state.

The decision in regard to the number and nature of independent state variables is based on by virtue of the intended generality of the constitutive theory. It is usually preceeded by questioning which physical quantities may be uniquely associated with a given thermodynamic state. For example, the classical model of thermoelastic behaviour requires one scalar and one tensorial (of second rank) independent state variable to describe the thermal and deformational aspects of thermodynamic state. The specific entropy s or the absolute temperature θ is the most frequent choice for the thermal state independent variable, while the deformational state is usually described by the independent components of either the stress tensor σ_{ij} or the elastic strain tensor $\varepsilon_{ij}^{(e)}$. In the case of inelastic deformation, changes in the internal material structure occur in addition to thermal and dimensional changes (on the macroscopic scale), indicating a need for additional scalar and/or tensorial state

variables. The isotropic hardening model of plastic flow, exclusively used in further considerations, is based on one additional scalar variable κ, which may be introduced either as the strain-hardening or as the work-hardening parameter* [8,19,29,53]. The simplest plasticity model accounting for hardening anisotropy (kinematic hardening model) would require extending the set of independent state variables to include the independent components of another symmetrical tensor of rank two.

If the elastic strain tensor $\varepsilon_{ij}^{(e)}$, the absolute temperature θ, and the work-hardening parameter κ are selected as independent state variables, than all other state variables, such as the specific internal energy e, specific entropy s or stress tensor σ_{ij}, become functions of the independent components of $\varepsilon_{ij}^{(e)}$, as well as θ and κ. Then, the derivation of the constitutive relationships is best facilitated by the use of the specific free energy (also called Helmholtz function) ψ, which is formally defined as:

$$\psi(\varepsilon_{ij}^{(e)}, \theta, \kappa) = e(\varepsilon_{ij}^{(e)}, \theta, \kappa) - \theta\, s(\varepsilon_{ij}^{(e)}, \theta, \kappa) \qquad (4.4.1)$$

---

* According to Lehmann [31], neither the inelastic strain tensor $\varepsilon_{ij}^{(p)}$ nor the total strain tensor ε_{ij} does qualify as a state variable, and therefore cannot be included in the set of independent state variables. The reason quoted is the experimental evidence indicating a possibility of attaining very different states of hardening corresponding to the same values of inelastic (or total) strains. Usage of either the strain- or the work-hardening parameter depends on the postulated evolution equation.

Its time derivative may be computed either as

$$\frac{d\psi}{dt} = \frac{de}{dt} - \theta \frac{ds}{dt} - s \frac{d\theta}{dt} \tag{4.4.2}$$

or as

$$\frac{d\psi}{dt} = \frac{\partial \psi}{\partial \varepsilon_{ij}^{(e)}} \dot{\varepsilon}_{ij}^{(e)} + \frac{\partial \psi}{\partial \theta} \dot{\theta} + \frac{\partial \psi}{\partial \kappa} \dot{\kappa} \tag{4.4.3}$$

Eliminating the internal energy and entropy rates of change in (4.4.2) with the use of balance equations (4.3.3) and (4.3.7) leads to the following equation*:

$$\rho \frac{d\psi}{dt} = \sigma_{ij} \dot{\varepsilon}_{ij}^{(e)} + \sigma_{ij} \dot{\varepsilon}_{ij}^{(p)} - \rho s \dot{\theta} - D \tag{4.4.4}$$

Assuming further, that internal energy dissipation is exclusively associated with plastic deformations (i.e. that D does not include elastic power component), comparison of (4.4.3) and (4.4.4) yields:

$$\sigma_{ij} = \rho \frac{\partial \psi}{\partial \varepsilon_{ij}^{(e)}} \tag{4.4.5}$$

$$s = - \frac{\partial \psi}{\partial \theta} \tag{4.4.6}$$

$$\sigma_{ij} \dot{\varepsilon}_{ij}^{(p)} - D = \rho \frac{\partial \psi}{\partial \kappa} \dot{\kappa} \tag{4.4.7}$$

---

* Using the identity (4.2.15) and the strain rate tensor decomposition (4.1.5)

Equations (4.4.5) and (4.4.6) define the dependent state variables σ_{ij} and s as functions of independent state variables, and are known as thermic and caloric equations of state, respectively.

Equation (4.4.7) involves quantities other than state variables, and according to Lehmann [36], should be considered as the additional thermodynamic requirement (the other being Clausius-Duhem inequality) with which the thermodynamic process description should be compatible.

To make use of the thermic and caloric equations of state the specific free energy function $\psi(\varepsilon_{ij}^{(e)},\theta,\kappa)$ does not have to be explicitly specified. It would be sufficient to postulate the explicit forms of the dependencies $\sigma_{ij}(\varepsilon_{ij}^{(e)},\theta,\kappa)$ and $s(\varepsilon_{ij}^{(e)},\theta,\kappa)$. In practice, however, another dependent state variable, known as the specific heat capacity at constant elastic strains and internal parameters, and defined as

$$c_\varepsilon = c_\varepsilon(\varepsilon_{ij}^{(e)},\theta,\kappa) = \theta \frac{\partial s(\varepsilon_{ij}^{(e)}, \theta, \kappa)}{\partial \theta} \qquad (4.4.8)$$

is postulated (from experimental measurements, for example) instead of the specific entropy s. Equation (4.4.8), although distinct from (4.4.6), is also sometimes called the caloric equation of state.

The previously assumed independence of elastic deformations on the plastic behaviour (see CHAPTER 3) implies no coupling between the state variables $\varepsilon_{ij}^{(e)}$ and κ in the specific free energy function $\psi(\varepsilon_{ij}^{(e)},\theta,\kappa)$. This, in turn, leads to the additive decomposition

$$\psi(\varepsilon_{ij}^{(e)},\theta,\kappa) = \psi^{(e)}(\varepsilon_{ij}^{(e)},\theta) + \psi^{(p)}(\theta,\kappa) \qquad (4.4.9)$$

where $\psi^{(e)}$ denotes the thermoelastic component of the specific free energy. Then, the thermic equation of state (4.3.5) takes the form derived in thermoelasticity. For the isotropic thermoelastic behaviour there is:

$$\sigma_{ij} = \frac{E}{(1+\nu)(1-2\nu)}\varepsilon_{kk}^{(e)}\,\delta_{ij} + \frac{E}{1+\nu}\,\varepsilon_{ij}^{(e)} - \frac{E\alpha}{1-2\nu}\,(\theta-T_o)\delta_{ij} \qquad (4.4.10)$$

where δ_{ij} is the Kronecker's delta with values of 1 for i=j and zero otherwise.

The thermoelastic constants: Young's modulus E, Poisson's ratio ν, and the coefficient of thermal expansion α are in general functions of instantenous temperature, and T_o is the temperature of the strain free reference state. Equation (4.4.10), known as the Duhamel-Neumann form of the generalized Hooke's law [5,50] may be conveniently rewritten as:

$$\sigma_{ij} = C_{ijrs}^{(e)}\,(\varepsilon_{rs}^{(e)} - \varepsilon_{rs}^{(th)}) = C_{ijrs}^{(e)}\,(\varepsilon_{rs} - \varepsilon_{rs}^{(p)} - \varepsilon_{rs}^{(th)}) \qquad (4.4.11)$$

where the elastic stiffness fourth rank tensor $C_{ijrs}^{(e)}$ is

$$C_{ijrs}^{(e)} = \frac{E\nu}{(1+\nu)(1-2\nu)}\,\delta_{ij}\delta_{rs} - \frac{E}{2(1+\nu)}\,(\delta_{ir}\delta_{js} + \delta_{is}\delta_{jr}) \qquad (4.4.12)$$

and the (apparent) thermal strain is:

$$\varepsilon_{ij}^{(th)} = \alpha\,(\theta - T_o)\,\delta_{ij} = \alpha T\,\delta_{ij} \qquad (4.4.13)$$

4.4.2 Constitutive Relations Resulting from the Thermodynamic Process Description

Despite the appeal of the thermodynamic state variables approach it becomes clear that the phenomenological description of inelastic features of deformation exclusively on the grounds of that theory (e.g. by postulating the explicit form of the Helmholtz free energy as a function of state variables) is inadequate [31]. Further variables are required to describe processes which occur in the non-equilibrium systems. These may be gradients or rates of change of the state variables, or any other quantity needed to specify processes occuring in the material. Such quantities are called process variables and are governed by (process) evolution equations which may involve both state and process variables [31].

According to Lehmann [36], the required constitutive relationships in process description of coupled thermoplasticity consist of:

(i) the evolution laws for the dependent external process variables q_i and ε_{ij} (conjugated to the independent external process variables θ and σ_{ij}).

(ii) the evolution laws for the internal process variables (where the internal state variable κ is selected as the only internal process variable for isotropic hardening plasticity).

(iii) the evolution law for the specific entropy production.

Following the simplified but common approach, which originates from the thermodynamics of homogeneous processes, all the evolution laws, with the exception of the constitutive equation for the heat flux q_i, are postulated in the form of ordinary differential equations* (possibly subject to auxilliary conditions). With the absence of experimental evidence to the contrary, it is usually assumed that heat flux q_i is independent of the history of past deformation (e.g. q_i is not a function of κ), and the evolution equations for the internal state variables are independent of the temperature gradient [43]. Also, the evolution law for the specific entropy production is sometimes replaced by the equivalent statement regarding the internal dissipation rate D (see equation (4.4.3)).

The evolution law for the heat flux q_i, known as the heat conduction law, will be assumed to be:

$$q_i = - k \, \theta,_i \qquad (4.4.14)$$

---

* Lehmann defines the rate-insensitive thermomechanical process, as one for which all the evolution laws are of the equilibrium type, i.e. for which the rates of the dependent process variables are related to the rates of independent process variables, [36]. This condition expressed mathematically states that all evolution laws must take the form of homogenous ordinary differential equations in the time domain. In this sense the rate-independent isothermal plasticity becomes rate-dependent in non-isothermal conditions.

where the thermal conductivity k of the isotropic material may be a function of temperature.

In view of the separation of the total strain into elastic and inelastic parts and identification of the elastic strain tensor as an independent state variable the evolution equation for the strain tensor may be concerned with the evolution of the plastic strain components only. This evolution law, known as a <u>flow rule</u>, is usually postulated in the form of the <u>normality condition</u>:

$$\dot{\varepsilon}^{(p)}_{ij} = \begin{cases} \lambda \dfrac{\partial F}{\partial \sigma_{ij}} & \text{if} \quad F = 0 \quad \text{and} \quad \lambda \geq 0 \\ 0 & \text{if} \quad F = 0 \quad \text{and} \quad \lambda < 0 \\ 0 & \text{if} \quad F < 0 \end{cases} \tag{4.4.15}$$

which assumes existence of a convex <u>yield surface</u> $F = 0$ in the stress deviator space. It states that when the stress state of a material point comes into contact with this yield surface, the resulting plastic strain increment is along the outward normal at the point of contact [15]. The yield surface is usually assumed to be of second degree with respect to the stress deviator components, and the most widely used form for the isotropic plasticity is due to von Mises, Huber and Hencky (known also as the J_2 flow theory):

$$F(\sigma_{ij}, \kappa, \theta) = \frac{1}{2} \sigma'_{ij} \sigma'_{ij} - \frac{1}{3} \sigma_y^2 \tag{4.4.16}$$

The deviatoric stress tensor is defined as

$$\sigma'_{ij} = \sigma_{ij} - \frac{1}{3}\sigma_{kk}\delta_{ij} \tag{4.4.17}$$

and σ_y denotes the yield stress, which for non-isothermal plasticity is a function of both the hardening parameter κ and the temperature:

$$\sigma_y = \sigma_y(\kappa,\theta) \tag{4.4.18}$$

It is assumed that a relationship between σ_y, κ and θ can be derived from the data obtained in a series of isothermal tensile tests. The evolution equation for the hardening parameter κ, known as the hardening rule provides, along with the temperature θ, a description of the changing size of the yield surface during plastic flow. Selecting κ as the work-hardening parameter, the appropriate hardening rule is:

$$\dot{\kappa} = \sigma'_{ij}\dot{\varepsilon}^{(p)}_{ij} \tag{4.4.19}*$$

It is known that for the von Mises-Huber-Hencky yield surface (4.4.16) equivalent formulation of isotropic hardening plasticity may be obtained if the strain-hardening hypothesis is employed [53,63].

---

* With the usual assumption of incompressibility of plastic deformation $\varepsilon^{(p)}_{kk} = 0$, there is $\varepsilon^{(p)}_{ij} = \frac{1}{3}\varepsilon^{(p)}_{kk}\delta_{ij} + \varepsilon^{(p)'}_{ij} = \varepsilon^{(p)'}_{ij}$, and $\dot{\kappa} = \sigma'_{ij}\dot{\varepsilon}^{(p)}_{ij} = (\sigma_{ij} - \frac{1}{3}\sigma_{kk}\delta_{ij})\dot{\varepsilon}^{(p)'}_{ij} = \sigma_{ij}\dot{\varepsilon}^{(p)'}_{ij} = \sigma_{ij}\dot{\varepsilon}^{(p)}_{ij}$.

Then, the only internal variable is selected in the form of the strain-hardening (Odqvist) parameter $\bar{\varepsilon}^{(p)}$, also known as the equivalent plastic strain. The corresponding strain-hardening rule may be considered as the definition of the equivalent plastic strain rate:

$$\dot{\bar{\varepsilon}}^{(p)} = \left(\frac{2}{3}\dot{\varepsilon}_{ij}^{(p)}\dot{\varepsilon}_{ij}^{(p)}\right)^{1/2} \tag{4.4.20}$$

The work-hardening parameter κ seems to be more often employed in the theoretical development of plasticity theory [43,44,62], while the equivalent plastic strain appears to be more convenient in the computational plasticity formulations.

Both of these hardening parameters will be employed in further presentation of the constitutive theory and numerical formulation of the boundary value problem. To avoid confusion, it should be stressed, however, that only one scalar hardening parameter is necessary to consider in isotropic plasticity.

During plastic straining there is $F = 0$ and $\lambda \geq 0$ (see 4.4.15), and the proportionality factor is determined from the consistency condition [23]:

$$\frac{\partial F}{\partial \sigma_{ij}}\dot{\sigma}_{ij} + \frac{\partial F}{\partial \theta}\dot{\theta} + \frac{\partial F}{\partial \kappa}\dot{\kappa} = 0 \tag{4.4.21}$$

resulting from the fact that at any instant the yield surface passes through the stress point. The partial derivatives of the yield function are:

$$\frac{\partial F}{\partial \sigma_{ij}} = \sigma'_{ij} = \sigma_{ij} - \frac{1}{3}\sigma_{kk}\delta_{ij} \qquad (4.4.22)$$

$$\frac{\partial F}{\partial \kappa} = -\frac{2}{3}\sigma_y \frac{\partial \sigma_y}{\partial \kappa} \qquad (4.4.23)$$

$$\frac{\partial F}{\partial \theta} = -\frac{2}{3}\sigma_y \frac{\partial \sigma_y}{\partial \theta} \qquad (4.4.24)$$

and equations (4.4.11) and (4.4.15) yield:

$$\dot{\sigma}_{ij} = C^{(e)}_{ijrs}\,(\dot{\varepsilon}_{rs} - \lambda\,\sigma'_{rs} - \dot{\varepsilon}^{(th)}_{rs}) + \dot{C}^{(e)}_{ijrs}\,(\varepsilon^{(e)}_{rs} - \varepsilon^{(th)}_{rs}) \qquad (4.4.25)$$

Then, substituting (4.4.19) and (4.4.22-25) into (4.4.21), and solving for λ, gives

$$\lambda = \frac{C^{(e)}_{ijrs}\,(\dot{\varepsilon}_{rs} - \dot{\varepsilon}^{(th)}_{rs})\,\sigma'_{ij} + \dot{C}^{(e)}_{ijrs}\,(\varepsilon^{(e)}_{rs} - \varepsilon^{(th)}_{rs})\,\sigma'_{ij} - \frac{2}{3}\sigma_y \frac{\partial \sigma_y}{\partial \theta}\dot{\theta}}{\frac{4}{9}\sigma_y^3 \frac{\partial \sigma_y}{\partial \kappa} + C^{(e)}_{ijrs}\,\sigma'_{ij}\,\sigma'_{rs}} \qquad (4.4.25)$$

In order to obtain a more coincise expression for λ it is convenient to consider additional moduli. They will be introduced in Section 4.5.1, and will enable λ to be expressed as a linear combination of total strain and temperature rates.

The final constitutive relation that has to be considered is a statement regarding the functional form of the internal energy dissipation rate D (or equivalently specific entropy production). Notwithstanding the fact that such relationship forms a part of the thermodynamic process description, it is convenient to discuss it

separately, along with other coupling effects appearing in the energy balance equation.

4.4.3 Coupling Effects in the Energy Balance Equation

To make full use of the internal energy balance (4.2.13) one has to be able to effectively compute the time rate of the specific internal energy ρ (de/dt). The thermodynamic framework, outlined in the previous sections, makes it possible through associating internal energy rates due to the temporal changes of independent state variables with changes of other (state or process) variables, which are postulated by the constitutive relationships. The internal energy rates corresponding to the rates of individual independent state variables can often be assigned further physical interpretations as rates of the subclasses of internal energy which may lead to the identification of their mutual conversions and arriving at their separate balances.

For the case in which one scalar internal state variable κ, the elastic strain rate $\varepsilon_{ij}^{(e)}$ and temperature θ selected as independent external state variables, the time rate of the specific internal energy ρe also treated as a state variable, is:

$$\rho \frac{de}{dt} = \rho \frac{\partial e}{\partial \varepsilon_{ij}^{(e)}} \overset{\bullet}{\varepsilon}{}_{ij}^{(e)} + \rho \frac{\partial e^{\bullet}}{\partial \theta} \theta + \rho \frac{\partial e^{\bullet}}{\partial \kappa} \kappa \qquad (4.4.27)$$

The additive decomposition of the free energy (4.4.9) renders a similar decomposition of the internal energy:

$$e(\epsilon_{ij}^{(e)},\theta,\kappa) = e^{(e)}(\epsilon_{ij}^{(e)},\theta) + e^{(p)}(\theta,\kappa) \tag{4.4.28}$$

Upon using the definition of Helmholtz free energy (4.4.1) and equations (4.4.5-8), it is easy to verify that the respective components of $\rho(de/dt)$ are:

$$\rho \frac{\partial e}{\partial \epsilon_{ij}^{(e)}} \dot{\epsilon}_{ij}^{(e)} = \rho \frac{\partial e^{(e)}}{\partial \epsilon_{ij}^{(e)}} \dot{\epsilon}_{ij}^{(e)} = (\sigma_{ij} - \theta \frac{\partial \sigma_{ij}}{\partial \theta}) \dot{\epsilon}_{ij}^{(e)} \tag{4.4.29}$$

$$\rho \frac{\partial e}{\partial \theta} \dot{\theta} = \rho c_\epsilon \dot{\theta} \tag{4.4.30}$$

$$\rho \frac{\partial e}{\partial \kappa} \dot{\kappa} = \rho \frac{\partial e^{(p)}}{\partial \kappa} \dot{\kappa} = \sigma_{ij} \dot{\epsilon}_{ij}^{(p)} - D - \rho\theta \frac{\partial}{\partial \theta} (\frac{\partial \psi}{\partial \kappa}) \dot{\kappa} \tag{4.4.31}$$

Substituting (4.4.27-31) and (4.4.27) into the internal energy balance equation (4.2.13) will yield:

$$\rho c_\epsilon \dot{\theta} = \theta \frac{\partial \sigma_{ij}}{\partial \theta} \dot{\epsilon}_{ij}^{(e)} + D + \rho\theta \frac{\partial}{\partial \theta} (\frac{\partial \psi}{\partial \kappa}) \dot{\kappa} + \rho r - q_{i,i} \tag{4.4.32}$$

Equation (4.4.32) is called coupled heat conduction equation, and it appears in similar forms in the works of Kratochvil and Dillon [28], Raniecki and Sawczuk [55] and Mróz and Raniecki [43]. The former two works offer an interpretation of the term $\rho(\partial e/\partial \kappa)\dot{\kappa}$ as the rate of internal energy being stored on the microlevel. Proceeding further with this type of interpretation, the term $\rho[\partial e/\partial \epsilon_{ij}^{(e)}]\dot{\epsilon}_{ij}^{(e)}$ may be identified as the rate of internal energy stored within the crystal lattice, i.e. elastic strain energy rate, while $\rho(\partial e/\partial \theta)\dot{\theta}$ may be termed the rate of internal energy stored as thermal energy.

Then, euqation (4.4.32) may be interpreted as the balance of thermal energy, with its rate of storage equal to $\rho c_\varepsilon \dot{\theta}$. The balance equation (4.4.32) indicates the following modes of thermal energy changes:

- exchange with the surroundings to be represented by the heat flux q_i;

- conversion with electromagnetic and other energies (excluding the kinetic energy) to be represented by the volumetric density ρr;

- conversions with the other two subclasses of internal energy (i.e. with the elastic strain energy and energy stored on the microscale).

The latter conversions are represented in the coupled heat conduction equation (4.4.32) by the first three terms on the right hand side. The reversible conversion between thermal and elastic strain energies is accounted for through the heat of elastic deformation, which may be computed using (4.4.10), as:

$$\theta \frac{\partial \sigma_{ij}}{\partial \theta} \overset{\bullet}{\varepsilon}{}^{(e)}_{ij} = \theta\{ - C^{(e)}_{ijrs}[\alpha + \frac{\partial \alpha}{\partial \theta}(\theta - T_o)]\delta_{rs}$$

$$+ \frac{\partial C^{(e)}_{ijrs}}{\partial \theta}[\varepsilon^{(e)}_{rs} - \alpha(\theta - T_o)\delta_{rs}]\}\overset{\bullet}{\varepsilon}{}^{(e)}_{ij} \qquad (4.4.33)$$

and which represents the (passive) thermoelastic coupling effect [15]. The conversion between thermal and stored on the microscale energies is a partially reversible and partially irreversible process. Its reversible aspect is represented in the balance equation (4.4.32) by the heat of plastic deformation $\rho\theta(\partial/\partial\theta)(\partial\psi/\partial\kappa)\dot{\kappa}$, while the internal dissipation rate D accounts for the irreversible conversion [43]. The irreversibility of the internal dissipation process reflects the fact that only part of the energy stored on the microscale and converted into thermal energy may be converted back to its previous form.

Equations (4.4.29) and (4.4.31) may be viewed as separate balances of the elastic strain energy and energy stored on microlevel. They do not provide any essentially new information, because the explicit forms of the functions $e^{(e)}(\varepsilon_{ij}^{(e)},\theta)$ and $e^{(p)}(\kappa,\theta)$, or equivalently $\psi^{(e)}(\varepsilon_{ij}^{(e)},\theta)$ and $\psi^{(p)}(\kappa,\theta)$, were not postulated. Nevertheless, the above mentioned equations, along with the coupled heat conduction equation (4.3.32), allow a clear realization of the mutual conversions between the internal energy subclasses. FIGURE 2 schematically illustrates these processes, interprets the individual terms in the balance equations (4.4.29, 31-32), and identifies the various types of (passive) thermomechanical couplings arising within the employed phenomenological description.

At this point, it is worthwhile to note that the coupled heat conduction equation (4.4.32) is still in quite a general form. Neither the constitutive relations resulting from the thermodynamic process description nor the explicit form of the thermic equation of

state were used in its derivation. In particular, no specific assumption regarding inelastic behaviour, except the assumption (4.4.28) concerning the lack of direct coupling between elastic and inelastic deformations, was involved.

The final constitutive relationship to be postulated concerns the internal dissipation rate D. It should be however, considered in close connection with the heat of plastic deformation $\rho\theta(\partial/\partial\theta)(\partial\psi/\partial\kappa)\dot{\kappa}$, in view of the fact that some authors treat these quantities together as a thermoplastic coupling in the energy equation.

It should be recognized that to postulate a general but adequate model for the rate of conversion between internal energy stored on the microlevel and thermal energy is a difficult task. Many simple approaches attempt to make use of experimental observations. They lead to the following conclusions:

(i) heat is generated when material is undergoing deviatoric deformations [14];

(ii) only part of the input plastic power $\sigma_{ij}\dot{\varepsilon}^{(p)}_{ij}$ * is stored, while most of it is dissipated as heat [14,30].

---

* $\sigma_{ij}\dot{\varepsilon}^{(p)}_{ij} \geq 0$ may be concluded on the basis of (4.3.6) and (4.4.14).

The latter observation, known as Taylor-Farren-Quinney effect [14,28,49], may form a basis for a simple model of the internal dissipation rate:

$$D = \xi \sigma_{ij} \dot{\varepsilon}^{(p)}_{ij} \tag{4.4.34}$$

where the positive factor ξ may be, in general, a function of both the absolute temperature θ and the internal state variable κ:

$$\xi = \xi(\theta, \kappa) \tag{4.4.35}$$

As quoted by many contemporary authors [17,30,40], the original research by Taylor and Farren, and Taylor and Quinney suggest that the value of the factor ξ remains between 0.9 and unity.

A review of selected models of thermoplastic coupling in the coupled heat conduction equation are summarized in Table 1. It indicates that most models use variations of equation (4.4.34) as constitutive postulates. All the reviewed models of thermoplastic coupling pertain to simple models of plastic behaviour, and are represented by no more than one scalar internal variable. However, some of the thermodynamic frameworks within which the models were developed (often not clearly stated) are not identical to the one adopted in this thesis. In particular, it is worthy mentioning that some of the quoted models [43,44,55] were arrived at by employing Ziegler's orthogonality principle in order to obtain the functional forms of the variables conjugated to the internal state variables.

The approach to the modelling of nonisothermal behaviour of simple isotropically hardening elastoplastic material as was taken by Lehmann [31,32,33,34,35,36,37] also differs to some extent from that pursued in this work. Advocating the idea of distinguishing between the internal state and process variables, he proposes to neglect the heat of plastic deformation (by postulating $\rho\psi^{(p)}(\theta,\kappa) = \kappa$). At the same time, by employing the constitutive relationship (4.4.34) in the consistency equation (4.4.7), he concludes that the evolution equation for the internal variable κ should be

$$\dot{\kappa} = (1 - \xi)\sigma_{ij}\dot{\varepsilon}_{ij}^{(p)} \tag{4.4.36}$$

which is different from the equation (4.4.19) as postulated earlier.

According to Raniecki and Sawczuk, the reversible heat of plastic deformation can usually be neglected in the applied thermoplasticity, resulting in the entropy and the specific heat for an elastoplastic material having the same form as in the case of an elastic solid [55]. Following this approach and at the same time accepting the evolution equation (4.4.19), one only needs to assume a constant value of the factor ξ in equations (4.4.34-35) to remain consistent with the adopted thermodynamic framework. The consistency condition (4.4.7) is then satisfied if

$$\rho \frac{\partial \psi}{\partial \kappa}^{(p)}\dot{\kappa} = \rho \frac{\partial e}{\partial \kappa}^{(p)}\dot{\kappa} = \rho(1 - \xi)\sigma_{ij}\dot{\varepsilon}_{ij}^{(p)} \tag{4.4.37}$$

where ξ = const for all values of θ and κ. Assuming a value of ξ close to unity one conforms to the basic feature of the Taylor-Farren-Quinney effect.

4.5 Temperature-Displacement Formulation of the Boundary Value Problem

4.5.1 Representation of the Constitutive Relationships in the Forms Convenient for the Boundary Value Problem Formulation

The objective of this section is to express the previously presented constitutive relationships in the forms suitable for easy inclusion into the formulation of the coupled temperature-displacement boundary value problem corresponding to the physical model described in CHAPTER 3. The aim is to extend the temperature-displacement formulation of the coupled linear thermoelasticity into the range of inelastic material behaviour, represented by the isotropic plasticity model of Section 4.4. Assuming the total strain components ε_{ij} and the excess temperature T (over the uniform temperature T_o at the reference state) as the basic independent variables, the initial thrust might be to attempt to express all the relevant constitutive relationships through these variables and their temporal derivatives $\dot{\varepsilon}_{ij}$ and $\dot{T}$. It is a known fact, however, that the adopted model of the Prandtl-Reuss material* precludes such a possibility and forces one to leave the stress components in certain expressions. Henceforth, the immediate task becomes to eliminate both the elastic and plastic strain tensors and their rates and to express the stress rate tensor

---

* The Prandtl-Reuss material is defined as the material for which the partial derivative of the yield function F with respect to the stress tensor σ_{ij} becomes $(\partial F/\partial \sigma_{ij}) = \sigma'_{ij}$.

as a linear combination of $\dot{\varepsilon}_{ij}$ and $\dot{T}$ [1,42]:

$$\dot{\sigma}_{ij} = C^{(ep)}_{ijkl}\dot{\varepsilon}_{kl} - \beta^{(ep,th)}_{ij}\dot{T} \tag{4.5.1}$$

where $C^{(ep)}_{ijkl}$ denotes a generalized elastoplastic stiffness tensor, and $\beta^{(ep,th)}_{ij}$ is a generalized thermal moduli tensor.

A suitable procedure of deriving the explicit expressions for $C^{(ep)}_{ijkl}$ and $\beta^{(ep)}_{ij}$ comprises the following steps:

(i) Decompose the total strain tensor rate as:

$$\dot{\varepsilon}_{ij} = \dot{\varepsilon}^{(e)}_{ij} + j\dot{\varepsilon}^{(p)}_{ij} \tag{4.5.2}$$

where the integer number j equals 0 for elastic loading and unloading, and 1 for plastic and neutral loading, i.e.

$$j = \begin{cases} 1 \text{ for } F = 0 \text{ and } \lambda \geq 0 \\ 0 \text{ for } F = 0 \text{ and } \lambda < 0 \\ 0 \text{ for } F < 0 \end{cases} \tag{4.5.3}$$

Here, F denotes the yield function given by equation (4.4.16), while λ is the proportionality factor in the normality condition (4.4.15). λ will be explicitly expressed later as a linear combination of $\dot{\varepsilon}_{ij}$ and $\dot{T}$.

(ii) Express the stress rate tensor as a linear combination of $\dot{\varepsilon}_{ij}$, $\dot{\varepsilon}^{(p)}_{ij}$ and $\dot{T}$.

To accomplish this, it is convenient to further develop the equation (4.4.25). Then it may be directly calculated that

$$C^{(e)}_{ijrs}\dot{\varepsilon}^{(th)}_{rs} - \dot{C}_{ijrs}(\varepsilon^{(e)}_{rs} - \varepsilon^{(th)}_{rs})$$

$$= C^{(e)}_{ijrs}(\alpha^{(e)}_{rs} + \alpha^{(th)}_{rs})\dot{T} \qquad (4.5.4)$$

where

$$\alpha^{(e)}_{rs} = \frac{\partial D^{(e)}_{ijrs}}{\partial T}\sigma_{ij} \qquad (4.5.5)$$

$$\alpha^{(th)}_{rs} = [\alpha + \frac{\partial \alpha}{\partial T}(T + T_o)]\delta_{rs} \qquad (4.5.6)$$

and $D^{(e)}_{ijrs}$ is the elastic compliance tensor*, which for the isotropic elasticity takes the form [64]:

$$D^{(e)}_{ijrs} = \frac{1+\nu}{2E}(\delta_{ir}\delta_{js} + \delta_{is}\delta_{jr}) - \frac{\nu}{E}\delta_{ij}\delta_{rs} \qquad (4.5.7)$$

Using (4.5.2-4) the equation (4.4.25) becomes:

$$\dot{\sigma}_{ij} = C^{(e)}_{ijrs}[\dot{\varepsilon}_{rs} - j\dot{\varepsilon}^{(p)}_{rs} - (\alpha^{(e)}_{rs} + \alpha^{(th)}_{rs})\dot{T}] \qquad (4.5.8)$$

(iii) Express the product $jC^{(e)}_{ijrs}\dot{\varepsilon}^{(p)}_{rs}$ in equation (4.5.8) as a linear combination of the rates $\dot{\varepsilon}_{ij}$ and $\dot{T}$.

To accomplish this, one has to express the proportionality factor λ as a function of the rates $\dot{\varepsilon}_{ij}$ and $\dot{T}$. Substituting equation (4.5.4) into (4.4.26), there is:

---

* The elastic stiffness and compliance tensors are related through the identity: $C^{(e)}_{ijkl}D^{(e)}_{klrs} = 1/2(\delta_{ir}\delta_{js} + \delta_{is}\delta_{jr})$.

$$\lambda = \frac{C^{(e)}_{ijrs}\sigma'_{ij}\dot{\varepsilon}_{rs} - [C^{(e)}_{ijrs}\sigma'_{ij}(\alpha^{(e)}_{rs} + \alpha^{(th)}_{rs}) + \frac{2}{3}\sigma_y \frac{\partial \sigma_y}{\partial T}]\dot{T}}{C^{(e)}_{ijrs}\sigma'_{ij}\sigma'_{rs} + \frac{4}{9}\sigma_y^3 \frac{\partial \sigma_y}{\partial \kappa}} \qquad (4.5.9)$$

Changing the dummy indices in (4.5.9), and premultiplying by $C^{(e)}_{ijrs}\sigma'_{rs}$, the normality condition (4.4.15) gives the desired result:

$$C^{(e)}_{ijrs}\dot{\varepsilon}^{(p)}_{rs} = \frac{C^{(e)}_{ijmn}\sigma'_{mn}\sigma'_{kl}C^{(e)}_{klrs}[\dot{\varepsilon}_{rs} - (\alpha^{(e)}_{rs} + \alpha^{(th)}_{rs})\dot{T}] - \frac{2}{3}\sigma_y \frac{\partial \sigma_y}{\partial T} C^{(e)}_{ijrs}\sigma'_{rs}\dot{T}}{C^{(e)}_{klmn}\sigma'_{kl}\sigma'_{mn} + \frac{4}{9}\sigma_y^3 \frac{\partial \sigma_y}{\partial \kappa}}$$

(4.5.10)

Equation (4.5.10) could be directly substituted into (4.5.8), but for the convenience of a more concise notation the following auxiliary quantities are introduced:

- <u>hardening modulus</u>:

$$h = \frac{4}{9}\sigma_y^3 \frac{\partial \sigma_y}{\partial \kappa} \qquad (4.5.11)$$

- auxiliary hardening modulus:

$$S = h + C^{(e)}_{klmn}\sigma'_{kl}\sigma'_{mn} \qquad (4.5.12)$$

- Yamada's plastic stiffness tensor [61]:

$$C^{(p)}_{ijrs} = \frac{C^{(e)}_{ijmn}\sigma'_{mn}\sigma'_{kl}C^{(e)}_{klrs}}{C^{(e)}_{klmn}\sigma'_{kl}\sigma'_{mn} + \frac{4}{9}\sigma_y^3\frac{\partial\sigma_y}{\partial\kappa}} = \frac{1}{S}C^{(e)}_{ijmn}\sigma'_{mn}\sigma'_{kl}C^{(e)}_{klrs} \qquad (4.5.13)$$

- coefficient of yield stress variation with temperature:

$$\alpha^{(p)}_{rs} = \frac{\frac{2}{3}\sigma_y\frac{\partial\sigma_y}{\partial T}\sigma'_{rs}}{C^{(e)}_{klmn}\sigma'_{kl}\sigma'_{mn} + \frac{4}{9}\sigma_y^3\frac{\partial\sigma_y}{\partial\kappa}} = \frac{1}{S}\frac{2}{3}\sigma_y\frac{\partial\sigma_y}{\partial T}\sigma'_{rs} \qquad (4.5.14)$$

Now, equation (4.5.10) may be written as:

$$C^{(e)}_{ijrs}\dot{\varepsilon}^{(p)}_{rs} = C^{(p)}_{ijrs}\dot{\varepsilon}_{rs} - [C^{(p)}_{ijrs}(\alpha^{(e)}_{rs} + \alpha^{(th)}_{rs}) + C^{(e)}_{ijrs}\alpha^{(p)}_{rs}]\dot{T} \qquad (4.5.15)$$

and (4.5.8) becomes:

$$\dot{\sigma}_{ij} = (C^{(e)}_{ijrs} - jC^{(p)}_{ijrs})\dot{\varepsilon}_{rs} - [(C^{(e)}_{ijrs} - jC^{(p)}_{ijrs})(\alpha^{(e)}_{rs} + \alpha^{(th)}_{rs}) - jC^{(e)}_{ijrs}\alpha^{(p)}_{rs}]\dot{T} \qquad (4.5.16)$$

Comparing equations (4.5.1) and (4.5.16), the elastoplastic stiffness tensor may be identified as:

$$C^{(ep)}_{ijrs} = C^{(e)}_{ijrs} - jC^{(p)}_{ijrs} \qquad (4.5.17)$$

and the generalized thermal moduli tensor as:

$$\beta^{(ep,th)}_{ij} = C^{(ep)}_{ijrs}(\alpha^{(e)}_{rs} + \alpha^{(th)}_{rs}) - jC^{(e)}_{ijrs}\alpha^{(p)}_{rs} \qquad (4.5.18)$$

It should be noted that both $C^{(ep)}_{ijrs}$ and $\beta^{(ep,th)}_{ij}$ in general depend on the instantenous temperature T, stress σ_{ij} and the work-hardening parameter κ. The latter enters into the coefficients $C^{(ep)}_{ijrs}$ and $\beta^{(ep,th)}_{ij}$ through the instantenous values of the yield stress σ_y and its derivatives $\frac{\partial \sigma_y}{\partial T}$ and $\frac{\partial \sigma_y}{\partial \kappa}$.

If one decides to use the strain-hardening parameter $\bar{\varepsilon}^{(p)}$ rather than κ, as it is preferred in most numerical formulations, the hardening modulus definition has to be altered. Then, defining

$$h = \frac{4}{9}\,\sigma_y^2\,\frac{\partial \sigma_y}{\partial \bar{\varepsilon}^{(p)}} \tag{4.5.19}$$

instead of (4.5.11), the second terms in the denominators of (4.4.26), (4.5.9) and (4.5.10) should undergo the appropriate changes. However, all derived relationships and other introduced expressions remain intact.

Using the auxiliary quantities introduced, a number of other useful relationships can be derived. Some of them, useful in the convenient expression of the coupling terms in the energy balance equation (4.4.32), are:

$$C^{(e)}_{ijrs}\dot{\varepsilon}^{(e)}_{rs} = C^{(ep)}_{ijrs}\dot{\varepsilon}_{rs} + j[C^{(p)}_{ijrs}(\alpha^{(e)}_{rs} + \alpha^{(p)}_{rs}) + C^{(e)}_{ijrs}\alpha^{(p)}_{rs}]\dot{T} \tag{4.5.20}$$

obtained by substituting (4.5.2) into (4.5.15) and using (4.5.17), and

$$\dot{\varepsilon}^{(p)}_{ij} = D^{(e)}_{ijkl}C^{(p)}_{klrs}\dot{\varepsilon}_{rs} - [D^{(e)}_{ijkl}C^{(p)}_{klrs}(\alpha^{(e)}_{rs} + \alpha^{(th)}_{rs}) + \alpha^{(p)}_{ij}]\dot{T} \tag{4.5.21}$$

obtained from (4.5.15), by changing the dummy indices and premultiplying both sides by $D^{(e)}_{ijkl}$.

Using equation (4.5.20) the thermoelastic coupling term (4.4.33) may be expressed as:

$$\theta \frac{\partial \sigma_{ij}}{\partial \theta} \dot{\varepsilon}^{(e)}_{ij} = - (T + T_0)(\alpha^{(e)}_{rs} + \alpha^{(th)}_{rs}) \{C^{(ep)}_{ijrs} \dot{\varepsilon}_{ij} + j[C^{(p)}_{ijrs}(\alpha^{(e)}_{ij} + \alpha^{(th)}_{ij}) + C^{(e)}_{ijrs}\alpha^{(p)}_{ij}]\dot{T}\} \qquad (4.5.22)$$

The thermoplastic coupling term in the energy balance equation (4.4.32) (assuming that heat of plastic deformation is neglected) becomes :

$$D = j\xi\sigma'_{ij}\dot{\varepsilon}^{(p)}_{ij} = j\xi\{D^{(e)}_{ijkl}C^{(p)}_{klrs}\sigma'_{ij}\dot{\varepsilon}_{rs} - [D^{(e)}_{ijkl}C^{(p)}_{klrs}(\alpha^{(e)}_{rs} + \alpha^{(th)}_{rs}) + \alpha^{(p)}_{ij}]\sigma'_{ij}\dot{T}\} \qquad (4.5.23)$$

The above expression could be further simplified, if the product $D^{(e)}_{ijkl}\sigma'_{ij}$ were expressed by the components of elastic strain tensor $\varepsilon^{(e)}_{kl}$. However, in the derivation procedure followed in this section an attempt is made to exclude the components of strains (but not their rates) from the formulation. Henceforth, the appearance of the quantity σ'_{ij} in equation (4.5.23) is preferred to $\varepsilon^{(e)}_{kl}$.

Thus far in the presentation of the constitutive relations in this section no use was made of the explicit expressions for the elastic stiffness and compliance tensors (4.4.12) and (4.5.7).

Neither was the assumption regarding incompressibility of plastic deformation directly utilized.

The latter assumption, which may be expressed as

$$\dot{\varepsilon}^{(p)}_{kk} = \varepsilon^{(p)}_{kk} = 0 \tag{4.5.24}$$

when considered in conjunction with the normality condition (4.4.15) leads to the conclusion that the trace of the stress deviator must remain zero during plastic straining.

$$\sigma'_{kk} = 0 \tag{4.5.25}$$

A number of simplifications arise in the previously presented relationships, if equations (4.4.12), (4.4.16), (4.5.7) and (4.5.25) are taken into consideration. For example, it may be directly verified that:

$$C^{(e)}_{ijrs}\sigma'_{ij} = \frac{E}{1+\nu}\sigma'_{rs} \tag{4.5.26}$$

$$C^{(e)}_{ijrs}\sigma'_{ij}\sigma'_{rs} = \frac{E}{1+\nu}\sigma'_{rs}\sigma'_{rs} = \left(\frac{2\sigma_y}{3}\right)^2 \frac{3E}{2(1+\nu)} \tag{4.5.27}$$

$$\alpha^{(e)}_{rs} = \frac{\partial}{\partial T}\left(\frac{1-2\nu}{E}\right)\frac{\sigma_{kk}}{3}\delta_{rs} + \frac{\partial}{\partial T}\left(\frac{1+\nu}{E}\right)\sigma'_{rs} \tag{4.5.28}$$

$$C^{(e)}_{ijrs}(\alpha^{(e)}_{rs} + \alpha^{(th)}_{rs}) = \frac{E}{1-2\nu}\left[\frac{\partial}{\partial T}\left(\frac{1-2\nu}{E}\right)\frac{\sigma_{kk}}{3} + \alpha + \frac{\partial \alpha}{\partial T}(T + T_0)\right]\delta_{ij} + \frac{E}{1+\nu}\frac{\partial}{\partial T}\left(\frac{1+\nu}{E}\right)\sigma'_{ij} \tag{4.5.29}$$

$$S = h + \left(\frac{2\sigma_y}{3}\right)^2 \frac{3E}{2(1+\nu)} = \left(\frac{2\sigma_y}{3}\right)^2 \left[\frac{\partial \sigma_y}{\partial \bar{\varepsilon}^{(p)}} + \frac{3E}{2(1+\nu)}\right] \tag{4.5.30}$$

$$C^{(p)}_{ijrs} = \frac{1}{S}\left(\frac{E}{1+\nu}\right)^2 \sigma'_{ij}\sigma'_{rs} = \left(\frac{3}{2\sigma_y}\right)^2 \frac{\left(\frac{E}{1+\nu}\right)^2}{\frac{\partial \sigma_y}{\partial \bar{\varepsilon}^{(p)}} + \frac{3E}{2(1+\nu)}} \sigma'_{ij}\sigma'_{rs} \tag{4.5.31}$$

$$\alpha^{(p)}_{rs} = \frac{3}{2\sigma_y} \frac{\frac{\partial \sigma_y}{\partial T}}{\frac{\partial \sigma_y}{\partial \bar{\varepsilon}^{(p)}} + \frac{3E}{2(1+\nu)}} \sigma'_{rs} \tag{4.5.32}$$

$$\lambda = \frac{1}{S}\left\{\frac{E}{1+\nu}\sigma'_{rs}\dot{\varepsilon}_{rs} - \frac{2\sigma_y}{3}\left[\frac{E}{1+\nu}\frac{\partial}{\partial T}\left(\frac{1+\nu}{E}\right)\sigma_y + \frac{\partial \sigma_y}{\partial T}\right]\dot{T}\right\} \tag{4.5.33}$$

$$C^{(p)}_{ijrs}(\alpha^{(e)}_{rs} + \alpha^{(th)}_{rs}) = \frac{3}{2} \frac{\left(\frac{E}{1+\nu}\right)^2}{\frac{\partial \sigma_y}{\partial \bar{\varepsilon}^{(p)}} + \frac{3E}{2(1+\nu)}} \frac{\partial}{\partial T}\left(\frac{1+\nu}{E}\right)\sigma'_{ij} \tag{4.5.34}$$

$$C^{(e)}_{ijrs}\alpha^{(p)}_{rs} = \frac{3}{2\sigma_y}\frac{E}{1+\nu} \frac{\frac{\partial \sigma_y}{\partial T}}{\frac{\partial \sigma_y}{\partial \bar{\varepsilon}^{(p)}} + \frac{3E}{2(1+\nu)}} \sigma'_{ij} \tag{4.5.35}$$

$$D^{(e)}_{ijkl} C^{(p)}_{klrs} = \left(\frac{3}{2\sigma_y}\right)^2 \frac{\frac{E}{1+\nu}}{\frac{\partial \sigma_y}{\partial \bar{\varepsilon}^{(p)}} + \frac{3E}{2(1+\nu)}} \sigma'_{ij} \sigma'_{rs} \tag{4.5.36}$$

$$D^{(e)}_{ijkl} C^{(p)}_{klrs} \sigma'_{ij} = \frac{\frac{3E}{2(1+\nu)}}{\frac{\partial \sigma_y}{\partial \bar{\varepsilon}^{(p)}} + \frac{3E}{2(1+\nu)}} \sigma'_{rs} \tag{4.5.37}$$

$$D^{(e)}_{ijkl} C^{(p)}_{klrs} (\alpha^{(e)}_{rs} + \alpha^{(th)}_{rs}) = \frac{\frac{3E}{2(1+\nu)}}{\frac{\partial \sigma_y}{\partial \bar{\varepsilon}^{(p)}} + \frac{3E}{2(1+\nu)}} \frac{\partial}{\partial T}\left(\frac{1+\nu}{E}\right) \sigma'_{ij} \tag{4.5.38}$$

$$D^{(e)}_{ijkl} C^{(p)}_{klrs} (\alpha^{(e)}_{rs} + \alpha^{(th)}_{rs}) \sigma'_{ij} = \left(\frac{2\sigma_y}{3}\right)^2 \frac{\frac{3E}{2(1+\nu)}}{\frac{\partial \sigma_y}{\partial \bar{\varepsilon}^{(p)}} + \frac{3E}{2(1+\nu)}} \frac{\partial}{\partial T}\left[\frac{2(1+\nu)}{3E}\right] \tag{4.5.39}$$

$$\alpha^{(p)}_{ij} \sigma'_{ij} = \frac{\sigma_y \frac{\partial \sigma_y}{\partial T}}{\frac{\partial \sigma_y}{\partial \bar{\varepsilon}^{(p)}} + \frac{3E}{2(1+\nu)}} \tag{4.5.40}$$

The above stated equations result in much simpler expressions for the stress rate tensor $\dot{\sigma}_{ij}$, plastic strain rate tensor $\dot{\varepsilon}^{(p)}_{ij}$, proportionality factor λ and both the thermoelastic and thermoplastic terms, than those derived before. Table 2 contains the summary of the respective expressions in the simplified forms, obtained with the help

of equations (4.5.26-40). These are the forms of the constitutive relationships which are required in the temperature-displacement formulation of the boundary value problem to be used in the next section.

A brief examination of the content of Table 2 confirms the earlier expressed assertions that the constitutive theory of isotropic thermoplasticity adopted in this thesis requires the following material property data obtained from isothermal tests:

(i) uniaxial yield stress dependence on the accumulated plastic strain (i.e. equation (4.4.18)) which can be derived from the stress-strain data obtained in a series of tensile tests at different temperatures using virgin material specimens,

(ii) variations of Young's modulus and Poisson's ratio (or any other two elastic constants for isotropic material) with temperature,

(iii) variation of the coefficient of thermal expansion with temperature,

(iv) variations of the specific heat at constant elastic strain and thermal conductivity with temperature.

The yield stress dependence on the accumulated plastic strain is assumed to be valid irrespective of the loading path followed in

the process of plastic straining. The coefficients of yield stress variations with plastic strain and temperature:

$$H' = \frac{\partial \sigma_y}{\partial \bar{\varepsilon}^{(p)}} \tag{4.5.41}$$

and

$$H'' = \frac{\partial \sigma_y}{\partial T} \tag{4.5.42}^{*}$$

are assumed to be possible to obtain from (4.4.18) by direct differentiation, and in addition, H' is assumed to be a monotonically increasing function of $\bar{\varepsilon}^{(p)}$**. The details of calculating H' and H" for the particular form of the stress-strain relationship will be discussed later in conjunction with the numerical formulation.

Finally, as one may notice from Table 2, the shear (Kirchhoff's) modulus G and the compressibility (bulk) modulus K seem to be more convenient to use than Young's modulus E and Poisson's ratio ν. However, if only Young's modulus but not Poisson's ratio exhibits temperature dependence, then there is:

$$\frac{1}{G}\frac{\partial G}{\partial T} = \frac{1}{K}\frac{\partial K}{\partial T} = \frac{1}{E}\frac{\partial E}{\partial T} \tag{4.5.43}$$

and the expressions in Table 2 render further simplifications.

---

* The symbol H" is introduced here after Mondkar and Powell [42].

** H' > 0 for all values of $\bar{\varepsilon}^{(p)}$ excludes a possibility of strain softening. However, for most materials with well defined isothermal hardening behaviour there is H" < 0, which accounts for a thermal softening.

4.5.2 Differential Formulation

The differential (local, strong) formulation of the boundary value problem for the thermoelastoplastic material makes use of the local forms of the momentum and internal energy balances, constitutive relationships and appropriate boundary and initial conditions. The temperature-displacement approach designates the excess temperature and the components of the displacement vector to be the primary dependent variables. It tends to exclude other variables from the formulation. Some of those variables, like the density and certain stress tensor components have been eliminated previously (see Section 4.2), and are given by the equations (4.2.11) and (4.2.14). Some others, like the heat flux q_i and the components of the total strain tensor ε_{ij}, are easy to eliminate through the use of the constitutive equation (4.4.14) and the kinematic relations (4.1.1-2), respectively. In contrast to the purely thermoelastic case, however, the remaining components of the stress tensor, as well as the internal state variable $\bar{\varepsilon}^{(p)}$, were impossible to eliminate from the rate forms of the constitutive relationships (stated in Table 2) and must remain a part of the present formulation. Therefore, the corresponding rate equations for $\dot{\sigma}_{ij}$ and $\dot{\bar{\varepsilon}}^{(p)}$ must be considered together with the momentum and energy balance equations.

The local equilibrium equation (4.2.12), representing the local balance of momentum, may be written in the rate form as:

$$\dot{\sigma}_{ij,j} + \rho\dot{b}_i = 0 \qquad (4.5.44)$$

The rate form is preferred, because it allows easy elimination of the stress rate tensor. Using equations (4.5.1) and (4.1.2), and taking advantage of the symmetry of the tensor $C^{(ep)}_{ijkl}$, equation (4.5.44) yields:

$$(C^{(ep)}_{ijkl}\dot{u}_{k,l})_{,j} - (\beta^{(ep,th)}_{ij}\dot{T})_{,j} + \rho\dot{b}_i = 0 \qquad (4.5.45)$$

The local balance of energy (4.4.32) may be written in the following form by neglecting the heat of plastic deformation and using the rate expressions for the heat of elastic deformation and internal dissipation as given in Table 2:

$$(\rho c_\varepsilon + \tilde{\gamma})\dot{T} = - B_{ij}\dot{\varepsilon}_{ij} - q_{i,i} + \rho r \qquad (4.5.46)$$

where

$$\tilde{\gamma} = j\sigma_y \frac{\frac{\sigma_y}{G}\frac{\partial G}{\partial T}}{H' + 3G}\left[\xi - \frac{1}{G}\frac{\partial G}{\partial T}(T + T_0)\right] \qquad (4.5.47)$$

$$B_{ij} = \beta^{(e,th)}_{ij}(T + T_0) - j\frac{3G}{H' + 3G}\left[\xi - \frac{1}{G}\frac{\partial G}{\partial T}(T + T_0)\right]\sigma'_{ij} \qquad (4.5.48)$$

The expressions for $C^{(ep)}_{ijkl}$, $\beta^{(e,th)}_{ij}$ are stated in Table 2, and the coefficients H' and H" are defined by equations (4.5.41) and (4.5.42), respectively.

Expressing the strain rate tensor through the displacement rates, using the constitutive equation (4.4.14), and utilizing the

symmetry of B_{ij}, yields

$$(\rho c_\varepsilon + \tilde{\gamma})\dot{T} + B_{ij}\dot{u}_{i,j} = (kT_{,i})_{,i} + \rho r \qquad (4.5.49)$$

Equations (4.5.45) and (4.5.49) represent the system of four coupled partial differential equations for the displacement vector components u_i and the excess temperature T. They are assumed to be valid within a closed region R of the space which is said to be occupied by the solid medium under consideration and includes the region's boundary ∂R.

The boundary conditions in coupled thermomechanics are usually stated separately for the mechanical and thermal variables. Following this traditional approach, four types of boundary conditions will be considered:

(i) Displacement boundary condition:

$$\bar{a}_{ij}\dot{u}_j + \bar{a}_i = 0 \qquad \text{on } \partial R_u \qquad (4.5.50)$$

(ii) Pressure boundary condition:

$$\dot{\sigma}_{ij}n_j = -\dot{\bar{p}}n_i \qquad \text{on } \partial R_\sigma \qquad (4.5.51)$$

(iii) Temperature boundary condition:

$$T = \bar{T} \qquad \text{on } \partial R_T \qquad (4.5.52)$$

(iv) Heat flux boundary condition:

$$q_i n_i = \bar{q} + \bar{h}(T - \bar{T}_\infty) \qquad \text{on } \partial R_q \qquad (4.5.53)$$

where the portions $_{\smile}R_u$ and $_{\smile}R_\sigma$, and $_{\smile}R_T$ and $_{\smile}R_q$, of the boundary are mutually exclusive, and their corresponding logical sums represent the entire boundary, i.e.

$$\partial R_u \cap \partial R_\sigma = \emptyset \qquad \partial R_u \cup \partial R_\sigma = \partial R$$
$$\partial R_T \cap \partial R_q = \emptyset \qquad \partial R_T \cup \partial R_q = \partial R \tag{4.5.54}$$

Furthermore, the following barred quantities denote fields prescribed on the corresponding portions of the boundary:

$\bar{a}_{ij}, \bar{c}_i$ - prescribed constants

$\bar{p}$ - prescribed pressure rate

$\bar{T}$ - prescribed temperature

$\bar{q}$ - prescribed heat influx

$\bar{h}$ - prescribed heat transfer coefficient

$\bar{T}_\infty$ - prescribed bulk fluid temperature

The coefficients $\bar{a}_{ij}$ and $\bar{c}_i$ allow consideration of the so called skew displacement boundary conditions [3,4]. The quantities $\bar{q}_i$, $\bar{h}$ and $\bar{T}_\infty$ may be, in general, prescribed functions of local temperature. Zero initial boundary conditions at the instant $t = 0$ will be considered for the variables u_i, T, σ_{ij} and $\bar{\varepsilon}^{(p)}$. They reflect the earlier stated assumptions with regard to the absence of preloading, uniform initial temperature distribution $\theta = T_0$, and the virgin state of material.

As mentioned at the beginning of this section, the field equations (4.5.45) and (4.5.49) must be complemented by the appropriate equations for the undetermined components of σ_{ij}, and for $\bar{\varepsilon}^{(p)}$. These are:

$$\dot{\sigma}_{ij} = C^{(ep)}_{ijkl}\dot{\varepsilon}_{kl} - \beta^{(ep,th)}_{ij}\dot{T} \tag{4.5.1}$$

and

$$\dot{\bar{\varepsilon}}^{(p)} = \frac{2}{3}\lambda\sigma_y = \frac{3G}{\sigma_y(H' + 3G)}\sigma'_{ij}\dot{u}_{i,j} + \frac{\frac{\sigma_y}{G}\frac{\partial G}{\partial T} - H''}{H' + 3G}\dot{T} \tag{4.5.55}$$

The latter equation follows directly from the definition of $\bar{\varepsilon}^{(p)}$ given by (4.4.20).

The final point requiring clarification is concerned with the purely mathematical aspect of the posed problem. The mathematical formulation presented in this section did not address the difficulties associated with the existence of the inequality constraints (in the form of the normality condition (4.4.15)). Since they are known to be tractable in numerical formulations, the discussion of how to handle them is postponed to a later section.

4.5.3 Integral Formulation

The local formulation of the boundary value problem presented in the previous section could be considered a basis for an approximate formulation, obtained as a result of a certain discretization process. Such procedures are often used when finite difference formulations are desirable, but may also lead to finite element models [8]. The latter

are, however, more conveniently derived through other approaches whose common feature is the use of some kind of integral statement as a starting point in the search for an approximate solution. Many well known approaches, including variational formulations and formulations based on the principle of virtual work, may be stated independently from the latter approximate solution procedures in the form of a system of integral equations equivalent in some sense to the governing differential equations and boundary conditions of the local formulation. More often, however, the derivation of an integral formulation is directly inspired by the intended approximate formulation. Consequently, it is presented in such a way as to show how it naturally lends itself to the possibility of problem discretization.

The integral formulation of the coupled thermoelastoplastic problem formulated locally in the previous section will be considered here in the context of the future finite element approximation. The approach employed is known under many names, such as weighted residual method, conjugate approximation method, and projective method. The basic motivation is to distribute the errors resulting from the approximate only fulfillment of the governing equations and boundary conditions, over the volume of the region R and the surface area of its boundary ∂R. In the formulation pursued here, and termed the weak formulation in the classification of weighted residual method by Zienkiewicz [63] and others, the integral statement corresponding to a particular differential equation and its associated boundary conditions, takes the form:

$$\int_V \epsilon w dV = \int_{S_2} \epsilon_2 w dS \qquad (4.5.56)$$

Here, ϵ is the error function in the domain V, being a result of non-exact satisfaction of the governing differential equation, ϵ_2 is the error function on the boundary S_2, being a result of non-exact satisfaction of the natural boundary conditions*, and w is a weighting (or test) function. The error ϵ_1, resulting from the non-exact satisfaction of the essential boundary conditions* on the remaining part S_1 of the boundary S, is not taken into consideration in the statement (4.5.56). The present approach requires that essential boundary conditions be invoked separately, preferably on the discrete model directly.

In the local formulation presented in Section 4.5.2, equation (4.5.50) represents essential boundary condition, and equation (4.5.51) natural boundary condition, associated with the equation (4.5.45). Similarly, equation (4.5.52) represents essential boundary condition and equation (4.5.53) - natural boundary condition associated with the coupled heat conduction equation (4.5.49).

Denoting the approximations of the displacement and excess temperature fields by $\hat{u}_i$ and $\hat{T}$, respectively, the error functions corresponding to equations (4.5.45) and (4.5.49) and to the boundary

---

* The procedure of identification of natural and essential boundary conditions is the following:
If the differential operator in the governing differential equation contains at most m-th order derivatives, then the order of the derivatives in the essential boundary conditions is at most m-1. The boundary conditions involving higher order derivatives represent natural boundary conditions [3].

conditions (4.5.51) and (4.5.53) are:

$$\varepsilon_u = (C^{(ep)}_{ijkl}\dot{\hat{u}}_{k,l} - \beta^{(ep,th)}_{ij}\dot{\hat{T}})_{,j} + \rho\dot{b}_i \tag{4.5.57}$$

$$\varepsilon_T = (\rho c_\varepsilon + \tilde{\gamma})\dot{\hat{T}} + B_{ij}\dot{\hat{u}}_{i,j} - (k\hat{T}_{,i})_{,i} - \rho r \tag{4.5.58}$$

$$\varepsilon_\sigma = [C^{(ep)}_{ijkl}\dot{\hat{u}}_{k,l} - \beta^{(ep,th)}_{ij}\dot{\hat{T}} + \dot{\bar{p}}\delta_{ij}]n_j \tag{4.5.59}$$

$$\varepsilon_q = -(k\hat{T}_{,i} + \bar{q}_i)n_i - \bar{h}(\hat{T} - \bar{T}_\infty) \tag{4.5.60}$$

Introducing the test functions u^*_i and T^*, the weak formulation of the coupled thermoelastoplastic problem becomes:

$$\int_V \varepsilon_u u^*_i dV = \int_{S_\sigma} \varepsilon_\sigma u^*_i dS \tag{4.5.61}$$

$$\int_V \varepsilon_T T^* dV = \int_{S_q} \varepsilon_q T^* dS \tag{4.5.62}$$

where V is the volume integration domain corresponding to the region R, and S_σ and S_q are the surface integration domains corresponding to the ∂R_σ and ∂R_q portions of the boundary, respectively.

Application of the Gauss-Green-Ostrogradski's (divergence) theorem yields:

$$\int_V (C^{(ep)}_{ijkl}\hat{u}_{k,l} - \beta^{(ep,th)}_{ij}\hat{T})_{,j} u^*_i dV$$

$$= \int_{S_\sigma} (C^{(ep)}_{ijkl}\hat{u}_{k,l} - \beta^{(ep,th)}_{ij}\hat{T})u^*_i n_j dS - \int_V (C^{(ep)}_{ijkl}\hat{u}_{k,l} - \beta^{(ep,th)}_{ij}\hat{T})u^*_{i,j} dV \tag{4.5.63}$$

and

$$\int_V (k\hat{T}_{,i})_{,i} T^* dV = \int_{S_q} k\hat{T}_{,i} T^* n_i dS - \int_V k\hat{T}_{,i} T^*_{,i} dV \qquad (4.5.64)$$

Substitution of (4.5.59) and (4.5.60) into (4.5.57) and (4.5.58), respectively, leads to the following transformed form of the weak formulation:

$$\int_V C^{(ep)}_{ijkl} \dot{\hat{u}}_{k,l} u^*_{i,j} dV - \int_V \beta^{(ep,th)}_{ij} \dot{\hat{T}} u^*_{i,j} dV = \int_V \rho \dot{b}_i u^*_i dV - \int_{S_\sigma} \dot{\bar{p}} n_i u^*_i dS \qquad (4.5.65)$$

$$\int_V (\rho c_\varepsilon + \tilde{\gamma}) \dot{\hat{T}} T^* dV + \int_V k\hat{T}_{,i} T^*_{,i} dV + \int_V B_{ij} \dot{\hat{u}}_{i,j} T^* dV =$$

$$= - \int_{S_q} [\bar{q}_i n_i + \bar{h}(\hat{T} - \bar{T}_\infty)] T^* dS + \int_V \rho r T^* dV \qquad (4.5.66)$$

The transformed form of the weak formulation is preferrable to the original form given by equations (4.5.57-62) because it imposes reduced smoothness requirement on the trial functions $\hat{u}_i$ and $\hat{T}$. At the same time a higher degree of smoothness is required from the test functions u^*_i and T^*. The important point, however, is the following: If equations (4.5.65-66) hold for sufficiently many choices of the test functions u^*_i and T^*, which satisfy the homogenous essential boundary conditions (i.e. $u^*_i = 0$ on ∂R_u and $T^* = 0$ on ∂R_T), then they are equivalent to equations (4.5.45) and (4.5.49) with the corresponding boundary conditions (4.5.51) and (4.5.53), for sufficiently smooth solutions $\hat{u}_i$ and $\hat{T}$.

Therefore, spatial discretization of the weak equations (4.5.65-66) may be achieved by approximating the region R by $\tilde{R}$, and then approximating the fields u_i and T defined on R through the functions $\tilde{u}_i$ and $\tilde{T}$ defined on $\tilde{R}$. Specific choices for $\tilde{R}$, and $\tilde{u}_i$ and $\tilde{T}$ may lead to finite element approximations.

When the test functions are selected identical to the trial functions, i.e. when $u_i^* = \tilde{u}_i$ and $T^* = \tilde{T}$, the Galerkin approach results [4,63].

As the final point in the discussion of global formulation, it is necessary to recall that equations (4.5.61) and (4.5.62) do not fully describe the considered problem. They must be supplemented by the constitutive equations (4.5.1) and (4.5.52), the inequality representing the criterion of transition between loading and unloading states, and the appropriate initial and essential boundary conditions.

CHAPTER 5

FINITE ELEMENT APPROXIMATION AND SOLUTION

5.1 Finite Element Approximation

The finite element method is sometimes viewed as a general procedure of transforming "continuous" mathematical models into "discretized" ones. The first step of the discretization process consists of partitioning the domain of interest into a number of non-overlapping subregions, called finite elements. Associated with this division is a set of nodal points located on element boundaries and/or within their interiors. The second step involves approximating variations of the continuous physical quantities over elemental subregions through (usually linear) functions of their nodal values. These nodal values become the basic parameters of the discretized problem. The application of the outlined procedure to the previously formulated mathematical model of coupled thermomechanical behaviour is subject of the following sections. Discretization of the spatial domain leads to the discrete model in the form of a set of coupled ordinary differential equations, and time becomes the only independent variable.

5.1.1 Isoparametric Elements

Among the many different types of finite elements proposed until now the concept of isoparametric element, originated by Taig and

further developed by Irons, Zienkiewicz, and their coworkers [63], offers a very convenient way of construction and numerical implementation of multinode high order elements, for which curved boundaries are allowed. Regions with curved and/or irregular boundaries may be then accurately represented in the discrete model. This is accomplished through individual parametrization of each element domain, while employing the same set of functions which are later used for approximating problem variables.

The parametrization of elemental domain may be achieved by assigning a local nondimensionalized (natural) coordinate system * to it, with the origin at the centroid of the element. If the reference (global) coordinates x_i are assumed to be polynomial functions of the isoparametric (local) coordinates ξ_i

$$x_i = a_i + a_{ij}\xi_j + a_{ijk}\xi_j\xi_k + a_{ijkl}\xi_j\xi_k\xi_l + \cdots \qquad (5.1.1)$$

where $a_{ijk} = 0$ for $j = k$, $a_{ijkl} = 0$ for $j = k = l = 0$, and additional constraints are imposed on the coefficients a_{ijk} and a_{ijkl} in order to keep their number equal to the number of nodal coordinates, the assignment of the local coordinates of nodes fully defines the isoparametric transformation (5.1.1).

---

* In the natural coordinate system any point whose reference coordinates are x_i is represented by the numbers ξ_i, such that $|\xi_i| \leq 1$.

This well documented procedure results in the representation of the isoparametric transformation (5.1.1) in the form:

$$x_i = N_I^{(e)}(\xi_j)x_{Ii} \tag{5.1.2}$$

where x_{Ii} denote the global coordinates of the I-th node (I = 1,...,N) of the e-th element, and $N_I^{(e)}$ are the interpolation (shape) functions for this element, which are defined in the elemental natural coordinate system.

If one restricts one's considerations to two-dimensional quadrilateral elements, then the isoparametric transformation (5.1.2) may be viewed as a mapping of a unit square $-1 \leq \xi_1 \leq 1$, $-1 \leq \xi_2 \leq 1$ into the region of the Euclidean space occupied by the element which appears irregular in the x_i-coordinates. The shape functions derived for a four-nodes, straight-sides isoparametric quadrilateral element are [3,4]:

$$N_I^{(e)}(\xi_1,\xi_2) = \frac{1}{4}(1 + \xi_{I1}\xi_1)(1 + \xi_{I2}\xi_2) \tag{5.1.3}$$

where ξ_{Ii} (i = 1,2) are the local coordinates or the I-th node. If the local node numbering is done according to FIGURE 3, the local node coordinates are $\xi_{11} = \xi_{12} = \xi_{22} = \xi_{41} = 1$ and $\xi_{21} = \xi_{31} = \xi_{32} = \xi_{42} = -1$, and the shape functions (5.1.3) become:

$$N_1^{(e)}(\xi_1,\xi_2) = \frac{1}{4}(1 + \xi_1)(1 + \xi_2)$$

$$N_2^{(e)}(\xi_1,\xi_2) = \frac{1}{4}(1 - \xi_1)(1 + \xi_2)$$

$$N_3^{(e)}(\xi_1,\xi_2) = \frac{1}{4}(1 - \xi_1)(1 - \xi_2)$$

$$N_4^{(e)}(\xi_1,\xi_2) = \frac{1}{4}(1 + \xi_1)(1 - \xi_2) \qquad (5.1.4)$$

The element described above furnishes linear variation of a field variable along each of the constant local coordinate lines. A quadratic variation may be accomplished through addition of midside and/or interior nodes. The quadratic element belonging to the "Serendipity" family [63] has eight nodes located as shown in FIGURE 4. The shape functions derived for its corner nodes have the form:

$$N_I^{(e)}(\xi_1,\xi_2) = \frac{1}{4}(1 + \xi_{I1}\xi_1)(1 + \xi_{I2}\xi_2)(\xi_{I1}\xi_1 + \xi_{I2}\xi_2 - 1)$$

$$I = 1,2,3,4 \qquad (5.1.5)$$

while those derived for the midside-nodes are:

$$N_I^{(e)}(\xi_1,\xi_2) = \frac{1}{2}(1 + \xi_{I1}\xi_1)(1 + \xi_{I2}\xi_2)(1 - \xi_{I1}^2\xi_2^2 - \xi_{I2}^2\xi_1^2)$$

$$I = 5,6,7,8 \qquad (5.1.6)$$

For the local node numbering as indicated in Figure 1, there is

$$\xi_{11} = \xi_{12} = \xi_{22} = \xi_{41} = \xi_{52} = \xi_{81} = 1,$$

$$\xi_{21} = \xi_{31} = \xi_{32} = \xi_{42} = \xi_{61} = \xi_{72} = -1 \text{ and}$$

$$\xi_{51} = \xi_{62} = \xi_{71} = \xi_{82} = 0,$$

and the shape functions (5.1.5-6) become:

$$N_1^{(e)}(\xi_1,\xi_2) = \frac{1}{4}(1 + \xi_1)(1 + \xi_2)(\xi_1 + \xi_2 - 1)$$

$$N_2^{(e)}(\xi_1,\xi_2) = \frac{1}{4}(1 - \xi_1)(1 + \xi_2)(- \xi_1 + \xi_2 - 1)$$

$$N_3^{(e)}(\xi_1,\xi_2) = \frac{1}{4}(1 - \xi_1)(1 - \xi_2)(- \xi_1 - \xi_2 - 1)$$

$$N_4^{(e)}(\xi_1,\xi_2) = \frac{1}{4}(1 + \xi_1)(1 - \xi_2)(\xi_1 - \xi_2 - 1)$$

$$N_5^{(e)}(\xi_1,\xi_2) = \frac{1}{2}(1 + \xi_2)(1 - \xi_1^2) \qquad (5.1.7)$$

$$N_6^{(e)}(\xi_1,\xi_2) = \frac{1}{2}(1 - \xi_1)(1 - \xi_2^2)$$

$$N_7^{(e)}(\xi_1,\xi_2) = \frac{1}{2}(1 - \xi_2)(1 - \xi_1^2)$$

$$N_8^{(e)}(\xi_1,\xi_2) = \frac{1}{2}(1 + \xi_1)(1 - \xi_2^2) \qquad (5.1.7)$$

The quadratic element of the Lagrangian family of the isoparametric two-dimensional elements includes an additional node located at the origin of the local coordinate system [63]. The shape function corresponding to the ninth node has the form:

$$N_9^{(e)}(\xi_1,\xi_2) = (1 - \xi_1^2)(1 - \xi_2^2) \qquad (5.1.8)$$

and the shape functions corresponding to other nodes have to be modified to yield:

$$N_I^{(e)}(\xi_1,\xi_2) = \frac{1}{4}(1 + \xi_{I1}\xi_1)(1 + \xi_{I2}\xi_2)(\xi_{I1}\xi_1 + \xi_{I2}\xi_2 - 1) + \frac{1}{4}N_9(\xi_1,\xi_2)$$

$$= \frac{1}{4}(1 + \xi_{I1}\xi_1)(1 + \xi_{I2}\xi_2)\xi_{I1}\xi_1\xi_{I2}\xi_2 \qquad I = 1,2,3,4$$

$$N_I^{(e)}(\xi_1,\xi_2) = \frac{1}{2}(1 + \xi_{I1}\xi_1)(1 + \xi_{I2}\xi_2)(1 - \xi_{I1}\xi_1^2 - \xi_{I2}\xi_2^2) - \frac{1}{2}N_9(\xi_1,\xi_2)$$

$$= \frac{1}{2}(1 + \xi_{I1}\xi_1)(1 + \xi_{I2}\xi_2)(1 - \xi_{I1}\xi_1^2 - \xi_{I2}\xi_2^2)(\xi_{I1}\xi_1 + \xi_{I2}\xi_2)$$

$$I = 5,6,7,8$$

(5.1.9-10)

Quadrilateral isoparametric elements may be degenerated to triangular elements by coalescing the nodes of one edge. In such a case the shape functions require further modifications which are minor for the linear type elements and more extensive for the quadratic ones. The details of these modifications are given by Bathe [3].

The three types of isoparametric quadrilateral elements described above, as well as the straight edge triangular element obtained by collapsing any two adjacent nodes of the linear quadrilateral element, were incorporated in the finite element program TEPAP which was written in the course of this thesis research. The suitability of the isoparametric element concept to the formulation of the spatially discretized model of thermoelastoplastic solid will be further explored in the following section devoted to the discrete model equations' set-up.

5.1.2 Derivation of Discrete Model Equations

According to the previously outlined procedure for isoparametric finite elements, the field variables in every element can be approximated with the use of the same shape functions which

were employed for parametrization of the spatial domain. The formulation of the thermoelastoplastic problem, which was presented in Section 4.5, consisted of two integral and two differential equations, (4.5.65-66), (4.5.1) and (4.5.55). It involved four fields: displacement u_i, excess temperature T, stress σ_{ij} and equivalent plastic strain $\bar{\varepsilon}^{(p)}$. This formulation indicates the possibility of enforcing the assumed trial solutions u_i and T to obey the integral equations (4.5.65-66) while using the remaining equations (4.5.1) and (4.5.55) for determining the required values of σ_{ij} and $\bar{\varepsilon}^{(p)}$. Such an approach is motivated by the displacement formulation of elastic and thermoelastic problems when the stresses do not appear in the integral statements (4.5.65) and (4.5.66) at all. Then, it may be shown that there are certain interior points within isoparametric elements where the stresses computed from known displacements and temperatures (according to the Duhamel-Neumann constitutive equation analogical to (4.5.1)) exhibit the highest accuracy [3,4,63]. Furthermore, these interior locations within isoparametric elements coincide with the "sampling points" required in the Gauss-Legendre procedure of numerical evaluation of integrals which may be used when solving for displacements and temperatures.

By adopting the above described approach to elastoplastic problems one fixes the locations of points where stresses and plastic strains are determined [4,53,63]. In the case of the thermoelastoplastic problem this leads to the set of discrete variables consisting of the nodal displacement components and nodal excess temperatures complemented by the values of stresses and equivalent plastic strains

at the Gauss-Legendre sampling points*. Equations (4.5.51) and (4.5.52) are then enforced only at these points, and the yield condition is also checked there only.

Following the standard practice [3,4,63], the discrete model equations will be derived for a single element. The governing equations for the entire mesh may then be easily obtained by identifying nodal couplings with other elements nodes. This assembly procedure, often referred to as the direct stiffness method, could be introduced more formally through the use of the Boolean connectivity matrices [57].

The trial solutions for the displacement $\hat{u}_i$ and temperature $\hat{T}$ in the e-th element are assumed in the forms:

$$u_i(\xi_1,\xi_2) = N_I^{(e)}(\xi_1,\xi_2)u_{iI}^{(e)} \tag{5.1.11}$$

$$T(\xi_1,\xi_2) = N_I^{(e)}(\xi_1,\xi_2)T_I^{(e)} \tag{5.1.12}$$

Inserting equations (5.1.11) and (5.1.12) into the Galerkin form of the equations (4.5.65) and (4.5.66), written for a single element, yields:

$$\int_{V^{(e)}} C_{ijkl}^{(ep)} \frac{\partial N_K^{(e)}}{\partial x_l} \dot{u}_{kK}^{(e)} \frac{\partial N_I^{(e)}}{\partial x_j} u_{iI}^{(e)} dV^{(e)} - \int_{V^{(e)}} \beta_{ij}^{(ep,th)} N_J^{(e)} \dot{T}_J \frac{\partial N_I^{(p)}}{\partial x_j} u_{iI}^{(e)} dV^{(e)}$$

$$= \int_{V^{(e)}} \rho \dot{b}_i N_I^{(e)} u_{iI}^{(e)} dV^{(e)} - \int_{S^{(e)}} \dot{\bar{p}} n_i N_I^{(e)} u_{iI}^{(e)} dS^{(e)} \tag{5.1.13}$$

---

* The Gauss-Legendre sampling points do not usually coincide with the element nodes.

$$\int_{V^{(e)}} (\rho c_\varepsilon + \tilde{\gamma}) N_J^{(e)} \dot{T}_J N_I^{(e)} T_I^{(e)} dV^{(e)} + \int_{V^{(e)}} k \frac{\partial N_I^{(e)}}{\partial x_i} T_I^{(e)} \frac{\partial N_J^{(e)}}{\partial x_i} T_J^{(e)} dV^{(e)}$$

$$+ \int_{V^{(e)}} B_{ij} \frac{\partial N_J^{(e)}}{\partial x_j} \dot{u}_{iJ}^{(e)} N_I^{(e)} T_I^{(e)} dV^{(e)} + \int_{S^{(e)}} \bar{h} N_I^{(e)} T_I^{(e)} N_J^{(e)} T_J^{(e)} dS^{(e)}$$

$$= \int_{S^{(e)}} (\bar{h}\bar{T}_\infty - \bar{q}) N_I^{(e)} T_I^{(e)} dS^{(e)} + \int_{V^{(e)}} \rho r N_I^{(e)} T_I^{(e)} dV^{(e)} \qquad (5.1.14)$$

The volume integrations in the above equations extend over the elemental volume $V^{(e)}$, while the surface integrations are performed over the external surface $S^{(e)}$ of the element. The elemental matrix quantities may be defined as folows:

- <u>tangent stiffness matrix</u>:

$$K_{ijIJ}^{(e)} = \int_{V^{(e)}} C_{ijkl}^{(ep)} \frac{\partial N_I^{(e)}}{\partial x_k} \frac{\partial N_J^{(e)}}{\partial x_l} dV^{(e)} \qquad (5.1.15)$$

- <u>thermal expansivity matrix</u>:

$$E_{iIJ}^{(e)} = - \int_{V^{(e)}} \beta_{ij}^{(ep,th)} \frac{\partial N_I^{(e)}}{\partial x_j} N_J^{(e)} dV^{(e)} \qquad (5.1.16)$$

- <u>rate of external forces vector</u>:

$$F_{iI}^{(e)} = \int_{V^{(e)}} \rho \dot{b}_i N_I^{(e)} dV^{(e)} - \int_{S^{(e)}} \dot{\bar{p}} n_i N_I^{(e)} dS^{(e)} \qquad (5.1.17)$$

- generalized thermal capacitance matrix:

$$C_{IJ}^{(e)} = \int_{V^{(e)}} (\rho c_\varepsilon + \tilde{\gamma}) N_I^{(e)} N_J^{(e)} dV^{(e)} \tag{5.1.18}$$

- thermal conductance matrix:

$$S_{IJ}^{(e)} = \int_{V^{(e)}} k \frac{\partial N_I^{(e)}}{\partial x_i} \frac{\partial N_J^{(e)}}{\partial x_i} dV^{(e)} + \int_{S^{(e)}} \bar{h} N_I^{(e)} N_J^{(e)} dS^{(e)} \tag{5.1.19}$$

- thermomechanical coupling matrix:

$$R_{iIJ}^{(e)} = \int_{V^{(e)}} B_{ij} \frac{\partial N_J^{(e)}}{\partial x_j} N_I^{(e)} dV^{(e)} \tag{5.1.20}$$

- rate of heat generation vector:

$$Q_I^{(e)} = \int_{V^{(e)}} \rho r N_I^{(e)} dV^{(e)} + \int_{S^{(e)}} (\bar{\bar{h}} \bar{\bar{T}}_\infty - \bar{q}) N_I^{(e)} dV^{(e)} \tag{5.1.21}$$

Substituting expressions (5.1.15-21) into equations (5.1.13) and (5.1.14), and using the symmetry property of $C_{ijkl}^{(ep)}$, one obtains:

$$u_{iI}^{(e)} (K_{ijIJ}^{(e)} u_{jJ}^{\bullet(e)} + E_{iIJ}^{(e)} T_J^{\bullet(e)} - F_{iI}^{(e)}) = 0 \tag{5.1.22}$$

$$T_I^{(e)} (C_{IJ}^{(e)} T_J^{\bullet(e)} + S_{IJ}^{(e)} T_J^{(e)} + R_{iIJ}^{(e)} u_{iJ}^{\bullet(e)} - Q_I^{(e)}) = 0 \tag{5.1.23}$$

where I,J = 1,...,N and i,j = 1,2 for plane problems, and i,j = 1,2,3 for three-dimensional problems.

Since the foregoing equations must hold for arbitrary $u_{iI}^{(e)}$ and $T_I^{(e)}$, it follows that for any e-th element:

$$K_{ijIJ}^{(e)} \dot{u}_{jJ}^{(e)} + E_{iIJ}^{(e)} \dot{T}_J^{(e)} = F_{iI}^{(e)} \tag{5.1.24}$$

$$R_{jIJ}^{(e)} \dot{u}_{jJ}^{(e)} + C_{IJ}^{(e)} \dot{T}_J^{(e)} + S_{IJ}^{(e)} T_J^{(e)} = Q_I^{(e)} \tag{5.1.25}$$

i.e. for an element having N nodes there are N temperature and Nxn displacement equations, where n denotes the number of displacement field components.

It should be mentioned that the above equations were derived under an additional assumption concerning the interaction of elements. It has been assumed that the surface integrals over element interfaces vanished due to the cancelation of identical terms contributed to the assembled equations by adjacent elements.

Matrices $K_{ijIJ}^{(e)}$, $E_{iIJ}^{(e)}$, $R_{jIJ}^{(e)}$ and $C_{IJ}^{(e)}$ depend on the current local values of stress, effective plastic strain and temperature. Thermal conductance matrix $S_{IJ}^{(e)}$ and the vector of heat generation rate $Q_I^{(e)}$ also depend on the current local temperature values in view of the temperature dependencies of thermal conductivity k and heat transfer coefficient $\bar{h}$. These additional couplings may be conveniently accounted for in the numerical formulation when the Gauss-Legendre method is employed for approximate evaluation of volume and surface integrals. The integrands must then be evaluated only at

the Gauss-Legendre sampling points [3,4], and the values of stress, effective plastic strain and temperature only at these points are required.

Denoting the local coordinates of the K-th sampling point within an isoparametric element by ξ_{rK}, (r = 1,...,n) one needs to evaluate:

- the required independent variables at this point:

$$T_K = N_I^{(e)}(\xi_{rK})T_I^{(e)} \tag{5.1.26}$$

$$\sigma_{ijK} = \sigma_{ij}(\xi_{rK}) \tag{5.1.27}$$

$$\bar{\varepsilon}_K^{(p)} = \bar{\varepsilon}^{(p)}(\xi_{rK}) \tag{5.1.28}$$

- the required material properties at this point:

$$\sigma_{yK} = \sigma_y(\bar{\varepsilon}_K^{(p)}, T_K) \tag{5.1.29}$$

$$K_K = K(T_K) = \frac{E(T_K)}{3[1 - 2\nu(T_K)]} \tag{5.1.30}$$

$$G_K = G(T_K) = \frac{E(T_K)}{2[1 + \nu(T_K)]} \tag{5.1.31}$$

$$\alpha_K = \alpha(T_K) \tag{5.1.32}$$

$$k_K = k(T_K) \tag{5.1.33}$$

$$c_{\varepsilon K} = c_\varepsilon(T_K) \tag{5.1.34}$$

and their derivatives

$$K''_K = \frac{\partial K}{\partial T}\bigg|_{T=T_K} \tag{5.1.35}$$

$$G''_K = \frac{\partial G}{\partial T}\bigg|_{T=T_K} \tag{5.1.36}$$

$$\alpha''_K = \frac{\partial \alpha}{\partial T}\bigg|_{T=T_K} \tag{5.1.37}$$

$$H'_K = \frac{\partial \sigma_y}{\partial \bar{\varepsilon}^{(p)}}\bigg|_{T=T_K,\ \bar{\varepsilon}^{(p)}=\bar{\varepsilon}^{(p)}_K} \tag{5.1.38}$$

$$H''_K = \frac{\partial \sigma_y}{\partial T}\bigg|_{T=T_K,\ \bar{\varepsilon}^{(p)}=\bar{\varepsilon}^{(p)}_K} \tag{5.1.39}$$

Then, it is possible to compute the values of $C^{(ep)}_{ijklK}$, $\beta^{(ep,th)}_{ijK}$, B_{ijK} and $\tilde{\gamma}_K$ at the sampling points, following the expressions stated in Table 2, and (4.5.47-48).

In order to apply the Gauss-Legendre method for the evaluation of the surface integrals the sampling points have to be located on the elements' boundaries but otherwise the procedure remains identical. Then it may be necessary to sample the values of pressure rate $\dot{\bar{p}}$, prescribed heat flux $\bar{q}$, heat transfer coefficient $\bar{h}$ and bulk fluid temperature $\bar{T}_\infty$ on the boundaries.

The details of element matrices evaluation by the Gauss-Legendre procedure will be discussed in the following section for the case of axisymmetric problems. Realizing that the volume and the surface integrals are computed as weighted sums of their respective integrands at sampling points enables one to envisage the manner in which the sampling point values of stress σ_{ijK} and effective plastic strain $\bar{\varepsilon}_K^{(p)}$ are coupled with the nodal values, $u_{iI}^{(e)}$ and $T_I^{(e)}$, in the discrete model. The nodal equations (5.23-24) for the given element are coupled with the following equations, valid at M sampling points (K=1,...,M) of the e-th element:

$$\dot{\sigma}_{ijK} = C_{ijklK}^{(ep)} \frac{\partial N_I^{(e)}(\xi_{rK})}{\partial x_l} \dot{u}_{kI}^{(e)} - \beta_{ijK}^{(ep,th)} N_I^{(e)}(\xi_{rk}) \dot{T}_I^{(e)} \tag{5.1.40}$$

$$\dot{\bar{\varepsilon}}_K^{(p)} = \frac{3G_K}{\sigma_{yK}(H_K' + 3G_K)} \sigma'_{ijK} \frac{\partial N_I^{(e)}(\xi_{rK})}{\partial x_j} \dot{u}_{iI}^{(e)}$$

$$+ \frac{\frac{\sigma_{yK}}{G_K} G_K'' - H_K''}{H_K' + 3G_K} N_I^{(e)}(\xi_{rK}) \dot{T}_I^{(e)} \tag{5.1.41}$$

which result from (4.5.1), (4.5.55), (5.1.11) and (5.1.12).

While the element nodal equations (5.1.24-25) are subject to the assembling procedure which result in couplings between nodes not shared by one element, equations (5.1.40-41) involve couplings between nodal variables of one element only. The reason for this is that in contrast to the former equations, the latter were not derived from integral statements. As a result, the discrete model encompases weaker couplings between stresses and effective plastic strains at

adjacent sampling points than those between displacements and temperatures at adjacent nodes.

In summary, the discrete model equations consist of Nx(n+1) nodal equations (5.1.24-25) and $2MxN_{el}$ sampling point equations (5.1.40-41), where M denotes number of sampling points in one element and N_{el} is the total number of elements.

By referring to equation (4.5.3) which checks the yield condition (and determines the value of j) at the sampling points, the values of the yield function F_K and the proportionality factor λ_K at the K-th sampling are computed as follows:

$$F_K = \frac{1}{2}\,\sigma'_{ijK}\sigma'_{ijK} - \frac{1}{3}\,\sigma^2_{yK} \tag{5.1.42}$$

$$\lambda_K = \frac{2G_K}{(\frac{2}{3}\,\sigma_{yK})^2(H'_K + 3G_K)}\,\sigma'_{ijK}\,\frac{\partial N_I^{(e)}(\xi_{rK})}{\partial x_j}\,\dot{u}_{iI}^{(e)}$$

$$+\ \frac{\frac{\sigma_{yK}}{G_K}\,G''_K - H''_K}{\frac{2}{3}\,\sigma_{yK}(H'_K + 3G_K)}\,N_I^{(e)}(\xi_{rK})\dot{T}_I^{(e)} \tag{5.1.43}$$

5.1.3 Discrete Model For Axisymmetric Problems

Analyses of axisymmetric problems are most conveniently performed using the system of cylindrical coordinates r, θ and z, and assuming that all fields are functions of r- and z-coordinates only. All the relationships derived up to this point for the Cartesian components of vectors and tensors could be restated in cylindrical

coordinates, while employing the general tensorial notation for curvilinear coordinate systems [15]. However, for the sake of notational simplicity, it is convenient to utilize, from now on, the matrix language used in most of the literature on finite elements. Vectors and tensors will be represented through their physical components in cylindrical coordinates, and the required relationships involving partial derivatives will be stated explicitly.

Since all the second and fourth order tensors employed in the previous sections were symmetrical (in the sense that $\sigma_{ij} = \sigma_{ji}$, $C_{ijrs} = C_{rsij} = C_{jirs} = C_{ijsr}$, etc.), in the matrix notation they could be represented by 6x1 column vectors and 6x6 square matrices, respectively. For axisymmetric problems further simplifications arise, because only non-zero components need to be considered.

The non-zero components of the displacement vector for axisymmetric problems are u_1 and u_2 and it may be represented by the 2x1 column vector:

$$\{u\} = \begin{bmatrix} u_r \\ u_z \end{bmatrix} \tag{5.1.44}$$

The non-zero components of any symmetrical second order tensor correspond to the pairs of indicies: rr, θθ, zz and rz. The physical components of the strain tensor are represented by the 4x1 column vector $\{\varepsilon\}$ related to the displacement vector $\{u\}$ through the matrix differential operator $[\nabla_\varepsilon]$:

$$\{\varepsilon\} = \begin{bmatrix} \varepsilon_{rr} \\ \varepsilon_{zz} \\ \varepsilon_{\theta\theta} \\ 2\varepsilon_{rz} \end{bmatrix} = \begin{bmatrix} \frac{\partial}{\partial r} & 0 \\ 0 & \frac{\partial}{\partial z} \\ \frac{1}{r} & 0 \\ \frac{\partial}{\partial r} & \frac{\partial}{\partial z} \end{bmatrix} \begin{bmatrix} u_r \\ u_z \end{bmatrix} = [\nabla_\varepsilon]\ \{u\} \qquad (5.1.45)$$

The physical components of the temperature gradient form a 2x1 vector related to temperature through the gradient operator $\{\nabla_q\}$:

$$\{\nabla T\} = \begin{bmatrix} \frac{\partial}{\partial r} \\ \frac{\partial}{\partial z} \end{bmatrix} T = \{\nabla_q\}\ T \qquad (5.1.46)$$

The isoparametric elements described in Section 5.1.1 become the appropriate ring elements with the z-axis as the symmetry axis. The set of shape functions may be ordered to form the components of a column vector:

$$\{N^{(e)}\} = [N_1^{(e)}\ N_2^{(e)}\ \ldots\ N_N^{(e)}]^T \qquad (5.1.47)$$

where $N_I^{(e)}$ (I=1,...,N) are given by either (5.1.4) or (5.1.7-8). The displacements and temperature approximations within a given element may be represented as:

$$\begin{bmatrix} u_r \\ u_z \\ T \end{bmatrix} = \begin{bmatrix} \{N^{(e)}\}^T & 0 & 0 \\ 0 & \{N^{(e)}\}^T & 0 \\ 0 & 0 & \{N^{(e)}\}^T \end{bmatrix} \begin{bmatrix} \{u_r^{(e)}\} \\ \{u_z^{(e)}\} \\ \{T^{(e)}\} \end{bmatrix} = \begin{bmatrix} [N_u^{(e)}]^T & 0 \\ & \\ 0 & \{N_T^{(e)}\}^T \end{bmatrix} \begin{bmatrix} \{u^{(e)}\} \\ \\ \{T^{(e)}\} \end{bmatrix}$$

(5.1.48)

while the strain and temperature gradient fields are approximated as:

$$\{\varepsilon\} = [\nabla_\varepsilon][N_u^{(e)}]^T\{u^{(e)}\} = [H_u^{(e)}]\{u^{(e)}\} \tag{5.1.49}$$

$$\{\nabla T\} = \{\nabla_q\}\{N_T^{(e)}\}^T\{T^{(e)}\} = [H_T^{(e)}]\{T^{(e)}\} \tag{5.1.50}$$

The matrices $[H_u^{(e)}]$ and $[H_T^{(e)}]$ are computed explicitly as:

$$[H_u^{(e)}] = \begin{bmatrix} \frac{\partial N_1^{(e)}}{\partial r} & 0 & \frac{\partial N_2^{(e)}}{\partial r} & 0 & \cdots & 0 \\ 0 & \frac{\partial N_1^{(e)}}{\partial z} & 0 & \frac{\partial N_2^{(e)}}{\partial z} & \cdots & \frac{\partial N_N^{(e)}}{\partial z} \\ \frac{N_1^{(e)}}{r} & 0 & \frac{N_2^{(e)}}{r} & 0 & \cdots & 0 \\ \frac{\partial N_1^{(e)}}{\partial r} & \frac{\partial N_1^{(e)}}{\partial z} & \frac{\partial N_2^{(e)}}{\partial r} & \frac{\partial N_2^{(e)}}{\partial z} & \cdots & \frac{\partial N_N^{(e)}}{\partial z} \end{bmatrix}$$

(5.1.51)

$$[H_T^{(e)}] = \begin{bmatrix} \frac{\partial N_1^{(e)}}{\partial r} & \frac{\partial N_2^{(e)}}{\partial r} & & \frac{\partial N_N^{(e)}}{\partial r} \\ \frac{\partial N_1^{(e)}}{\partial z} & \frac{\partial N_2^{(e)}}{\partial z} & & \frac{\partial N_N^{(e)}}{\partial z} \end{bmatrix} \tag{5.1.52}$$

The element matrices expressing material properties of individual elements may be constructed in complete analogy to equations (5.1.15-21), using constitutive matrices summarized in Table 3, and matrices $[N_u^{(e)}]$, $\{N_T^{(e)}\}$, $[H_u^{(e)}]$ and $[H_T^{(e)}]$, provided by the equations (5.1.47-48) and (5.1.51-52).

To facilitate the integration in the natural coordinates, the differentiation with respect to cylindrical coordinates must be replaced with appropriate operations in the isoparametric domain. Using the chain rule, one obtains [3,4,53,63]:

$$\begin{bmatrix} \frac{\partial}{\partial r} \\ \frac{\partial}{\partial z} \end{bmatrix} = [j]^{-1} \begin{bmatrix} \frac{\partial}{\partial \xi_1} \\ \frac{\partial}{\partial \xi_2} \end{bmatrix} = \frac{1}{\det[j]} \begin{bmatrix} \frac{\partial z}{\partial \xi_2} & -\frac{\partial z}{\partial \xi_1} \\ -\frac{\partial r}{\partial \xi_2} & \frac{\partial r}{\partial \xi_1} \end{bmatrix} \begin{bmatrix} \frac{\partial}{\partial \xi_1} \\ \frac{\partial}{\partial \xi_2} \end{bmatrix} \tag{5.1.53}$$

where the Jacobian of isoparametric transformation is given by

$$[j(\xi_1,\xi_2)] = \begin{bmatrix} \frac{\partial r}{\partial \xi_1} & \frac{\partial z}{\partial \xi_1} \\ \frac{\partial r}{\partial \xi_2} & \frac{\partial z}{\partial \xi_2} \end{bmatrix} \tag{5.1.54}$$

Equation (5.1.53) must be utilized when computing the shape function derivatives with respect to the cylindrical coordinates, as required by the equations (5.1.51-52).

Finally, for evaluation of element integrals one needs to know how to determine the components of an outward unit vector normal to the element's boundary surface, and the volume and surface differentials transformed to isoparametric coordinates.

The outward unit vector, normal to the external surface of an axisymmetric ring element, may be split into the radial and axial components n_r and n_z, tangent to r- and z-coordinate lines, respectively. When the boundary surface is given by the equation $\xi_1 = \pm 1$, these components may be expressed as:

$$\begin{bmatrix} n_r \\ n_z \end{bmatrix} = \frac{\xi_1}{\sqrt{\left(\frac{\partial r}{\partial \xi_2}\right)^2 + \left(\frac{\partial z}{\partial \xi_2}\right)^2}} \begin{bmatrix} \frac{\partial z}{\partial \xi_2} \\ -\frac{\partial r}{\partial \xi_2} \end{bmatrix} \tag{5.1.55}$$

and the differential surface area is:

$$dS^{(e)} = 2\pi r \sqrt{\left(\frac{\partial r}{\partial \xi_2}\right)^2 + \left(\frac{\partial z}{\partial \xi_2}\right)^2}\, d\xi_2 \tag{5.1.56}$$

When the boundary surface is given by the equation $\xi_2 = \pm 1$, the radial and axial components of the outward unit normal become:

$$\begin{bmatrix} n_r \\ n_z \end{bmatrix} = \frac{\xi_2}{\sqrt{\left(\frac{\partial r}{\partial \xi_1}\right)^2 + \left(\frac{\partial z}{\partial \xi_1}\right)^2}} \begin{bmatrix} -\frac{\partial z}{\partial \xi_1} \\ \frac{\partial r}{\partial \xi_1} \end{bmatrix} \tag{5.1.57}$$

and the differential surface area is

$$dS^{(e)} = 2\pi r \sqrt{\left(\frac{\partial r}{\partial \xi_1}\right)^2 + \left(\frac{\partial z}{\partial \xi_1}\right)^2}\, d\xi_1 \qquad (5.1.58)$$

The elementary differential volume may be expressed in natural coordinates as:

$$dV^{(e)} = 2\pi r \det[j] d\xi_1 d\xi_2 \qquad (5.1.59)$$

Using the aforementioned equations, the elemental stiffness, thermal expansivity, thermal conductance, thermal capacitance and thermomechanical coupling matrices, as well as the rate of external forces and the rate of heat generation vectors, may be constructed for axisymmetric problems set up in the cylindrical coordinates. Table 4 contains the respective expressions written in matrix notation. The symbol $\underset{m}{\Sigma}$ used there refers to the assembly of element matrices rather than to their summation.

The Gauss-Legendre procedure of numerical integration in a natural coordinate system [3,4], yields the following expressions for volume and surface integrals evaluation:

$$\int_{v^{(e)}} f(r,z)dV^{(e)} = 2\pi \int_{-1}^{+1}\int_{-1}^{+1} \bar{f}(\xi_1,\xi_2)r(\xi_1,\xi_2)\det[j(\xi_1,\xi_2)]d\xi_1 d\xi_2$$

$$2\pi \sum_{K=1}^{M} W_K \bar{f}(\xi_{1K},\xi_{2K})r(\xi_{1K},\xi_{2K})\det[j(\xi_{1K},\xi_{2K})] \qquad (5.1.60)$$

$$\int_{S^{(e)}} f(r,z)dS^{(e)} = 2\pi \int_{-1}^{+1} \bar{f}(\xi_1,\pm 1)r(\xi_1,\pm 1)\sqrt{[\frac{\partial r(\xi_1,\pm 1)}{\partial \xi_1}]^2 + [\frac{\partial z(\xi_1,\pm 1)}{\partial \xi_1}]^2}\, d\xi_1$$

$$= 2\pi \sum_{K=1}^{M'} W'_K \bar{f}(\xi_{1K},\pm 1)r(\xi_{1K},\pm 1) \sqrt{[\frac{\partial r(\xi_1,\pm 1)}{\partial \xi_1}]^2 + [\frac{\partial z(\xi_1,\pm 1)}{\partial \xi_1}]^2}$$

for $\xi_2 = \pm 1$

$$\int_{S^{(e)}} f(r,z)dS^{(e)} = 2\pi \int_{-1}^{+1} \bar{f}(\pm 1,\xi_2)r(\pm 1,\xi_2)\sqrt{[\frac{\partial r(\pm 1,\xi_2)}{\partial \xi_2}]^2 + [\frac{\partial z(\pm 1,\xi_2)}{\partial \xi_2}]^2}\, d\xi_2$$

$$= 2\pi \sum_{K=1}^{M'} W'_K \bar{f}(\pm 1,\xi_{2K})r(\pm 1,\xi_{2K}) \sqrt{[\frac{\partial r(\pm 1,\xi_2)}{\partial \xi_2}]^2 + [\frac{\partial z(\pm 1,\xi_2)}{\partial \xi_2}]^2}$$

for $\xi_1 = \pm 1$

(5.1.61)

Here, $f(r,z)$ denotes an arbitrary function of the cylindrical coordinates r and z, and $\bar{f}(\xi_1,\xi_2) = \bar{f}(r(\xi_1,\xi_2),z(\xi_1,\xi_2))$ is its natural counterpart. The integrands of both types of integrals are sampled at a number of points located within their integration domains, and multiplied by respective weighting factors W_K and W'_K. The locations of sampling points and the numerical values of weighting factors are determined for a given order of integration [3,4,63]. When the same order is used for both volume and surface integration, the respective numbers of sampling points are related through the formula: M = M'xM'.

5.2 Computational Solution Algorithm

The spatially discretized model of thermoelastoplastic solid behaviour, presented in Section 5.1, consisted of the system of non-

linear oridinary differential equations, summarized in Table 4, and the additional inequalities aimed at determining whether yielding takes place at some preselected points in the structure. Numerical solution of the initial value problem cannot be accomplished by straightforward application of the standard methods developed for the systems of oridinary differential equations. Instead, the discretization in the time domain must be combined with a procedure for handling the inequality constraints. One basic difficulty is associated with the fact that activation and/or deactivation of an inequality constraint is always accompanied by discontinuous changes of some of the system's parameters. Another difficulty results from the solution's essential dependence on the history of material response (known as solution's path dependence), and requires that any acceptable solution algorithm assures that the unknown path corresponding to the exact solution is followed closely [42].

Among several approaches to solving elastoplastic problems the incremental procedures utilizing iterative methods are most widely used, [4,42,53,58]. The solution is advanced through time in finite steps, and computations pertaining to each step involve two phases: solving the nodal equations, and state determination* [42]. In the context of the temperature-displacement formulation pursuit in this thesis, the nodal equations are solved during the first phase,

---

* The meaning of the term "state" used in this Section (and common in the literature on computational plasticity) is broader than that used in Section 4.4. The state determination phase includes computations involving relationships, such as yield condition, which originate from the thermodynamic process description.

yielding temperature and displacement increments, while the second phase is concerned with determination of new stresses and equivalent plastic strains and assuring that yield conditions at the sampling points are satisfied. Since the incremental equations being dealt with in both phases of the solution process are non-linear, iterations are in general required. However, when an explicit time integration scheme is used during the state determination phase, one iterative cycle aimed at improving the satisfaction of nodal equations may be sufficient [4].

The following subsections deal with the formulation of incremental equations and the algorithm proposed for their solution.

5.2.1 Nodal Incremental Equations and Their Solution

Let's assume that the solution of the spatially discretized problem, represented by the equations given in Table 4, the inequality constraints and the appropriate initial conditions are available (exactly or approximately) at a given instant t. Using left superscripts to denote the time at which a quantity occurs, the following values are assumed to be known:

- nodal displacements ${}^{t}_{\iota}U$,
- nodal temperatures ${}^{t}\{T\}$
- stresses ${}^{t}\{\sigma\}$ at the integration points
- equivalent plastic strains ${}^{t-(p)}\varepsilon$ at the integration points
- indicators of plastic (or neutral) loading ${}^{t}j$ at the integration points

The temperatures at integration points may be easily calculated from their nodal values.

Time discretization of the nodal equations appearing in Table 4 requires approximations of the time derivatives $\{\dot{U}\}$ and $\{\dot{T}\}$. Restricting consideration to two-level schemes, the α-method successfully used in finite element inelastic and non-linear heat transfer problems [4,58] may be employed for this purpose.

The nodal displacements and temperatures at the instant $t + \Delta t$ are approximated as:

$$^{t+\Delta t}\{U\} = {}^{t}\{U\} + {}^{t+\alpha_1 \Delta t}\{\dot{U}\}\,\Delta t \tag{5.2.1}$$

$$^{t+\Delta t}\{T\} = {}^{t}\{T\} + {}^{t+\alpha_2 \Delta t}\{\dot{T}\}\,\Delta t \tag{5.2.2}$$

where the parameters α_1 and α_2 are between zero and unity. The displacements and temperatures variations over the interval Δt are assumed to be linear, i.e.

$$^{t+\alpha_1 \Delta t}\{U\} = (1-\alpha_1)\,{}^{t}\{U\} + \alpha_1\,{}^{t+\Delta t}\{U\} \tag{5.2.3}$$

$$^{t+\alpha_2 \Delta t}\{T\} = (1-\alpha_2)\,{}^{t}\{T\} + \alpha_2\,{}^{t+\Delta t}\{T\} \tag{5.2.4}$$

It is worth noting that when the parameters α_1 and α_2 assume the values of 0 and 1, the Euler forward (explicit) and backward (implicit) schemes result. Additionaly, if α_1 and α_2 equal $\frac{1}{2}$, the Crank-Nicholson (trapezoidal, midpoint) scheme is obtained.

When the increments of nodal displacements and temperatures over the time step Δt are introduced:

$$\{\Delta U\} = {}^{t+\Delta t}\{U\} - {}^{t}\{U\} \tag{5.2.5}$$

$$\{\Delta T\} = {}^{t+\Delta t}\{T\} - {}^{t}\{T\} \tag{5.2.6}$$

equations (5.2.1-2) yield:

$${}^{t+\alpha_1\Delta t}\{\dot{U}\} = \frac{1}{\Delta t}\{\Delta U\} \tag{5.2.7}$$

$${}^{t+\alpha_2\Delta t}\{\dot{T}\} = \frac{1}{\Delta t}\{\Delta T\} \tag{5.2.8}$$

$${}^{t+\alpha_1\Delta t}\{U\} = {}^{t}\{U\} + \alpha_1\{\Delta U\} \tag{5.2.9}$$

$${}^{t+\alpha_2\Delta t}\{T\} = {}^{t}\{T\} + \alpha_2\{\Delta T\} \tag{5.2.10}$$

The incremental nodal equations are postulated in the form:

$$[K]\,{}^{t+\alpha_1\Delta t}\{\dot{U}\} + [E]\,{}^{t+\alpha_2\Delta t}\{\dot{T}\} = {}^{t+\alpha_1\Delta t}\{F\} \tag{5.2.11}$$

$$[R]\,{}^{t+\alpha_1\Delta t}\{\dot{U}\} + [C]\,{}^{t+\alpha_2\Delta t}\{\dot{T}\} + [S]\,{}^{t+\alpha_2\Delta t}\{T\} = {}^{t+\alpha_2\Delta t}\{Q\} \tag{5.2.12}$$

With the use of equations (5.2.7-10) they could be conveniently written as:

$$\begin{bmatrix} [K] & [E] \\ [R] & [C] + \alpha_2 \Delta t[S] \end{bmatrix} \begin{bmatrix} \{\Delta U\} \\ \{\Delta T\} \end{bmatrix} = \begin{bmatrix} {}^{t+\alpha_1 \Delta t}\{F\} \\ {}^{t+\alpha_2 \Delta t}\{Q\} \end{bmatrix} \Delta t$$

$$- \begin{bmatrix} [0] & [0] \\ [0] & \Delta t[S] \end{bmatrix} \begin{bmatrix} {}^{t}\{U\} \\ {}^{t}\{T\} \end{bmatrix} \qquad (5.2.13)$$

It is understood that the assembled matrices [K], [E], [R], [C] and [S] are evaluated using the sampling point values

$${}^{t+\alpha_2 \Delta t}T, \quad {}^{t+\alpha_1 \Delta t}\{\sigma\}, \quad {}^{t+\alpha_1 \Delta t}\underline{\varepsilon}(p) \quad \text{and} \quad {}^{t+\alpha_1 \Delta t}j.$$

While evaluating the nodal vectors

$${}^{t+\alpha_1 \Delta t}\{F\} \quad \text{and} \quad {}^{t+\alpha_2 \Delta t}\{Q\},$$

the rates $\bar{b}$ and $\dot{\bar{p}}$ are sampled at the instant $t+\alpha_1 \Delta t$, while the values of r, $\bar{T}_\infty$, $\bar{q}$ and $\bar{h}$ are evaluated at time $t+\alpha_2 \Delta t$.

The matrix equation (5.2.13) represents a set of nonlinear algebraic equations. They are usually linearized to enable iterative solution. The solution of the linearized nodal equations represents the first phase of computations performed during one iterative cycle. The quantities associated with the sampling points are not affected in this phase of computation. Their corrected values calculated during the state determination phase may be, however, utilized during the nodal equations solution phase of the next iteration cycle.

When a simple solution strategy based on the Newton-Rapshon method is adopted [4,53], the increments of nodal quantities corresponding to the i-th iteration cycle are decomposed as:

$$\begin{bmatrix} \{\Delta U\}^{(i)} \\ \{\Delta T\}^{(i)} \end{bmatrix} = \begin{bmatrix} \{\Delta U\}^{(i-1)} \\ \{\Delta T\}^{(i-1)} \end{bmatrix} + \begin{bmatrix} \{\delta U\}^{(i)} \\ \{\delta T\}^{(i)} \end{bmatrix} \tag{5.2.14}$$

where the right superscripts refer to the iteration cycle number and the linearized equations solved in the i-th cycle ($i=1,\ldots,n_c$) are:

$$\begin{bmatrix} [K]^{(i-1)} & [E]^{(i-1)} \\ [R]^{(i-1)} & [C]^{(i-1)}+\alpha_2\Delta t[S]^{(i-1)} \end{bmatrix} \begin{bmatrix} \{\delta U\}^{(i)} \\ \{\delta T\}^{(i)} \end{bmatrix} = \Delta t \begin{bmatrix} {}^{t+\alpha_1\Delta t}\{F\} \\ {}^{t+\alpha_2\Delta t}\{Q\}^{(i-1)} \end{bmatrix}$$

$$- \begin{bmatrix} [K]^{(i-1)} & [E]^{(i-1)} \\ [R]^{(i-1)} & [C]^{(i-1)}+\alpha_2\Delta t[S]^{(i-1)} \end{bmatrix} \begin{bmatrix} \{\Delta U\}^{(i-1)} \\ \{\Delta T\}^{(i-1)} \end{bmatrix}$$

$$- \begin{bmatrix} [0] & [0] \\ [0] & \alpha_2\Delta t[S]^{(i-1)} \end{bmatrix} \begin{bmatrix} {}^{t}\{U\} \\ {}^{t}\{T\} \end{bmatrix} \tag{5.2.15}$$

In the first iteration cycle it is assumed that $\{\Delta U\}^{(0)} = \{0\}$ and $\{\Delta T\}^{(0)} = \{0\}$. The starting values of temperatures, stresses equivalent plastic strains and plastic (or neutral) loading indicators are assumed equal to the final values calculated in the previous time step, i.e. ${}^{t+\Delta t}T^{(0)} = {}^{t}T$, ${}^{t+\Delta t}\{\sigma\}^{(0)} = {}^{t}\{\sigma\}$, ${}^{t+\Delta t}\bar{\varepsilon}^{(p)(0)} = {}^{t}\bar{\varepsilon}^{(p)}$, ${}^{t+\Delta t}j^{(0)} = {}^{t}j$. The number of iteration cycles n_{cyc} depends on the criterion employed for the termination of the iterative process.

In the equation (5.2.13) the second matrix term on the right hand side represents the out-of-balance forces and heat inputs resulting from the approximate satisfaction of the nodal incremental equations in the previous iteration. The tangent matrix is updated in every cycle of computation. The modified Newton-Raphson scheme, simpler from the computational point of view, does not require updating of the tangent matrix, which remains unaltered during all iteration cycles performed during time-step computations [53].

If the modified Newton-Raphson scheme is implemented with the values of parameters $\alpha_1 = 1$ and $\alpha_2 = \frac{1}{2}$, then the two most widely used types of incremental equations, the fully implicit Euler scheme and the Crank-Nicholson scheme, are obtained for uncoupled elastoplastic and heat conduction problems, respectively.

5.2.2 State Determination

Given the approximate values of nodal displacements and temperatures at times t and $t+\Delta t$, i.e. ${}^{t}\{U\}$, ${}^{t}\{T\}$, ${}^{t+\Delta t}\{U\}^{(i)} = {}^{t}\{U\} + \{\Delta U\}^{(i)}$ and ${}^{t+\Delta t}\{T\}^{(i)} = {}^{t}\{T\} + \{\Delta T\}^{(i)}$, the approximate values of stresses and effective plastic strains at time $t+\Delta t$ are computed during the state determination phase of the i-th iteration cycle. The newly computed values ${}^{t+\Delta t}\{\sigma\}^{(i)}$ and ${}^{t+\Delta t}\bar{\varepsilon}^{(p)(i)}$ must reflect a possible appearance (or disappearance) of plastic flow during the time interval Δt, and to assure that detected yielding constraints the stress path to the yield surface.

A simple state determination algorithm for isotropic thermo-elastoplasticity was developed on the basis of analogical algorithms proposed for isothermal elastoplastic problems [4,19]. The algorithm employs explicit integration scheme for state variables (i.e. stresses and effective plastic strain) and uses a simple subincrementation technique [4,60] to enhance the control of stress path over the time interval t. However, the main difference between this and other state determination algorithms is in the use of a smooth representation of the isothermal stress-strain relationship, which obviates the need to explicitely identify the elastoplastic transition [23].

The concept of smooth representation of uniaxial isothermal stress-strain relationship is both physically justified (plastic deformation occurs in the subyield state), and computationally viable. Activation of plastic straining becomes possible at any time during the history of deformation, and the two-parameter ($\bar{\varepsilon}^{(p)}$ and T) family of yield surfaces, constructed from the uniaxial isothermal stress-strain curves, includes the degenerated surface represented by the point $\sigma_{rr} = \sigma_{zz} = \sigma_{\theta\theta} = \sigma_{rz} = 0$ in the stress space. Purely elastic straining starts upon the first unloading, when the point representing the stress state (in the stress space) leaves the virgin yield surface. A family of secondary yield surfaces is followed after the first reloading, etc.

A convenient analytical form of the family of isothermal stress-strain curves was proposed by Hsu et al. [10,23]:

$$\sigma_y = \tilde{\sigma}_y(\bar{\varepsilon}) = \frac{E\bar{\varepsilon}}{\{1 + [\frac{E\bar{\varepsilon}}{(1 - \frac{E'}{E})\sigma_{kink} + E'\bar{\varepsilon}}]^n\}^{1/n}} \qquad (5.2.16)$$

where the curve parameters, kink stress σ_y and plastic modulus E', are temperature dependent and are indicated in FIGURE 5. Since an analytical inversion of (5.2.16) to the form $\bar{\varepsilon} = \bar{\varepsilon}(\sigma_y)$ is not possible, the uniaxial relationship

$$\bar{\varepsilon} = \frac{\sigma_y}{E} + \bar{\varepsilon}^{(p)} \qquad (5.2.17)$$

must be used in iterative calculation of the yield stress for given values of T and $\bar{\varepsilon}^{(p)}$:

$$\sigma_y = \tilde{\sigma}_y(\bar{\varepsilon}^{(p)} + \frac{\sigma_y}{E}) \qquad (5.2.18)$$

When a secondary yield surface originates upon reloading, as shown in FIGURE 6, its analytical representation is given by the equation (5.2.16), provided the values of $\bar{\varepsilon}^{(p)}$ and σ_{kink} are replaced by $\bar{\varepsilon}^{(p)}_{-\varepsilon_y}$ and $\overset{*}{\sigma}_{kink}$.

The procedure of state determination at an element sampling point may be summarized as follows:

The quantities known at the start of calculations are:

${}^t\{\varepsilon\}$, $\{\Delta\varepsilon\}$ – strains at time t and approximate strain increments over the time step Δt,

${}^{t}T$, ΔT - temperature at time t and approximate temperature increment over the time step Δt,

${}^{t}\{\sigma\}$, ${}^{t}\bar{\varepsilon}^{(p)}$, ${}^{t}j$ - stresses, equivalent plastic strain and plastic strain indicator at time t,

ε_y - equivalent plastic strain accumulated up to the last unloading.

The sequence of computations is the following:

(i) Calculate the stress increment assuming elastic behaviour [1,2]:

$$\{\Delta\sigma^*\} = {}^{t+\Delta t}[C^{(e)}]\{\Delta\varepsilon\} - {}^{t+\Delta t}\{\beta^{(e,th)}\}\Delta T \qquad (5.2.19)$$

(ii) Calculate the trial stresses

$$\{\sigma^*\} = {}^{t}\{\sigma\} + \{\Delta\sigma^*\}$$

and trial effective stress:

$$\bar{\sigma}^* = \frac{3}{2}\sqrt{\{\sigma^{*'}\}^T\{\sigma^{*'}\}} \qquad (5.2.20)$$

(iii) Find the value of the yield stress corresponding to ${}^{t+\Delta t}T$ and ${}^{t}\bar{\varepsilon}^{(p)}$ (i.e. following the assumption on purely elastic behaviour $\Delta\bar{\varepsilon}^{(p)} = 0$), by solving iteratively

$$\sigma_y = \tilde{\sigma}_y({}^{t}\bar{\varepsilon}^{(p)} + \frac{\sigma_y}{{}^{t+\Delta t}E}) \qquad (5.2.21)$$

using ${}^{t+\Delta t}\sigma_{kink}$, ${}^{t+\Delta t}E$ and ${}^{t+\Delta t}E'$.

If secondary (tertiary, etc.) yield surface was already initiated by reloading (i.e. when $\varepsilon_y > 0$ and ${}^{t}j = 1$), the values of ${}^{t}\bar{\varepsilon}(p)$ and ${}^{t+\Delta t}\sigma_{kink}$ in equation (5.2.16) should be replaced by

$${}^{t}\bar{\varepsilon}(p) - \varepsilon_y$$

and

$${}^{t+\Delta t}\sigma_{kink} + \varepsilon_y \frac{{}^{t+\Delta t}E \; {}^{t+\Delta t}E'}{{}^{t+\Delta t}E - {}^{t+\Delta t}E'}, \quad \text{respectively.}$$

(iv) If $\bar{\sigma}^* \leq \sigma_y$ the step is elastic (neutral loading or unloading). Then set

$${}^{t+\Delta t}\{\sigma\} = \{\sigma^*\} \tag{5.2.22}$$

$${}^{t+\Delta t}\bar{\varepsilon}(p) = {}^{t}\bar{\varepsilon}(p) \tag{5.2.23}$$

$$\varepsilon_y = {}^{t}\bar{\varepsilon}(p) \tag{5.2.24}$$

$${}^{t}j = 0 \tag{5.2.25}$$

and <u>return</u>.

If $\bar{\sigma}^* > \sigma_y$ <u>continue</u>.

(v) If ${}^{t}j = 1$ yielding continues on the same yield surface, and <u>go to</u> (vi).

If ${}^{t}j = 0$ a new yield surface has to be initiated. In order to accomplish this, compute

$$t\bar{\sigma} = \sqrt{\frac{3}{2}\, t\{\sigma'\}^T\{\sigma'\}} \tag{5.2.26}$$

and find the new value of $\varepsilon_y^{(new)}$ from the relationship

$$t\bar{\sigma} = \sigma_y\left(t\bar{\varepsilon}^{(p)} - \varepsilon_y^{(new)} + \frac{t\bar{\sigma}}{t+\Delta t_E}\right) \tag{5.2.27}$$

using the new value of $\sigma_{kink}^{(new)}$ equal to

$$\sigma_{kink}^{(new)} = \sigma_{kink}^{(old)} + \varepsilon_y^{(new)} \frac{t+\Delta t_E \; t+\Delta t_{E'}}{t+\Delta t_E - t+\Delta t_{E'}} \tag{5.2.28}$$

(vi) Subdivide the strain and temperature increments, $\{\Delta\varepsilon\}$ and ΔT, into M increments:

$$\{\delta\varepsilon\} = \frac{1}{M}\{\Delta\varepsilon\} \tag{5.2.29}$$

$$\delta T = \frac{1}{M}\Delta T \tag{5.2.30}$$

(vii) For each i-th time-step subincrement (i=1,...,M) compute

$$\{\delta\varepsilon^{(p)}\} = \frac{1}{2G}\left([C^{(p)}]^{(i-1)}\{\delta\varepsilon\} - \{\beta^{(p,th)}\}^{(i-1)}\delta T\right) \tag{5.2.31}$$

$$^{(i)}\bar{\varepsilon}^{(p)} = \sqrt{\frac{2}{3}\{\delta\bar{\varepsilon}^{(p)'}\}^T\{\delta\bar{\varepsilon}^{(p)'}\}} + {}^{(i-1)}\bar{\varepsilon}^{(p)} \tag{5.2.32}$$

$$^{(i)}\{\sigma\} = [C^{(ep)}]^{(i-1)}\{\delta\varepsilon\} - \{\beta^{(ep,th)}\}^{(i-1)}\delta T + {}^{(i-1)}\{\sigma\} \tag{5.2.33}$$

where the values of stresses and effective plastic strain at time $t + \frac{i\Delta t}{M}$ are denoted by $^{(i)}\{\sigma\}$ and $^{(i)}\bar{\varepsilon}^{(p)}$.

The subscripts appearing on the right hand sides of constitutive matrices in equations (5.2.31-33) indicate the values of temperatures, stresses and effective plastic strains, at which they are evaluated.

Since the stresses $^{(i)}\{\sigma\}$ do not satisfy the yield surface equation at time $t + \frac{i\Delta t}{M}$, i.e.

$$\frac{3}{2}\,{}^{(i)}\{\sigma'\}^T\,{}^{(i)}\{\sigma'\} \neq \sigma_y^2({}^{(i)}\bar{\varepsilon}^{(p)}, {}^{(i)}T) \tag{5.2.34}$$

an elastic correction (presuming no change of $^{(i)}\bar{\varepsilon}^{(p)}$) may be considered. Assuming the corrective term as

$$^{(i)}\{\delta\sigma\} = -c^{(i)}\{\sigma'\} \qquad (0 \leq c^{(i)} \ll 1) \tag{5.2.35}$$

the value of $c^{(i)}$ is obtained from the condition

$$\frac{3}{2}\,(^{(i)}\{\sigma'\}^T - c^{(i)}\{\sigma'\}^T)(^{(i)}\{\sigma'\} - c^{(i)}\{\sigma'\}) = \sigma_y^2({}^{(i)}\bar{\varepsilon}^{(p)}, {}^{(i)}T)$$

and it may be directly calculated as:

$$c^{(i)} = 1 - \frac{\sigma_y({}^{(i)}\bar{\varepsilon}^{(p)}, {}^{(i)}T)}{\sqrt{\frac{3}{2}\,{}^{(i)}\{\sigma'\}^T\,{}^{(i)}\{\sigma'\}}} = 1 - \frac{{}^{(i)}\sigma_y}{{}^{(i)}\bar{\sigma}} \tag{5.2.36}$$

Then, the corrected value of stress is:

$$^{(i)}\{\sigma\}^{corr} = {}^{(i)}\{\sigma\} - (1 - \frac{{}^{(i)}\sigma_y}{{}^{(i)}\bar{\sigma}})\,{}^{(i)}\{\sigma'\} \tag{5.2.37}$$

(viii) The final values of stresses and effective plastic strains are:

$$t+\Delta t_{\{\sigma\}} = (M)_{\{\sigma\}}^{corr} \tag{5.2.38}$$

$$t+\Delta t\bar{\varepsilon}(p) = (M)\bar{\varepsilon}(p) \tag{5.2.39}$$

CHAPTER 6

IMPLEMENTATION OF THE COUPLED THERMOELASTOPLASTIC ANALYSIS IN THE FORM OF THE 'TEPAP' CODE

Program TEPAP (Thermo-Elasto-Plastic Analysis Program), written in standard FORTRAN IV, was developed as an implementation of the theory presented in CHAPTERS 4 and 5. It is intended to carry the coupled thermo-elasto-plastic finite element stress and heat conduction analyses for two-eimensional solids under the assumptions discussed in CHAPTER 3. At present only the case of axisymmetric analysis has been implemented, and the iterative schemes proposed for refinement of nodal variables and quantities evaluated at integration sampling points are not included. However, extensions to plane strain and plane stress cases are quite straightforward, and the existing version of the TEPAP code includes provisions for such additions. Implementation of the iterative schemes suggested in CHAPTER 5 would probably involve more programming effort, but it might prove worthwhile when attempting to reduce the dependence of code results on the time marching imposed by the user.

In the following sections the structure of TEPAP code and some implementation details are briefly discussed. In view of its length (in excess of 3000 lines) the code listing is not provided.

6.1 Code Organization and Structure

The basic layout of the TEPAP code follows the concepts of a finite element program organization as outlined by Bathe and Wilson [4]. The equation solver for the non-symmetric systems of linear equations is adopted from the chapter on Finite Element Programming written by Taylor and included in Zienkiewicz's monograph [63].

The advanced programming features described in these references, and implemented in TEPAP include: dynamic storage allocation, variable column height (skyline) storage of system matrices, a method of identification and elimination of constrained degrees of freedom, and several others. Since the code is intended for solving middle-sized problems, the data storage and solution process are arranged to use the core memory only. The dynamic storage allocation feature relieves the user from the necessity of declaring large matrices in one or more routines. Instead of this, all the matrices are stored vectorially, and the lengths of individual vectors are case dependent and calculated once for a given input. Core memory is allocated by the user through declaration of one large pool array. Declaration of insufficient core storage results in an error message, which provides information on the correct storage requirement. This feature combined with the option of running the code in the data check mode allows for easy and quick debugging of new case data.

TEPAP code is structured modularly in an effort to separate the functions it performs. The functional structure of the main program is illustrated in FIGURE 7, and indicates the separation of the data input phase from the solution phase. The former handles

input of all data except the specification of parameters $\dot{\bar{p}}$, $\bar{q}$, $\bar{h}$ and $\bar{T}_\infty$, which have to be supplied as functions of time and location on the boundary in the forms of individual, case dependent routines. During the solution phase a time-step loop is executed and each passage involves a check of the yielding zone extent. In a case of incorrect assumption appropriate correction is made, and all the calculations pertaining to the current time-step are repeated.

The subroutine tree depicted in FIGURE 8 indicates schematically the cross-communication among all the code subprograms. They may be classified as either the general routines independent of the type of finite element employed, or those developed specifically for linear and quadratic 2-D isoparametric elements. Introduction of such a classification allows easy extensions of TEPAP by either including more complex constitutive models or by adding new types of finite elements while leaving the code's basic structure intact.

6.2 Implementation Details

The routines developed for four-to-nine-node isoparametric elements enable both full and reduced integration over elemental volumes and surfaces. The full volume integration requires nine and four samplings over (r,z)-domain for quadratic and linear elements, respectively. The full surface integration requires three or two samplings over a one-dimensional domain. Reduced integrations involve appropriately fewer samplings.

No elemental matrices are permanently stored in core, instead they are computed at every time step and assembled into the global system matrix and global RHS-vector.

The active column profile (or skyline) storage scheme used in the code recognizes the fact that the matrix of coefficients in the system of linear equations in the finite element analysis (here called the global system matrix) has not only banded form, but the locations of non-zero elements differs greatly from column to column. The non-zero elements, which are most distant from the matrix diagonal, form the skyline of the matrix and it is imperative that all zero elements outside the skyline be excluded from the equation solution.

The required parts of the upper and lower triangular portions of the system matrix are stored, respectively, by columns and rows as two vectors. Two additional integer vectors of lengths equal to the number of equations in the system, have to be used for storing individual column heights and addresses of the diagonal elements. Despite the lack of symmetry of the system matrix, its profile, which is determined by the topology of the finite element mesh, may always be assumed to be symmetric. For this reason there is no need to store separately the row lengths of the lower triangular portion of the system matrix. The zero elements within the skyline of the system matrix must be, however, stored and operated upon, since they often become non-zero elements during the matrix reduction process [4].

The handling of essential boundary conditions, which were left unaccounted for in the integral formulation presented in CHAPTER 4, is in many cases not difficult. In the TEPAP code the nodal excess temperatures and the nodal displacement components may be requested to have zero values, and the r-component of the displacement of a node

may be required to be proportional to the z-component. Physically, these constraints represent isothermal nodes and roller supports arbitrarly oriented on the (r,z)-plane.

The elimination of constrained degrees of freedom is accomplished during the input phase using an integer array of constraint type identifiers. If a nodal degree of freedom is fully constrained (e.g. constant temperature or zero displacement in either r- or z-direction) the equation corresponding to it is not formed during the assembling process. In the case of a skew roller support, the roles of master and slave degrees of freedom must be assigned. In TEPAP the displacement component in the direction of sliding is assumed as the active (master) degree of freedom, while the component along the direction orthogonal to sliding is treated as fully constrained (slave). The stiffness matrix of the element with the roller node must be appropriately modified. The array of identifiers may then be filled with equation numbers corresponding to unconstrained degrees of freedom with zero entries representing eliminated temperatures and displacement components.

A system of linear algebraic equations is solved at each time-step by the Gaussian elimination technique. Diagonal dominance of system matrices allows one to avoid searches for pivoting elements and renumbering of equations.

CHAPTER 7

EXAMPLE CASES

In the course of the development of the 'TEPAP' code a number of test cases were prepared and used to validate the individual parts of the program. The tests, which are not reported here, involved comparisons between 'TEPAP' predictions and the known solutions of elastic, elastoplastic and heat transfer problems [21, 23]. The numerical examples discussed in this chapter were aimed at assessing 'TEPAP' capability to solve coupled thermomechanical problems as well as at providing some insight into the effects resulting from the inclusion of the passive thermoelastic and thermoplastic couplings in the models. To the best of the author's knowledge, this approach has not been attempted by any other existing analytical model.

7.1 Thermal Shock on Ceramic Tube

Hsu and Gillespie [24] considered the thermoelastic response of a silicon carbide thick wall tube whose outside surface was thermally insulated, and whose internal surface was suddenly subjected to convective heating. Assuming temperature independent material properties they derived analytical solutions for temperature and stress fields during thermal shock transients in an infinitely long cylinder. These solutions were used for comparison with the results of 'TEPAP' simulations obtained with the FE model presented in FIGURE 9.

The following geometric and material properties data were used in the computations:

- tube outside diameter — $d_o = 4$ in $= .1016$ m
- tube inside diameter — $d_i = 3$ in $= .0762$ m
- Young's modulus — $E = 54 \times 10^6$ psi $= 3.7232 \times 10^{11}$ Pa
- virgin yield stress — $\sigma_y = 18.65 \times 10^3$ psi $= 1.2859 \times 10^8$ Pa
- Poisson's ratio — $\nu = 0.31$
- linear thermal expansion coeff. — $\alpha = 2.6 \times 10^{-6}$ $1/^oF = 4.68 \times 10^{-6}$ $1/K$
- mass density — $\rho = 193.5$ $lb/ft^3 = 3.1 \times 10^6$ g/m^3
- specific heat capacity — $c_\varepsilon = 0.34$ Btu/(lb.^oF) $= 1.4226$J (g.K)
- thermal conductivity — $k = 41.6$ Btu/(hr.ft.^oF) $= 72.01$ W/(m.k)

The tube was assumed to initially remain at a temperature $T_o = 100^oF = 37.78^oC$. The bulk temperature of the hot fluid was assumed as $\bar{T}_\infty = 1470^oF = 798.89^oC$, and the heat transfer coefficient as $\bar{h} = 129.79$ Btu/(hr.ft.^{2o}F) $= 735.91$ W/(m^2.K).

The comparison between analytical and 'TEPAP' solutions (for the case when thermoelastic coupling in the heat conduction equation is neglected) are presented for time instants $t = .158$ s and $t = .790$ s in FIGURES 10, 11 and 12. The temperatures and tangential stresses predicted by 'TEPAP' agree well with the corresponding analytical solutions. Poorer agreement between axial stresses appears as the result of the tube top and bottom being axially constrained in order to simulate the plain strain condition [24]. The axial end-load

effect is pronounced because only one layer of elements was used to model the full length of the tube. If more axial layers were used in the FE model the axial restraint effect would appear more localized.

The temperature and stress distributions predicted by 'TEPAP' at t = 1s, with and without taking the thermoelastic coupling in the heat conduction equation into account, are compared in Table 6. Both the temperature and stress fields are only minutely affected by the inclusion of the passive thermoelastic coupling in the model. The differences between coupled and uncoupled solutions are smaller than the respective discrepancies between uncoupled solutions predicted by 'TEPAP' and 'TEPSA' - another FE code available for thermoelasto-plastic analyses [23]. 'TEPSA' predictions of temperature and stress fields are shown in Table 7.

7.2 Semi-infinite Space Subjected to Suddenly Imposed Convective Heating (Second Danilovskaya's Problem)

Among the first initial/boundary value problems studied in the theory of dynamic thermoelasticity was the (first) Danilovskaya's problem concerning a linear elastic half-space subjected to a uniform sudden temperature change on its bounding plane which was assumed to remain traction free [13]. This problem, along with its modified version involving half-space suddenly exposed to a high ambient temperature through a boundary layer of finite thermal conductance (the second Danilovskaya's problem), were among the most extensively studied thermoelastic problems, in both uncoupled and coupled formulations [6,26,46,50]. An approximate analytical solution

(confirmed by the finite element results) to the coupled dynamic version of the second Danilovskaya's problem was reported by Nickel and Sackman [46], and contrasted with the dynamic uncoupled case.

Following the formulation presented in Reference [46] the second Danilovskaya's problem may be cast in the dimensionless form:

$$\frac{\partial^2 \bar{u}_z}{\partial \bar{z}^2} = \frac{\partial^2 \bar{u}_z}{\partial \bar{t}^2} + \frac{\partial \bar{T}}{\partial \bar{z}} \qquad \text{for} \quad 0 \leq \bar{z} < \infty \qquad (7.2.1\text{-}2)$$

$$\frac{\partial^2 \bar{T}}{\partial \bar{z}^2} = \frac{\partial \bar{T}}{\partial \bar{t}} + \delta \frac{\partial^2 \bar{u}_z}{\partial \bar{z} \partial \bar{t}} \qquad \text{and} \quad 0 \leq \bar{t} < \infty$$

$$\bar{u}_z(\bar{z},0) = \frac{\partial \bar{u}_z(z,0)}{\partial \bar{t}} = \bar{T}(\bar{z},0) = 0 \qquad \text{for } 0 \leq \bar{z} < \infty \qquad (7.2.3)$$

$$\bar{\sigma}_{zz}(0,\bar{t}) = \frac{\partial \bar{u}_z(0,t)}{\partial z} - \bar{T}(0,\bar{t}) = 0 \qquad \text{for } 0 \leq \bar{t} < \infty \qquad (7.2.4)$$

$$\frac{\partial \bar{T}(0,\bar{t})}{\partial \bar{z}} = \bar{H}[\bar{T}(0,t) - \bar{T}_\infty] \qquad \text{for } 0 \leq \bar{t} < \infty \qquad (7.2.5)$$

where equations (7.2.3) represent initial conditions, and equations (7.2.4-5) represents boundary conditions.

The dimensionless parameters are defined as:

$$\bar{z} = \frac{c_\varepsilon}{k} \sqrt{\rho(K + \frac{4}{3} G)}\, z \qquad (7.2.6)$$

$$\bar{t} = \frac{c_\varepsilon}{k} (K + \frac{4}{3} G)t \qquad (7.2.7)$$

$$\bar{u}_z = \frac{c_\varepsilon}{k\alpha T_0} \frac{K + \frac{4}{3}G}{3K} \sqrt{\rho\left(K + \frac{4}{3}G\right)}\, u_z \tag{7.2.8}$$

$$\bar{\sigma}_{zz} = \frac{\sigma_{zz}}{3K\alpha T_0} \tag{7.2.9}$$

$$\bar{T} = \frac{\theta - T_0}{T_0} = \frac{T}{T_0} \tag{7.2.10}$$

$$\bar{T}_\infty = \frac{\theta_\infty - T_0}{T_0} = \frac{T_\infty}{T_0} \tag{7.2.11}$$

$$\bar{H} = \frac{\bar{h}}{\rho c_\varepsilon \sqrt{\rho\left(K + \frac{4}{3}G\right)}} \tag{7.2.12}$$

$$\delta = \frac{9\, K^2 \alpha^2 T_0}{\rho c_\varepsilon \left(K + \frac{4}{3}G\right)} \tag{7.2.13}$$

where all quantities used in the right-hand sides of these equations are defined in the NOMENCLATURE. The appropriate regularity requirements at infinity are assumed to supplement the boundary conditions [26,46].

The uncoupled case corresponds to the thermomechanical coupling parameter $\delta = 0$. Nickell and Sackman used three values for this coupling parameter $\delta = 0$, $\delta = 0.36$ and $\delta = 1.0$, and two values of the dimensionless heat transfer coefficient $\bar{H} = 0.5$ and $\bar{H} = 5.0$ in their studies, while assuming $\bar{T}_\infty = 1$. They presented temperature, displacement and stress histories at the location corresponding to $\bar{z} = 1$. While their displacement and stress solutions, obtained within the

framework of dynamic thermoelasticity theory, could not be verified with 'TEPAP' (whose modelling capability is restricted to quasistatic processes), the temperature solution in the uncoupled case offered this possibility. In addition to temperatures verification for $\delta = 0$, the effect of thermomechanical coupling on the temperature predictions in the quasistatic case, which does not seem to have been reported in published literature, has been assessed with the use of 'TEPAP'.

The semi-infinite space was approximated by a finite length and finite radius cylinder, modelled with 20 ring elements equally spaced in the axial direction, as shown in FIGURE 13. To conform to the dimensionless coefficients $\delta = 1.0$, $\overline{H} = 0.5$, and $\overline{T}_{\infty} = 1$, representing one of the sets employed in Nickell and Sackmann calculations, and to assure at the same time that the assumed cylinder length L = 20 m was represented by the dimensionless value $\overline{L} \gg 1$, the following fictitious material properties were used in the simulation:

- Young's modulus $E = \frac{2}{3}$ Pa
- Poisson's ratio $\nu = \frac{1}{3}$
- linear thermal expansion coefficient $\alpha = 0.5\ K^{-1}$
- mass density $\rho = 1.0\ kg.m^{-3}$
- specific heat capacity $c_{\varepsilon} = 1\ J.kg^{-1}.K^{-1}$
- thermal conductivity $k = 1W.m^{-1}.K^{-1}$

Assuming further that T_0 = 1K, θ_∞ = 2K, and $\bar{h}$ = 0.5 $W.m^{-2}.K^{-1}$, the dimensionless time and distance become $\bar{t}$ = t and $\bar{z}$ = z, in addition to δ = 1 and $\bar{H}$ = 0.5. The interface of the first and the second elements, located 1m away from the semi-space bounding surface (see FIGURE 13), is then represented by the coordinate $\bar{z}$ = 1.

The temperature history at this position, predicted by 'TEPAP' for the described above input data, is depicted in FIGURE 14 along with the prediction for δ = 0 which was practically identical to that of Reference [46]. The results of another case study shown in Figure 15 correspond to $\bar{H}$ = 0.5, $\bar{T}_\infty$ = 1.0 and δ = 2.0, and were obtained from the 'TEPAP' run using α = 1.0 K^{-1}, T_0 = 0.5K, while leaving the remaining data unchanged.

The 'TEPAP' simulation of the uncoupled case indicates that the finite element approximation of the semi-infinite space geometry is good for the considered values of parameters. The predicted temperatures are strongly affected by the presence/absence of the coupling term in the heat conduction equation, despite the neglect of inertia effects. The temperatures predicted by the quasistatic theory tend to be bounded from above by the uncoupled solution and from below by the solution computed according to the dynamic coupled theory.

The absence of the thermal wave which appears in the dynamic coupled solution [46] seems to be responsible for the monotonically increasing temperatures during transients predicted by the coupled quasistatic model. In the studied case the net contribution of the passive thermoelastic coupling is that of a heat sink whose intensity

may be characterized by the dimensionless number δ. The predicted magnitudes of displacements and stresses were however too small (in particular when compared to the corresponding values of the dynamic solution) to draw meaningful conclusions with regard to these fields' direct effects on the temperature distributions.

7.3 Initial Stage of Hydrostatic Extrusion

In this study, motivated by the publication of Iwata et al. [25], a thermoelastoplastic analysis of the initial non-steady state hydrostatic extrusion process was carried out.

The process in which a material is subjected to high hydrostatic pressure and forced out through a die is of continuing high interest to the metalworking technology [25], and it represents a perplexing problem for modelling. Within the capability of 'TEPAP' code a number of important features of the process could not be modelled: large bulk and localized deformations of the billet, frictional forces and heat generation at the die contact surfaces, rate dependent effects of material deformation (particularly important for high speed extrusion), etc. Practical considerations (concerns with execution times, lack of code's restart capability) dictated further simplifications, and resulted in assuming a rather crude finite element model depicted in FIGURE 16.

The workpiece (billet) was modelled as an assembly of 32 eight-nodes elements forming a mesh of 121 nodes. For comparison, the model employed by Iwata et al used 181 triangular constant strain elements, and 112 nodes. The boundary conditions for the stress

analysis part were assumed identical to those indicated in the frictionless axisymmetric studies by Iwata et al, i.e. prescribed hydrostatic pressure acting on the free surfaces at the die entrance, and sliding supports along the billet-die interface were assumed. At the die exit the displacement vector of node 25 (see FIGURE 16) was constrained to have axial direction, in an attempt to realistically model an uncertain detail of the boundary conditions specification in Reference [25]. The other surfaces of the billet were considered traction free and the sliding supports were assumed along the centreline. For the thermal part of the problem a uniform temperature of $20^{o}C$ was assumed to be maintained in the workpiece prior to its deformation, and adiabatic wall conditions were assumed on all billet surfaces throughout the transient.

The billet material was assumed to be pure annealed copper with the following temperature independent material properties:

- Young's modulus — $E = 12.5 \times 10^{3}\ kG.mm^{-2} = .1226 \times 10^{12}\ Pa$
- hardening modulus — $H' = 55.0\ kG.mm^{-2} = .5396 \times 10^{9}\ Pa$
- virgin yield stress — $\sigma_y = 8.0\ kG.mm^{-2} = .7848 \times 10^{8}\ Pa$
- Poisson's ratio — $\nu = 0.34$
- linear thermal expansion coeff. — $\alpha = 0.277 \times 10^{-5}\ K^{-1}$

- mass density $\rho = 8.94 \times 10^{6}\ g.m^{-3}$

- specific heat capacity $c_{\varepsilon} = 0.381\ J.g^{-1}.K^{-1}$

- thermal conductivity $k = 388.0\ W.m^{-1}.K^{-1}$

Numerical simulations were conducted using 'TEPAP', for the pressure rate $\dot{\bar{p}} = 100$ MPa/s, and for both uncoupled and coupled (with $\xi = 0$) thermoelastoplastic models. It was found that no significant plastic straining takes place during the first 0.1 x of the transient, and consequently, the first four time steps were marched with $\Delta t = 0.025$ s. The value $\Delta t = 0.00125$ s was used in the simulations for times $t > 0.1$ s, after it was found not to lead to any noticeable instabilities.

Reduced Gaussion integration ($M' = 2$, see Section 5.1.3) was employed in all calculations which were continued until the pressure $\bar{p} = 57.0$ MPa was attained. Attempts to continue the calculations past this point resulted in nonphysical predictions and were abandoned. Excessive and divergent deformations and varying temperatures predicted for the applied pressure range $\bar{p} \geq 57.0$ MPa suggest that the limit of model validity has been reached.

The predicted axial displacements of nodes 1 and 9 (made dimensionless by dividing them by the radius of the undeformed billet) are compared in FIGURE 17 with the corresponding (dimensionless) average axial displacement of the back face of the billet reported in the Reference [25]. According to 'TEPAP' predictions, the incipient bend in the applied pressure - displacement curves occurs at the

pressure $\bar{p} \sim 50$ MPa, which is lower than that of $\bar{p} \sim 75$ MPa reported by Iwata et al. This discrepancy may be attributed to differences between both the models and solution algorithms. The constant strain triangles could be expected to result in a generally stiffer behaviour than isoparametric elements used in conjunction with the reduced order Gauss integration. The reduced integration employs fewer number of sampling points per element than the full integration and is recommended for isoparametric elements [3,4,63], but results in poorer resolution of stresses and plastic strains and may lead to excessive underestimation of integrated quantities such as stiffness. The representation of the stress-strain relationship used in 'TEPAP' (the smooth stress-strain curve) should also be expected to result in earlier material plasticization than the bilinear representation used in Reference [25].

This effect could have played significant role in the simulations discussed, since only the moderate value of the exponent n = 20 (in the analytical representation of the smooth stress-strain curve (5.2.16)) was used. The close resemblance of the smooth stress-strain curve to the bilinear representation is achieved for large values of n, but these necessitate the usage of very small load increments in the elastoplastic transition regime and have to be avoided. Finally, the distinct ways of computing stresses and effective plastic strains (at nodes, by averaging the values calculated for surrounding triangles, in Reference [25], and at integration sampling points in 'TEPAP'), along with possible differences in boundary conditions, could also be viewed as factors contributing to differences in predictions.

The displacements, strains and stresses computed during 'TEPAP' simulations were not noticeably affected by the inclusion of the passive thermomechanical coupling in the model. The analysis of temperatures predicted for the coupled cases explains the former finding: The maximum increase of a local temperature did not exceed 1.08 K during the entire transient, and was much too low to result in any significant additional thermal strains and/or stresses. The rate independent model of mechanical behaviour (with the absence of temperature dependent material properties) results in the same stress and strain values predicted for a given value of applied (external) pressure, irrespective of its rate of change. The model indicates that for the applied pressure rate as high as 100 MPa/s, the internal dissipation rate is still too low to lead to considerable local temperature increases. The temperatures of nodes 58 and 72 (the nodes which exhibited the highest temperature rises) are ploted versus time in Figure 18. The slow temperature increases during the first phase of the transient correspond to the prevailing contribution of thermoelastic heating, when the compressive stresses result in negative dillation, and the negative sign of the strain tensor trace ε_{ii} (see equation (4.5.46)). The more rapid heating follows local yielding, which for these nodes occured at pressure $p \sim 35.0$ MPa. Thermoplastic dissipation then dominates and the net heating rate is controlled by the heat outflow through conduction.

CHAPTER 8

CONCLUSIONS AND RECOMMENDATIONS

The following conclusions can be drawn from the investigation pursued in this thesis:

(i) The coupled theory of quasistatic isotropic thermoelasto-plasticity admits the formulation of the boundary value problem consisting of the balance equations for linear momentum and thermal energy, constitutive equations for the rates of stress tensor and one scalar internal state variable, the inequality determining extent of yielding, and the appropriate initial and boundary conditions. The unknown fields in such a formulation are: displacement vector, temperature, independent components of stress tensor, and the internal state variable employed.

(ii) The Finite Element Method represents a plausible solution tool for the formulated non-linear boundary value problem of the coupled thermoelastoplasticity. A proposed computational algorithm has been proven to perform well for the linear thermoelastic problems. The implementation of its simplified version (code 'TEPAP') has been successfully employed for the

solution of one essentially two-dimensional problem in coupled thermoelastoplasticity.

(iii) A very limited assesment of the relevance of passive thermo-mechanical coupling is possible on the basis of the results of numerical simulations. The dimensionless number

$$\delta = \frac{27K^2\alpha^2T_0}{\rho c_\varepsilon(3K+4G)}$$

seems to represent a good measure of the significance of thermoelastic coupling, when compared with unity. For the thermal shock on ceramic tube case, when almost no effect of the coupling was detected in the simulations, the value of this parameter may be calculated as $\delta \simeq 0.0247$. The effect of thermoplastic couplings in the energy equation has not been systematically studied, but the appearance of the thermo-plastic heating (due to transformation of plastic strain energy into heat) upon onset of yielding was clearly demonstrated. It seems that this effect would be more pro-nounced in the latter stage of the studied process. Extension of the model into this range would require, however, reformulation of the theory within a general setting of non-linear kinematics.

The limited scope of this thesis investigation indicates numerous areas where improvements, generalizations and more extensive studies are possible and desirable. The following topics of further research are particularly recommended:

(i) Studies of the numerical aspects and practical performances of the computational solution algorithms, particularly with respect to the numerical conditioning of the systems of equations, the selection of the most suitable iteration schemes for both the solution of nodal incremental equations and the state determination stages, and the effects of time-stepping on numerical stability and accuracy.

(ii) Extension of the constitutive modelling of material behaviour to include newer, more realistic, and preferably physically based models, encompassing the rate and memory effects.

(iii) Extension of the presented theory and boundary value problem formulation to the general case of solid continuum undergoing finite straining and rotations.

(iv) Modelling and systematic simulation studies of the problems from areas where the passive thermomechanical effects are believed to be important, or even critical, for the proper understanding of the physical phenomena (metalworking, micro-mechanics, fracture, and other branches of mechanics mentioned in the discussion in CHAPTER 1).

REFERENCES

[1] Allen, D.H. and Haisler, W.E., "A Theory for Analysis of Thermoplastic Materials", Computers and Structures, 13, 1981, pp. 129-135.

[2] Allen, D.H., "Computational Aspects of the Nonisothermal Classical Plasticity", Computers and Structures, 15, 1982, pp. 589-599.

[3] Bathe, K.J., "Finite Element Procedures in Engineering Analysis", Prentice-Hall, Englewood Cliffs, New Jersey, 1982.

[4] Bathe, K.J. and Wilson, E.L., "Numerical Methods in Finite Element Analysis", Prentice-Hall, Englewood Cliffs, New Jersey, 1976.

[5] Bhandari, D.R. and Oden, J.T., "A Large Deformation Analysis of Crystalline Elastic-Viscoplastic Materials", Nucl. Engng. and Design, 29, 1974, pp. 360-369.

[6] Boley, B.A. and Weiner, J.H., "Theory of Thermal Stresses", John Wily and Sons, New York, 1960.

[7] Buyukozturk, O., "Numerical Models for Coupled Thermo-Conduction and Stress Analysis of Structures", Lecture Notes for the One-Day-Workshop on "Finite Element Analysis of Coupled Fluid-Thermoelastic Problems", November 1974, School of Engineering, Old Dominion University, Newport News, Virginia.

[8] Chan, A.S.L., "Finite Element Method in Plasticity Problems", presented at the Educational Conference on "Application of Finite Element Method in Non-linear Problems of Elasticity and Plasticity", Jablonna (Poland), Sept. 1974 (in Polish).

[9] Cheng, S.Y. and Hsu, T.R., "On Elasto-Plastic Stress-Strain Relationship for Multiaxial Stress States", Int. J. Num. Meth. Engng., 12, 1978, pp. 1617-1627.

[10] Cheng, S.Y., Hsu, T.R. and Too, J.M., "An Integrated Load Increment Method for Finite Elasto-Plastic Stress-Analysis", Int. J. Num. Engng., 15, 1980, pp. 833-842.

[11] Chung, T.J. and Yagawa, G., "The Incremental Theory of Three-Dimensional Transient Thermoelastoplasticity - Formulation and Solution", Developments in Mechanics, Vol. 7, Proceedings of the 13-th Midwestern Mechanics Conference, pp. 843-856.

[12] Coleman, B.D. and Gurtin, M.E., "Thermodynamics with Internal State Variables", J. Chem. Phys., 47, 1967, pp. 597-613.

[13] Danilovskaya, V.I., "Thermal Stresses in an Elastic Half-Space Due to a Sudden Heating of its Boundary", Prikl. Math. & Mekh., 14, 1950, p. 316 (in Russian).

[14] Dillon, O.W., "Coupled Thermoplasticity", J. Mech. Phys. Solids, 11, 1963, pp. 21-33.

[15] Fung, Y.C., "Foundation of Solid Mechanics", Prentice-Hall, Englewood Cliffs, New Jersey, 1965.

[16] Geradin, M., Idelsohn, S. and Hogge, M., "Computational Strategies for the Solution of Large Non-Linear Problems Via Quasi-Newton Methods", Comput. & Struct., 13, 1981, pp. 73-81.

[17] Guelin, P. and Boisserie, J.M., "The Heat Supply Trap Lying at the Origin of Thermo-Inelastic Analysis", Res Mechanica Letters, 2, 1982, pp. 13-17.

[18] Green, A.E. and Naghdi, P.M., "A General Theory of an Elastic-Plastic Continuum", Arch. Rat. Mech. Anal., 18, 1965, pp. 251-281.

[19] Halleux, J.P., "Modelling of Elasto-Plastic Material Behaviour", Nuclear Science and Technology, Joint Research Centre-Ispra Establishment-Italy, published by Commission of the European Communities, Brussels-Luxembourg, 1981.

[20] Head, J.L., "Inelastic Structural Analysis", Paper 6 presented at the British Nuclear Energy Society Symposium on "Trends in Structural Mechanics" in Berlin, Jan. 24, 1974, Nucl. Engng. and Design, 28, 1974, pp. 324-330.

[21] Hodge, P.g. jr. and White, G.N. jr., "A Quantitative Comparison of Flow and Deformation Theories of Plasticity", J. Appl. Mech., Trans. ASME, 72, 1950, pp. 180-184.

[22] Hsu, T.R., "On Behaviour of Fuel Elements Subject to Combined Cyclic Thermomechanical Loading", Nucl. Engng. and Design, 56, 1980, pp. 279-287.

[23] Hsu, T.R., "Transient Thermal Elastic-Plastic Stress Analysis on Nuclear Reactor Fuel Elements. Part I (Theory of TEPSA Computer Program)", Report No. 74-1-1, Thermomechanics and Composite Structures Laboratory, Dept. of Mech. Engineering, The University of Manitoba, Winnipeg, Canada.

[24] Hsu, T.R. and Gillespie, G.E., "Thermal Shock on Ceramic Tubes", Nucl. Engng. and Design, 16, 1971, pp. 45-58.

[25] Iwata, K., Osakada, K., Fujino, S., "Analysis of Hydrostatic Extrusion by the Finite Element Method", J. of Engrng. for Industry, Trans. ASME, 92, 1972, pp. 697-703.

[26] Keramidas, G.A. and Ting, E.C., "A Finite Element Formulation for Thermal Stress Analysis. Part I and II", Nucl. Engng. and Design, 39, 1976, pp. 267-289.

[27] Klepaczko, J., "Thermo-Mechanical Couplings in Metals", Report No. 11/1978, Polish Academy of Science, Inst. of Fundamental Technological Problems, Warsaw, 1978 (in Polish).

[28] Kratochvil, J. and Dillon, O.W., "Thermodynamics of Elasto-Plastic Materials as a Theory with Internal State Variables", J. Appl. Physics, 40, 1969, pp. 3207-3218.

[29] Krempl, E., "Cyclic Creep - An Interpretative Literature Survey", Bulletin No. 195, Welding Research Council, June 1974, pp. 63-123.

[30] Lee, E.H., "Elastic-Plastic Deformations at Finite Strains", J. Appl. Mech., 36, 1969, pp. 1-6.

[31] Lehmann, Th., "Some Thermodynamic Considerations of Phenomenological Theory of Non-Isothermal Elastic-Plastic Deformations", Arch. Mech., 24, 1972, pp. 975-989.

[32] Lehmann, Th., "Non-Isothermic Large Elastic-Plastic Deformations", Arch. Mech., 27, 1975, pp. 759-772.

[33] Lehmann, Th., "On the Theory of Large Non-Isothermic Elastic-Plastic and Elastic-Visco-Plastic Deformations", Arch. Mech., 29, 1977, pp. 393-409.

[34] Lehmann, Th., "Some Aspects of Non-Isothermic Large Inelastic Deformations", SM Archives, 3, 1978, pp. 261-317.

[35] Lehmann, Th., "Coupling Phenomena in Thermoplasticity", Invited Paper L1/1*, presented at the 5-th Intern. conf. on Struct. Mechanics in Reactor Technology, Berlin (West), August 1979.

[36] Lehmann, Th., "Coupling Phenomena in Thermoplasticity", Nucl. Engng. and Design, 57, 1980, pp. 323-332.

[37] Lehmann, Th., "On Constitutive Relations in Thermoplasticity", in "Three-Dimensional Constitutive Relations and Ductile Fracture", ed. S. Nemat-Nasser, North-Holland Pu. Co., 1981, pp. 289-306.

[38] Levy, A. and Pifko, A.B., "On Computational Strategies for Problems Involving Plasticity and Creep", Int. J. Num. Meth. Engng., 17, 1981, pp. 747-771.

[39] Levy, A., "High Temperature Inelastic Analysis", Comp. & Struct., 13, 1981, pp. 249-256.

[40] McClintock, F.A. and Argon, A.S., "Mechanical Behaviour of Materials", Adison Wesley, 1966.

[41] Mondkar, D.P. and Powell, G.H., "Evaluation of Solution Schemes for Nonlinear Structures", Comp. & Struct., 9, 1978, pp. 223-236.

[42] Mondkar, D.P. and Powell, G.H., "Finite Element Analysis of Thermo-Elasto-Plastic Structures", Proceedings of the Symposium on Applications of Computer Methods in Engineering, Los Angeles, Calif., August 23-26, 1977, pp. 1429-1438.

[43] Mróz, Z. and Raniecki, B., "On the Uniqueness Problem in Coupled Thermoplasticity", Int. J. Engng. Sci., 1976, 14, pp. 211-221.

[44] Mróz, Z. and Raniecki, B., "A Note on Variational Principles in Coupled Thermoplasticity", Bull. de l'Acad. Pol. des Sciences, Serie des Sciences Techniques, 23, 1975, pp. 133-139.

[45] Naghdi, P.M., "Stress-Strain Relations in Plasticity and Thermoplasticity", Proc. 2nd Symp. Naval Struct. Mech., Providence, 1960, Pergamon Press, New York, p. 121.

[46] Nickell, R.E. and Sackmann, J.L., "Approximate Solution in Linear Coupled Thermoelasticity", J. Appl. Mech., 35, 1968, pp. 255-266.

[47] Nied, H.A. and Battermann, S.C., "On Coupled Thermoplasticity: An Exact Solution for a Spherical Domain", Israel J. Techn., 9, 1971, pp. 37-46.

[48] Nied, H.A. and Battermann, S.C., "Effects of Coupled Thermoplasticity with Applications to a Hollow Sphere", Development of Mechanics, Vol. 7, Proceedings of the 13-th Midwestern Mechanics Conference, pp. 823-841.

[49] Nied, H.A. and Battermann, S.C., "On the Thermal Feedback Reduction of Latent Energy in the Heat Conduction Equation", Mater. Sci. Engng., 9, 1972, pp. 243-245.

[50] Nowinski, J.L., "Thermoelasticity with Applications", Sijthoff and Noordhoff, 1978.

[51] Nyssen, C., "An Efficient and Accurate Iterative Method Allowing Large Incremental Steps To Solve Elasto-Plastic Problems", Comp. & Struct., 13, 1981, pp. 63-71.

[52] Oden, J.T., "Finite Element Analysis of Nonlinear Problems in the Dynamical Theory of Coupled Thermoelasticity", Nucl. Eng. and Design, 19, 1969, pp. 465-475.

[53] Owen, D.R.J. and Hinton, E., "Finite Elements in Plasticity: Theory and Practice", Pineridge Press Limited, Swansea, U.K., 1980.

[54] Perzyna, P. and Sawczuk, A., "Problems of Thermoplasticity", Nucl. Engng. and Design, 24, 1973, pp. 1-55.

[55] Raniecki, B. and Sawczuk, A., "Thermal Effects in Plasticity", ZAMM, 55, 1975, Parts 1 and 2, pp. 333-341 and 363-373.

[56] Rebello, N. and Kobayashi, S., "A Coupled Analysis of Viscoplastic Deformation and Heat Transfer. Parts I and II", Int. J. Mech. Sci., 22, 1980, pp. 707-718.

[57] Rutkowski, J., "Introduction to Mass, Momentum, Energy and Entropy Balances", Warsaw Techn. Univ. Press, Warsaw, 1976 (in Polish).

[58] Snyder, M.D. and Bathe K.J., "A Solution Procedure for Thermo-Elastic-Plastic and Creep Problems", Nucl. Engng. and Design, 64, 1981, pp. 49-80.

[59] William, K.J., "Numerical Solution of Inelastic Rate Processes", Comp. & Struct., 8, 1978, pp. 511-531.

[60] Wissmann, J.W. and Hauck, Ch., "Efficient Elastic-Plastic Finite Element Analysis with Higher Order Stress-Point Algorithms", Comp. & Struct., 17, 1983, pp. 89-95.

[61] Yamada, Y., Yoshimura, N. and Sakurai, T., "Plastic Stress-Strain Matrix and Its Application for the Solution of Elastic-Plastic Problems by the Finite Element Method", Int. J. Mech. Sci., 10, 1968, pp. 343-354.

[62] Ziegler, H., "An Introduction to Thermomechanics", North-Holland, Amsterdam-New York, Oxford, 1977.

[63] Zienkiewicz, O.C., "The Finite Element Method", McGraw-Hill, London, 1977.

[64] Zudans, Z., Reddi, M.M., Fishmann, H.M. and Tsai, H.C., "Elastic-Plastic Creep Analysis of High Temperature Nuclear Reactor Components", Nucl. Engng. and Design, 28, 1974, pp. 414-445.

Table 1. Summary Overview of Thermoplastic Models Used by Various Authors.

Author (year)	Physical interpretation of scalar internal variable used, and additional assumptions	Rate of internal energy being stored on the microlevel $\rho\dot{e}^{(p)}$	Model for internal dissipation rate D	Model for heat of plastic deformation $\rho\dot{\theta}\frac{\partial}{\partial\theta}(\frac{\partial\psi}{\partial\theta})$
Dillon (1963)	no internal variables; incompressibility during plastic deformation and deviatoric plastic strains responsible for internal dissipation assumed	0	$\sigma_{ij}\dot{\varepsilon}_{ij}^{(p)} = \sigma'_{ij}\dot{\varepsilon}'_{ij}{}^{(p)}$	0
Lee (1969)	no internal variables; plastic work rate $\sigma_{ij}\dot{\varepsilon}_{ij}^{(p)}$ used as a (process) variable characterizes inelastic deformation at adiabatic loading	$(1-\xi)\sigma_{ij}\dot{\varepsilon}_{ij}^{(p)}$	$\xi\sigma_{ij}\dot{\varepsilon}_{ij}^{(p)}$ ξ - factor varying slowly from about 0.9 to unity with increasing plastic flow	0
Need and Batterman	κ - scalar internal state variable specified as the dislocation density evolution equation for κ: $\chi\dot{\kappa} = \sigma_{ij}\dot{\varepsilon}_{ij}^{(p)}$ χ - dislocation energy per unit length (constant)	$\Lambda\sigma_{ij}\dot{\varepsilon}_{ij}^{(p)}$	$(1-\Lambda)\sigma_{ij}\dot{\varepsilon}_{ij}^{(p)}$ Λ - increasing with temperature factor representing the ratio of rates of energy stored on the microscale to kinetic energy converted into internal energy during adiabatic inelastic deformation	$\dot{\theta}\chi\frac{\partial\Lambda}{\partial\theta}$ where $\frac{\partial\psi}{\partial\theta} = \frac{\Lambda}{\rho}\chi$

Author (year)	Physical interpretation of scalar internal variable used, and additional assumptions	Rate of internal energy being stored on the microlevel $\rho \frac{\partial e^{(p)}}{\partial \kappa} \dot{\kappa}$	Model for internal dissipation rate D	Model for heat of plastic deformation $\rho\dot{\theta}\frac{\partial}{\partial\theta}(\frac{\partial\psi}{\partial\kappa})$
Raniecki and Sawczuk (1975)	κ - scalar internal state variable distinct from work hardening parameter evolution equation for κ: $\dot{\kappa} = \omega(\sigma_{ij},\theta)\,\sigma_{ij}\dot{\varepsilon}^{(p)}_{ij}$ $\omega(\sigma_{ij},\theta)$ - integrating factor	$\chi(\kappa,\theta)\dot{\kappa}$ where the factor $\chi(\kappa,\theta)$ is proposed to be evaluated in an experimental program	$\sigma_{ij}\dot{\varepsilon}^{(p)}_{ij} - \pi\dot{\kappa}$ where $\pi = \pi(\theta,\kappa) = \rho\frac{\partial\psi}{\partial\kappa} = \rho\frac{\partial\psi}{\partial\kappa}^{(p)}$ is the variable conjugated to the internal state variable κ; it should be determined from the equation: $\pi(\theta,\kappa) - \theta\frac{\partial}{\partial\theta}\pi(\theta,\kappa) = \chi(\kappa,\theta)$	$\dot{\theta}\frac{\partial\pi}{\partial\theta}$
Lehmann (1975)	κ - scalar internal state variable distinct from work hardening parameter evolution equation for κ: $\dot{\kappa} = (1-\xi)\sigma_{ij}\dot{\varepsilon}^{(p)}_{ij}$	$\dot{\kappa} = (1-\xi)\sigma_{ij}\dot{\varepsilon}^{(p)}_{ij}$ because from $\rho\psi^{(p)} = \kappa$ it follows that $\rho\frac{\partial e^{(p)}}{\partial\kappa}\dot{\kappa} = [\rho\frac{\partial\psi^{(p)}}{\partial\kappa} - \theta\frac{\partial}{\partial\theta}(\rho\frac{\partial\psi^{(p)}}{\partial\kappa})]\dot{\kappa} = \dot{\kappa}$	$\xi\sigma_{ij}\dot{\varepsilon}^{(p)}_{ij}$	0
Mróz and Raniecki (1976)	κ - scalar internal state variable describing state of (osotropic) hardening. Yield function is assumed as: $F(\sigma_{ij},\pi,\kappa,\theta) = 0$, and evolution equation for κ is assumed as: $\dot{\kappa} = \lambda\frac{\partial F}{\partial\pi}$ λ - proportionality factor	$(\pi - \theta\frac{\partial\pi}{\partial\theta})\dot{\kappa}$	$\sigma_{ij}\dot{\varepsilon}^{(p)}_{ij} - \pi\dot{\kappa}$ where $\pi = \pi(\theta,\kappa) = \rho\frac{\partial\psi}{\partial\kappa} = \rho\frac{\partial\psi}{\partial\kappa}^{(p)}$ is the state equation for the variable π - power conjugated to the internal state variable κ, and either $\psi(\varepsilon^{(e)}_{ij},\theta,\kappa)$ or $\psi^{(p)}(\theta,\kappa)$ is known function. Another possibility is to postulate $D = D(\dot{\varepsilon}^{(p)}_{ij},\dot{\kappa},\kappa,\theta)$ as the convex plastic potential, and to use Ziegler's orthogonality principle [62] to obtain: $\pi = \frac{\partial D}{\partial\kappa}$	$\dot{\theta}\frac{\partial\pi}{\partial\theta}$

Table 1 (continued)

Table 2. Summary of Constitutive Rate Equations Resulting from the Theory of Coupled Isotropic Thermoelastoplasticity.

(continued on next page)

$$\dot{\sigma}_{ij} = C^{(ep)}_{ijrs}\dot{\varepsilon}_{rs} + \beta^{(ep,th)}\dot{T}$$

where:

$$C^{(ep)}_{ijrs} = C^{(e)}_{ijrs} - jC^{(p)}_{ijrs}$$

$$C^{(e)}_{ijrs} = G(\delta_{ir}\delta_{js} + \delta_{is}\delta_{jr}) + (K - \frac{2}{3}G)\delta_{ij}\delta_{rs}$$

$$C^{(p)}_{ijrs} = \frac{4G^2}{(\frac{2}{3}\sigma_y)^2(H' + 3G)}\sigma'_{ij}\sigma'_{rs}$$

$$\beta^{(ep,th)}_{ij} = \beta^{(e,th)}_{ij} - j\beta^{(p,th)}_{ij}$$

$$\beta^{(e,th)}_{ij} = [-\frac{1}{3K}\frac{\partial K}{\partial T}\sigma_{kk} + 3K(\alpha + \frac{\partial \alpha}{\partial T}(T + T_0))]\delta_{ij} - \frac{1}{G}\frac{\partial G}{\partial T}\sigma'_{ij}$$

$$\beta^{(p,th)}_{ij} = -\frac{3G}{\sigma_y}\frac{\frac{\sigma_y}{G}\frac{\partial G}{\partial T} - H''}{H' + 3G}\sigma'_{ij}$$

$$\lambda = \frac{2G}{(\frac{2}{3}\sigma_y)^2(H' + 3G)}\sigma'_{rs}\dot{\varepsilon}_{rs} + \frac{\frac{\sigma_y}{G}\frac{\partial G}{\partial T} - H''}{\frac{2}{3}\sigma_y(H' + 3G)}\dot{T}$$

$$\dot{\varepsilon}^{(p)}_{ij} = \frac{2G}{(\frac{2}{3}\sigma_y)^2(H' + 3G)}\sigma'_{ij}\sigma'_{rs}\dot{\varepsilon}_{rs} + \frac{\frac{\sigma_y}{G}\frac{\partial G}{\partial T} - H''}{\frac{2}{3}\sigma_y(H' + 3G)}\sigma'_{ij}\dot{T}$$

$$D = j\xi\frac{3G}{H' + 3G}\sigma'_{rs}\dot{\varepsilon}_{rs} + j\xi\frac{\frac{\sigma_y}{G}\frac{\partial G}{\partial T} - H''}{H' + 3G}\sigma_y\dot{T}$$

Table 2 (continued)

$$\theta \frac{\partial \sigma_{ij}}{\partial \theta} \dot{\varepsilon}_{ij} = - (\beta_{ij}^{(e,th)} + j \frac{3 \frac{\partial G}{\partial T}}{H' + 3G} \sigma'_{ij})(T + T_0)\dot{\varepsilon}_{ij}$$

$$- j \frac{\sigma_y}{G} \frac{\partial G}{\partial T} \frac{\frac{\sigma_y}{G} \frac{\partial G}{\partial T} - H''}{H' + 3G} (T + T_0)\dot{T}$$

Comment: The temperature dependent elastic constants are the shear and compressibility modulii:

$$G = \frac{E}{2(1 + \nu)} \qquad K = \frac{E}{3(1 - 2\nu)}$$

Table 3. Summary of Fundamental Constitutive Matrices for Thermo-elastoplastic Isotropic Axisymmetric Solid.

(continued on next page)

Elastic Stiffness

$$[C^{(e)}] = \begin{bmatrix} K + \frac{4}{3}G & K - \frac{2}{3}G & K - \frac{2}{3}G & 0 \\ K - \frac{2}{3}G & K + \frac{4}{3}G & K - \frac{2}{3}G & 0 \\ K - \frac{2}{3}G & K - \frac{2}{3}G & K + \frac{4}{3}G & 0 \\ 0 & 0 & 0 & G \end{bmatrix}$$

Plastic Stiffness

$$[C^{(p)}] = \frac{4G^2}{(\frac{2}{3}\sigma_y)^2(H' + 3G)} \{\sigma'\}\{\sigma'\}^T$$

Elastoplastic Stiffness

$$[C^{(ep)}] = [C^{(e)}] - j[C^{(p)}]$$

Elastic Thermal Moduli

$$\{\beta^{(e,th)}\} = [3K(\alpha + \frac{\partial\alpha}{\partial T}(T + T_0)) - \frac{1}{3K}\frac{\partial K}{\partial T}\{\sigma\}^T\{1\}]\{1\} - \frac{1}{G}\frac{\partial G}{\partial T}\{\sigma'\}$$

Plastic Thermal Moduli

$$\{\beta^{(p,th)}\} = \frac{3G}{\sigma_y}\frac{H'' - \frac{\sigma_y}{G}\frac{\partial G}{\partial T}}{H' + 3G}\{\sigma'\}$$

Table 3 (continued)

Elastoplastic Thermal Moduli

$$\{\beta^{(ep,th)}\} = \{\beta^{(e,th)}\} - j\{\beta^{(p,th)}\}$$

Thermoelastic Coupling Moduli

$$\{B^{(e)}\} = \{\beta^{(e,th)}\}(T + T_0)$$

Thermoplastic Coupling Moduli

$$\{B^{(p)}\} = \frac{3G}{H' + 3G}\left(\xi - \frac{1}{G}\frac{\partial G}{\partial T}(T + T_0)\right)\{\sigma'\}$$

Thermoplastic Heat Capacity

$$\gamma = \sigma_y \frac{H'' - \frac{\sigma_y}{G}\frac{\partial G}{\partial T}}{H' + 3G}\left(\xi - \frac{1}{G}\frac{\partial G}{\partial T}(T + T_0)\right)$$

Thermoelastoplastic Coupling Moduli

$$\{B^{(ep)}\} = \{B^{(e)}\} - j\{B^{(p)}\}$$

where

$$\{\sigma\} = [\sigma_{rr} \quad \sigma_{zz} \quad \sigma_{\theta\theta} \quad \sigma_{rz}]^T$$

$$\{\sigma'\} = \left(1 - \frac{1}{3}\{1\}\{1\}^T\right)\{\sigma\}$$

$$\{1\} = [1 \quad 1 \quad 1 \quad 0]^T$$

Table 4. Summary of Discrete Model Equations.

(continued on next page)

NODAL EQUATIONS FOR THE ENTIRE ASSEMBLY OF ELEMENTS

$$[K]\{\dot{U}\} + [E]\{\dot{T}\} = \{F\}$$

$$[R]\{\dot{U}\} + [C]\{\dot{T}\} + [S]\{T\} = \{Q\}$$

where

$$[K] = \sum_e [K^{(e)}] = \sum_e \int_{V^{(e)}} [H_u]^T [C^{(ep)}][H_u] dV^{(e)}$$

$$[E] = \sum_e [E^{(e)}] = -\sum_e \int_{V^{(e)}} [H_u]^T \{\beta^{(ep,th)}\}\{N_T\}^T dV^{(e)}$$

$$[R] = \sum_e [R^{(e)}] = \sum_e \int_{V^{(e)}} \{N_T\}\{B^{(ep)}\}^T [H_u] dV^{(e)}$$

$$[C] = \sum_e [C^{(e)}] = \sum_e \int_{V^{(e)}} (\rho c_\varepsilon + \gamma)\{N_T\}\{N_T\}^T dV^{(e)}$$

$$[S] = \sum_e [S^{(e)}] = \sum_e \int_{V^{(e)}} k[H_T]^T [H_T] dV^{(e)} + \sum_b \int_{S^{(b)}} \bar{h}\{N_T\}\{N_T\} dS^{(b)}$$

$$\{F\} = \sum_e \{F^{(e)}\} = \sum_e \int_{V^{(e)}} \rho[N_u]^T \{\dot{b}\} dV^{(e)} + \sum_b \int_{S^{(b)}} [N_u]^T \bar{\bar{p}}\{n\} dS^{(b)}$$

$$\{Q\} = \sum_e \{Q^{(e)}\} = \sum_e \int_{V^{(e)}} \rho r\{N_T\} dV^{(e)} + \sum_b \int_{S^{(b)}} (\bar{\bar{h}}\bar{\bar{T}}_\infty - \bar{q})\{N_T\} dS^{(b)}$$

$$\{U\} = \sum_e \{u^{(e)}\}$$

$$\{T\} = \sum_e \{T^{(e)}\}$$

Table 4 (Continued)

SAMPLING POINT EQUATIONS FOR EACH SAMPLING POINT

$$\{\dot{\sigma}\} = [C^{(ep)}][H_u]\{\dot{u}^{(e)}\} - \{\beta^{(ep,th)}\}\{N_T\}^T\{\dot{T}^{(e)}\}$$

$$\dot{\bar{\varepsilon}}^{(p)} = \frac{2G}{\frac{2}{3}\sigma_y(H' + 3G)}\{\sigma'\}^T[H_u]\{\dot{u}^e\} + \frac{\frac{\sigma_y}{G}\frac{\partial G}{\partial T} - H''}{H' + 3G}\{N_T\}^T\{\dot{T}^{(e)}\}$$

Table 5. Brief Functional Description of TEPAP Subprograms

ADDBAN	adds element contributions to global system matrix (e.g. upper or lower triangular components of the global system matrix) and global system RHS-vector
ADDRES	calculates addresses of diagonal elements in the global system matrix
BODAQ4	reads in boundary data and computes identifiers of natural boundary conditions
CL	evaluates fundamental constitutive matrices (see Table 3) at a given point of an element
CLEAR	clears matrices
COLHT	updates column height of the global system matrix
DOT	calculates scalar product of two given vectors
EFS	calculates effective stress or effective strain rate
ELAS	evaluates elastic stiffness matrix
ELDAQ4	reads in elemental data; assembles connection and connectivity matrices; calculates column heights and bandwidth
ERROR	prints messages when allocated core memory is exceeded

Table 5 (continued)

FHTC1*	evaluates heat transfer coefficient at a given boundary location
FTSUR*	calculates surroundings' (bulk fluid) temperature at a given boundary location
HEFLU1*	calculates prescribed normal to the boundary component of heat flux vector at a given boundary location
INT	locates a given value of a parameter in an appropriate range of tabulated values (to enable a linear interpolation)
NODATA	reads and/or generates initial nodal coordinates and temperatures; calculates equation numbers and stores them in the identification array; identifies code numbers of skew displacement boundary conditions and stores them in the identification array
PRESS1*	calculates external pressure rate at a given boundary location
Q4	manages elemental operations for linear and quadratic quadrilateral isoparametic elements
Q4CALL	determines addresses of starting elements of variables required in Q4
QUAD4	calculates elemental matrices for linear and quadratic quadrilateral isoparametric elements
SHAPEQ4	evaluates shape function matrices and its derivatives with respect to the global coordinates at a given point of linear quadrilateral isoparametric element

Table 5 (continued)

SHAPE2	extends the computations performed by SHAPEQ4 to the case of quadratic quadrilateral isoparametric element
SIG	calculates yield stress at given temperature and accumulated effective total strain
SIGY	calculates yield stress at given temperature and accumulated effective plastic strain
SIDEV	calculates mean stress and stress deviator components
STDG	calculates interpolation matrices for displacements, temperatures, strains and temperature gradients
TANMOD	calculates tangent modulus at given temperature and accumulated effective total strain
TEMPQ4	calculates initial temperatures at element sampling points
UACTCL	solves system of simultaneous linear equations in core using compacted, active column storage scheme
UPST	calculates control parameters indicating current stress state on effective stress vs effective strain curve; corrects the predicted stress vector increment by enforcing the yield condition
WRITE	prints nodal values of temperature and displacements

---

* case dependent subprogram to be supplied by the code user.

Table 6. Temperature and Stress Predictions for the Thermal Shock on the Ceramic Tube Case Study - Comparison between Uncoupled and Coupled Simulations with 'TEPAP'.

Radial Position	Temperature (°C)		Radial Stress (Pa)		Hoop Stress (Pa)		Axial Stress (Pa)	
	D	C	D	C	D	C	D	C
0.7537	768.292	768.422	0.406E+6	0.405E+6	0.560E+8	0.558E+8	0.708E+8	0.705E+8
0.7713	773.219	773.349	0.132E+7	0.132E+7	0.426E+8	0.425E+8	0.583E+8	0.581E+8
0.7787	776.425	776.553	0.182E+7	0.182E+7	0.340E+8	0.339E+8	0.503E+8	0.500E+8
0.7963	780.389	780.513	0.231E+7	0.230E+7	0.235E+8	0.234E+8	0.402E+8	0.400E+8
0.8037	782.892	783.012	0.254E+7	0.254E+7	0.170E+8	0.169E+8	0.339E+8	0.337E+8
0.8213	785.970	786.083	0.273E+7	0.272E+7	0.901E+7	0.894E+7	0.261E+8	0.259E+8
0.8287	787.861	787.969	0.277E+7	0.277E+7	0.419E+7	0.413E+7	0.214E+8	0.212E+8
0.8463	790.159	790.259	0.275E+7	0.274E+7	-.159E+7	-.163E+7	0.156E+8	0.154E+8
0.8537	791.540	791.634	0.267E+7	0.266E+7	-.500E+7	-.502E+7	0.121E+8	0.119E+8
0.8713	793.187	793.272	0.251E+7	0.250E+7	-.900E+7	-.900E+7	0.793E+7	0.777E+7
0.8787	794.158	794.237	0.236E+7	0.235E+7	-.113E+8	-.113E+8	0.547E+7	0.534E+7
0.8963	795.287	795.358	0.212E+7	0.211E+7	-.139E+8	-.139E+8	0.262E+7	0.251E+7
0.9037	795.941	796.006	0.192E+7	0.191E+7	-.154E+8	-.153E+8	0.972E+6	0.870E+6
0.9213	796.677	796.736	0.164E+7	0.163E+7	-.169E+8	-.169E+8	-.887E+6	-.972E+6
0.9287	797.092	797.147	0.142E+7	0.141E+7	-.178E+8	-.177E+8	-.194E+7	-.201E+7
0.9463	797.540	797.590	0.112E+7	0.112E+7	-.186E+8	-.185E+8	-.307E+7	-.313E+7
0.9537	797.781	797.827	0.901E+6	0.896E+6	-.190E+8	-.189E+8	-.367E+7	-.373E+7
0.9713	798.017	798.061	0.603E+6	0.599E+6	-.193E+8	-.192E+8	-.427E+7	-.432E+7
0.9787	798.126	798.168	0.388E+6	0.386E+6	-.193E+8	-.192E+8	-.455E+7	-.459E+7
0.9963	798.199	798.240	0.102E+6	0.101E+6	-.192E+8	-.191E+8	-.473E+7	-.477E+7

Table 7. Temperature and Stress Predictions for the Thermal Shock on the Ceramic Tube Case Study - Comparison between Uncoupled Simulations with 'TEPAP' and 'TEPSA'.

Radial Position	Temperature (°C)		Radial Stress (Pa)		Hoop Stress (Pa)		Axial Stress (Pa)	
	TEPAP	TEPSA	TEPAP	TEPSA	TEPAP	TEPSA	TEPAP	TEPSA
0.7500	766.10	766.56						
0.7537	768.29		0.406E+6	0.800E+6	0.560E+8	0.490E+8	0.708E+8	0.643E+8
0.7713	773.22		0.132E+7	0.800E+6	0.426E+8	0.490E+8	0.583E+8	0.643E+8
0.7750	774.63	775.12						
0.7787	776.43		0.182E+7	0.200E+7	0.340E+8	0.284E+8	0.503E+8	0.449E+8
0.7963	780.39		0.231E+7	0.200E+7	0.235E+8	0.284E+8	0.402E+8	0.449E+8
0.8000	781.50	781.89						
0.8037	782.89		0.254E+7	0.257E+7	0.170E+8	0.127E+8	0.339E+8	0.298E+8
0.8213	785.97		0.273E+7	0.257E+7	0.901E+7	0.127E+8	0.261E+8	0.298E+8
0.8250	786.83	787.12						
0.8287	787.86		0.277E+7	0.270E+7	0.419E+7	0.115E+7	0.214E+8	0.184E+8
0.8463	790.16		0.275E+7	0.270E+7	-.159E+7	0.115E+7	0.156E+8	0.184E+8
0.8500	790.81	790.94						
0.8537	791.54		0.267E+7	0.254E+7	-.500E+7	-.699E+7	0.121E+8	0.101E+8
0.8713	793.19		0.251E+7	0.254E+7	-.900E+7	-.699E+7	0.793E+7	0.101E+8
0.8750	793.66	793.67						
0.8787	794.16		0.236E+7	0.220E+7	-.113E+8	-.124E+8	0.547E+7	0.428E+7
0.8963	795.29		0.212E+7	0.220E+7	-.139E+8	-.124E+8	0.262E+7	0.429E+7
0.9000	795.68	795.56						
0.9037	795.94		0.192E+7	0.175E+7	-.154E+8	-.159E+8	0.972E+6	0.366E+6
0.9213	796.68		0.164E+7	0.175E+7	-.169E+8	-.159E+8	-.887E+6	0.366E+6
0.9250	796.89	796.78						
0.9287	797.09		0.142E+7	0.125E+7	-.178E+8	-.179E+8	-.194E+7	-.213E+7
0.9463	797.54		0.112E+7	0.125E+7	-.186E+8	-.179E+8	-.307E+7	-.213E+7
0.9500	797.67	797.50						
0.9537	797.78		0.901E+6	0.740E+6	-.190E+8	-.189E+8	-.367E+7	-.359E+7
0.9713	798.02		0.603E+6	0.740E+6	-.193E+8	-.189E+8	-.427E+7	-.359E+7
0.9750	798.08	797.94						
0.9787	798.13		0.388E+6	0.241E+6	-.193E+8	-.190E+8	-.455E+7	-.425E+7
0.9963	798.20		0.102E+6	0.241E+6	-.192E+8	-.190E+8	-.473E+7	-.425E+7
1.0000	798.20	798.05						

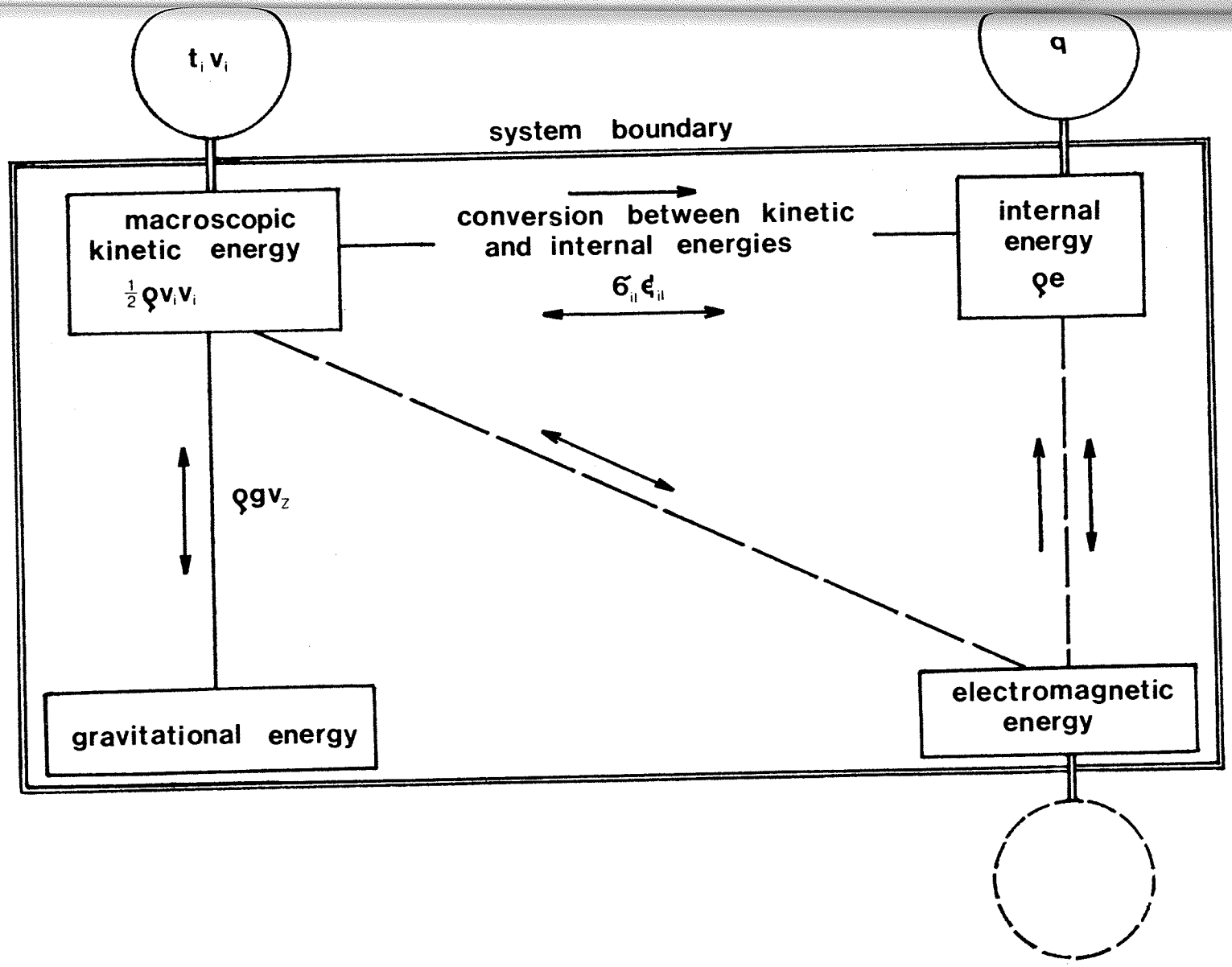

FIGURE I: Schematic Presentation of Energy Balance in a Solid Material Element (adopted from Rutkowski [57]).

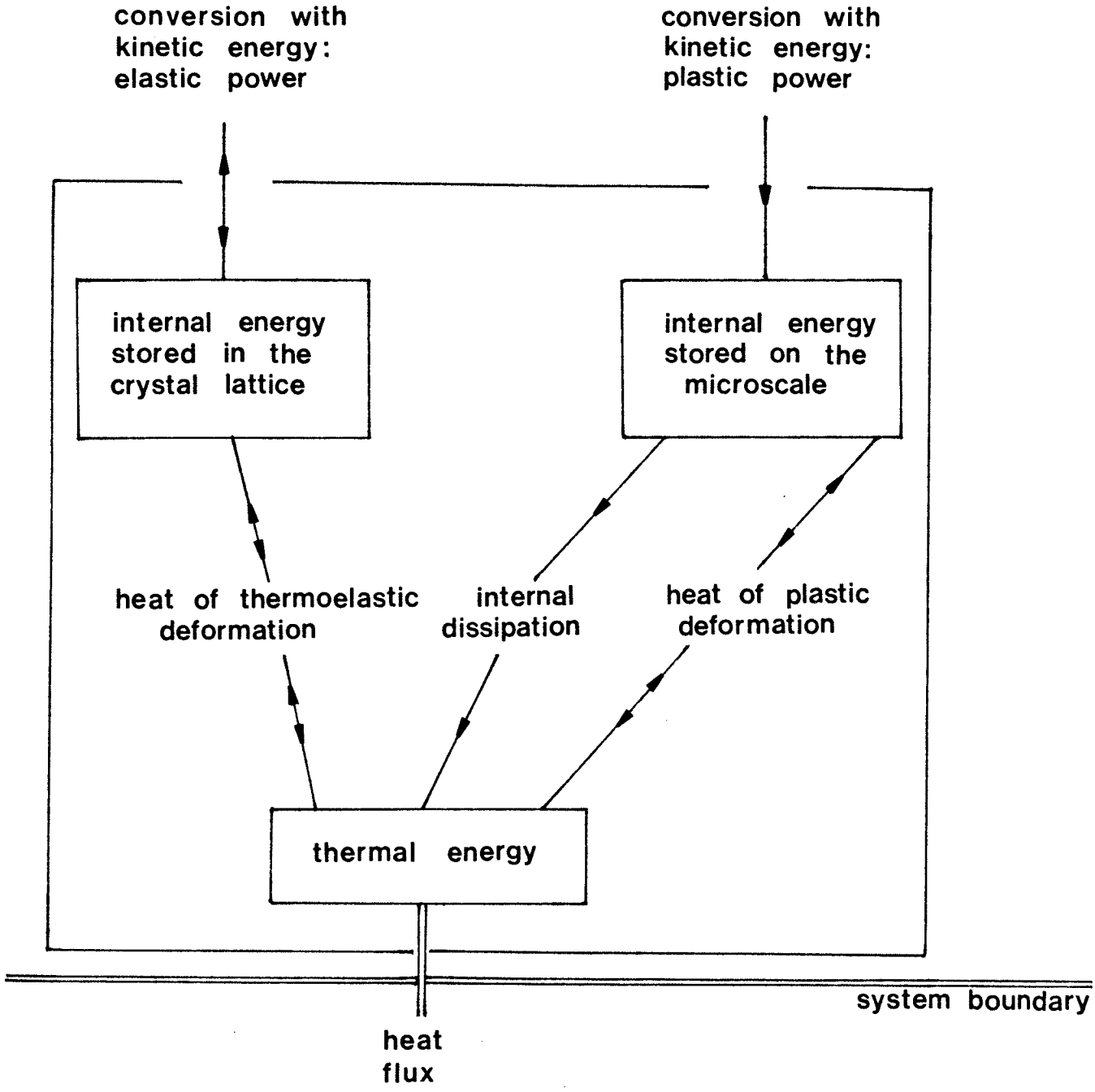

FIGURE 2: Schematic Presentation of Internal Energy Balance in a Thermoelastoplastic Material Element (as used in this thesis).

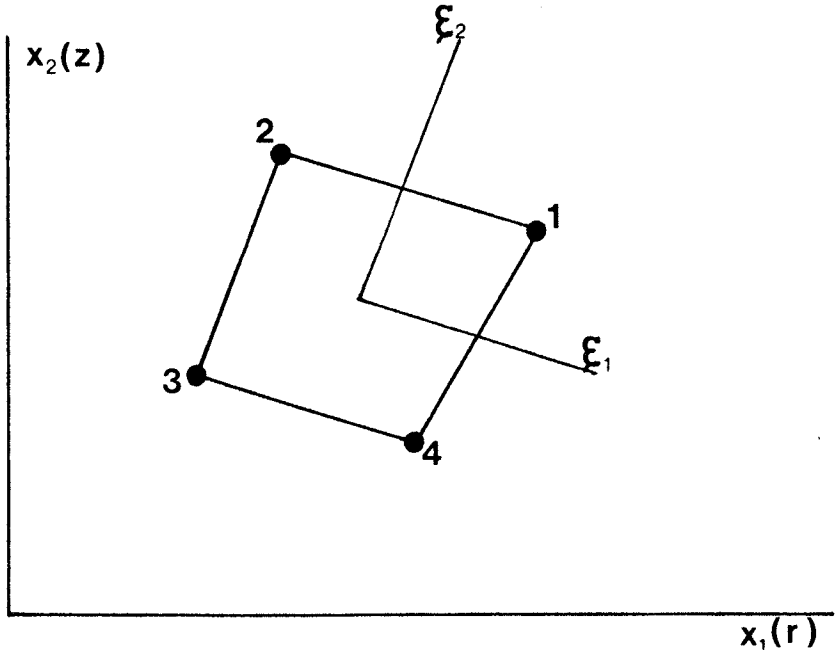

FIGURE 3: Four-nodes Isoparametric Element.

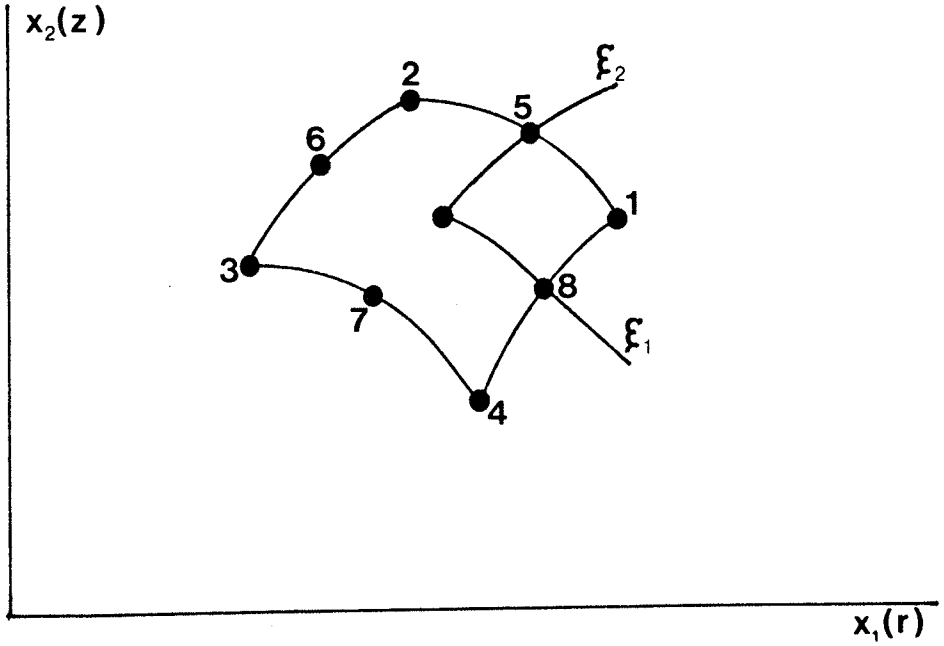

FIGURE 4: Nine-nodes Isoparametric Element.

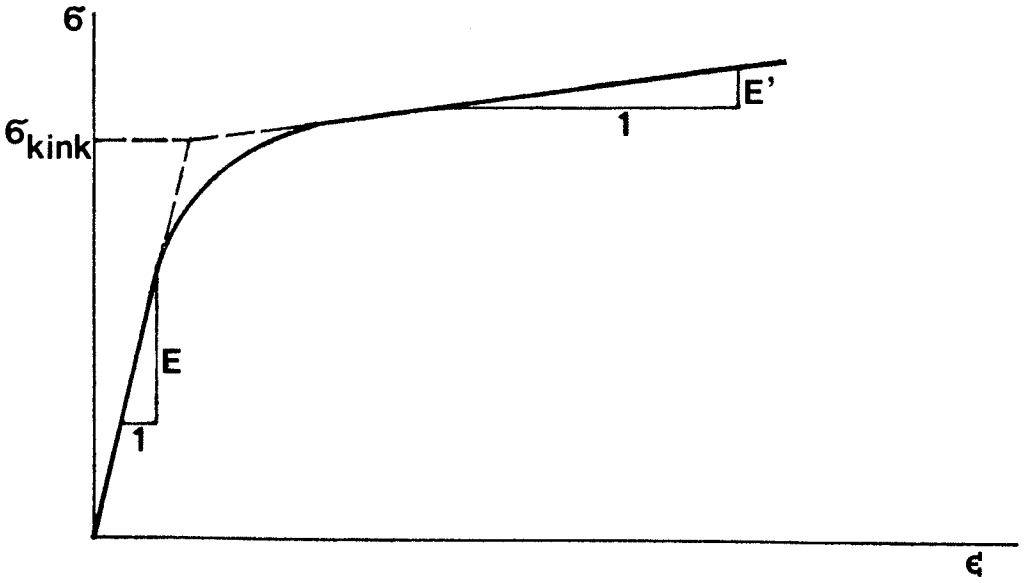

FIGURE 5: Isothermal Uniaxial Stress-Strain Curve.

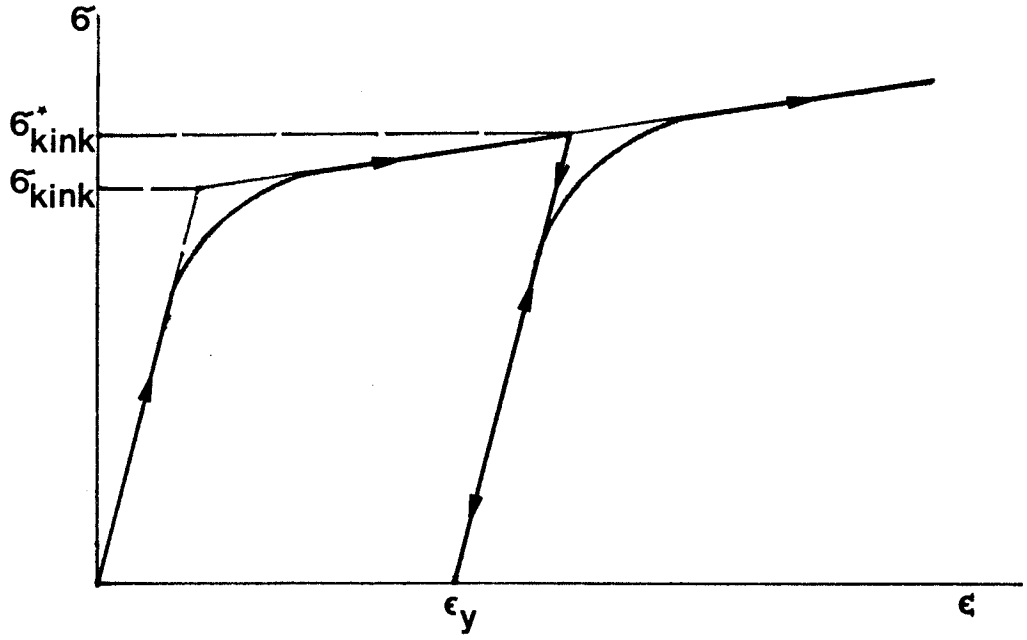

FIGURE 6: Definitions of Secondary Yield Surface Parameters σ^*_{kink} and ε_y.

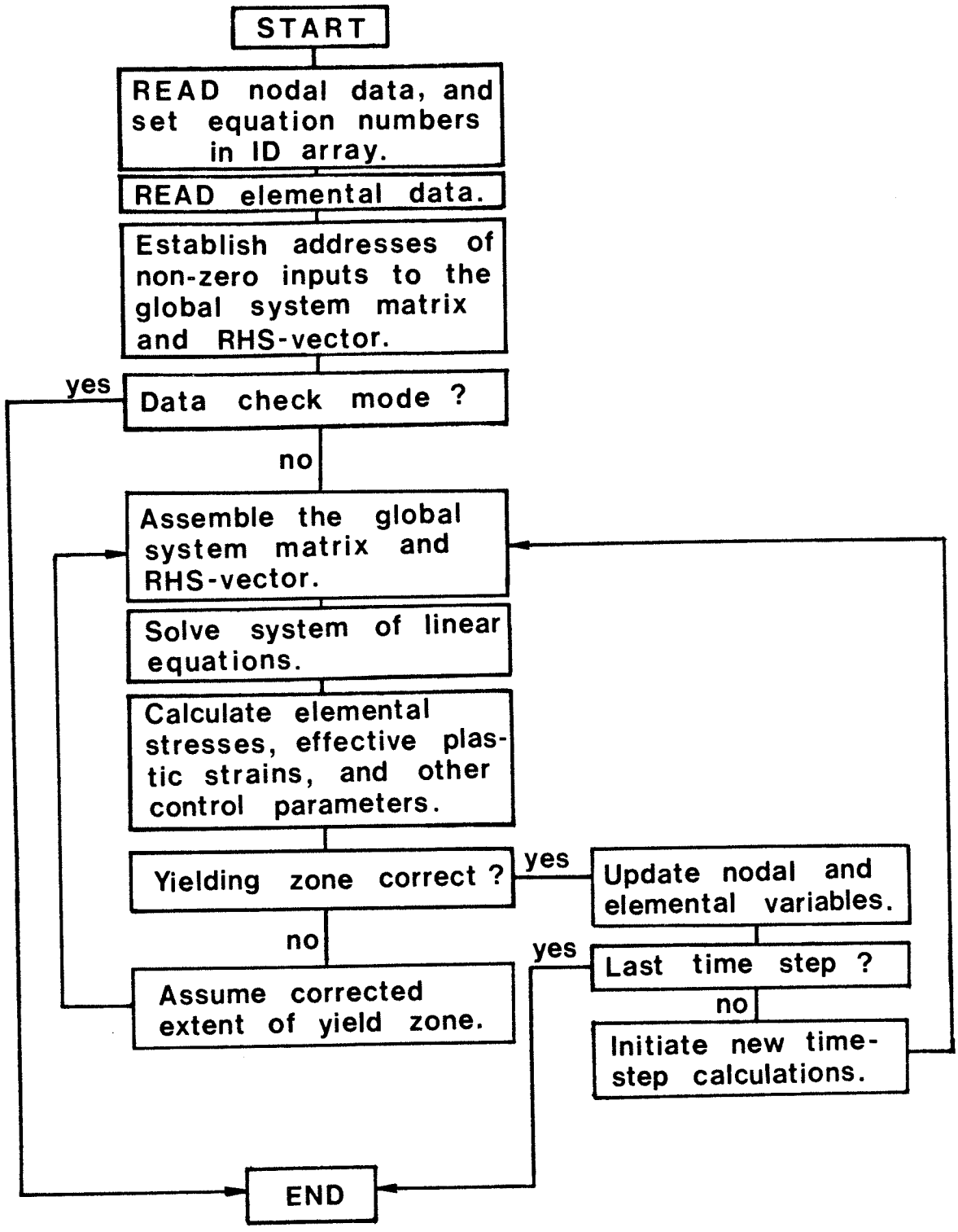

FIGURE 7: Flow Chart of 'TEPAP' Main Program.

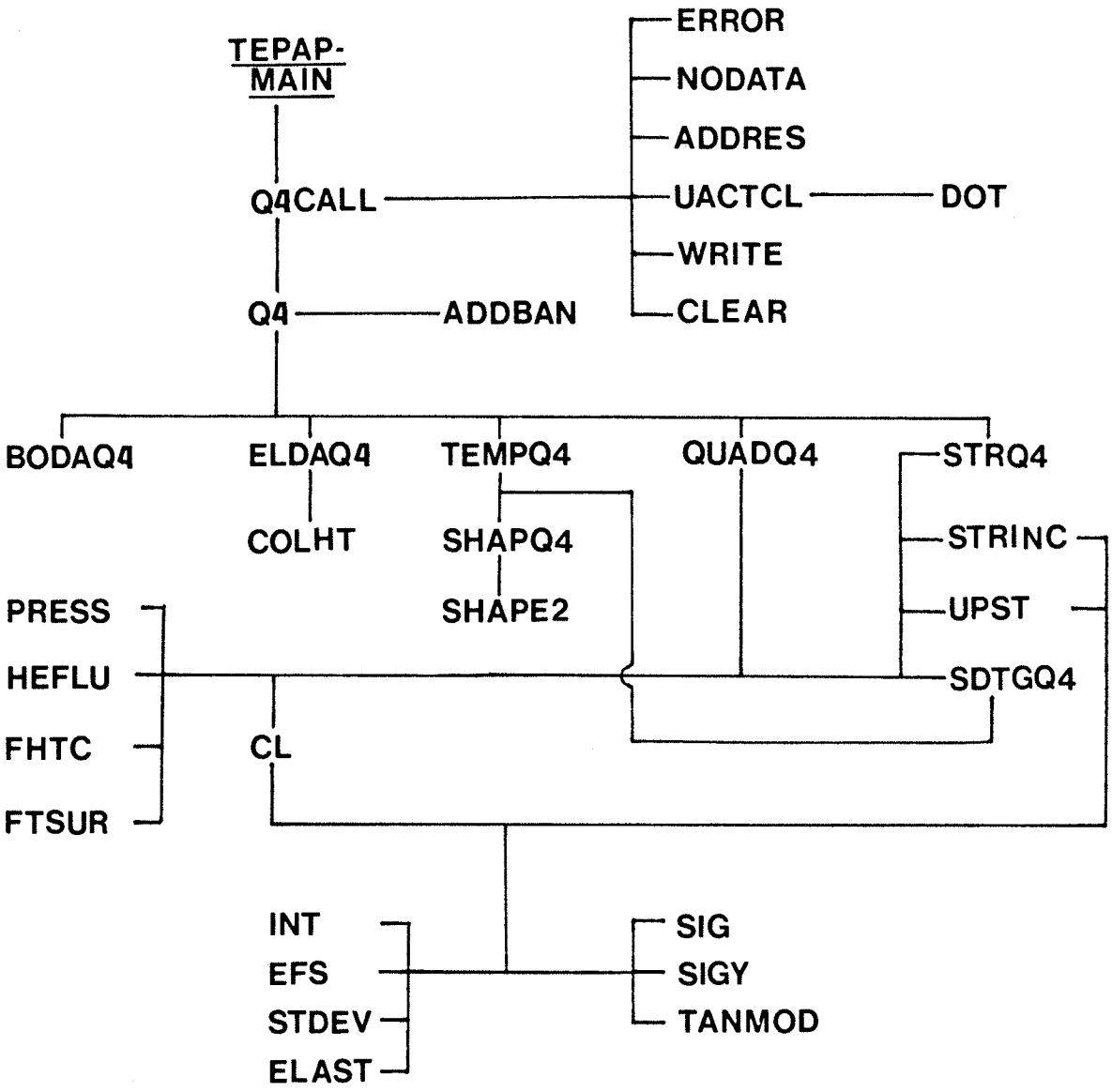

FIGURE 8: Subprograms' Tree for 'TEPAP'.

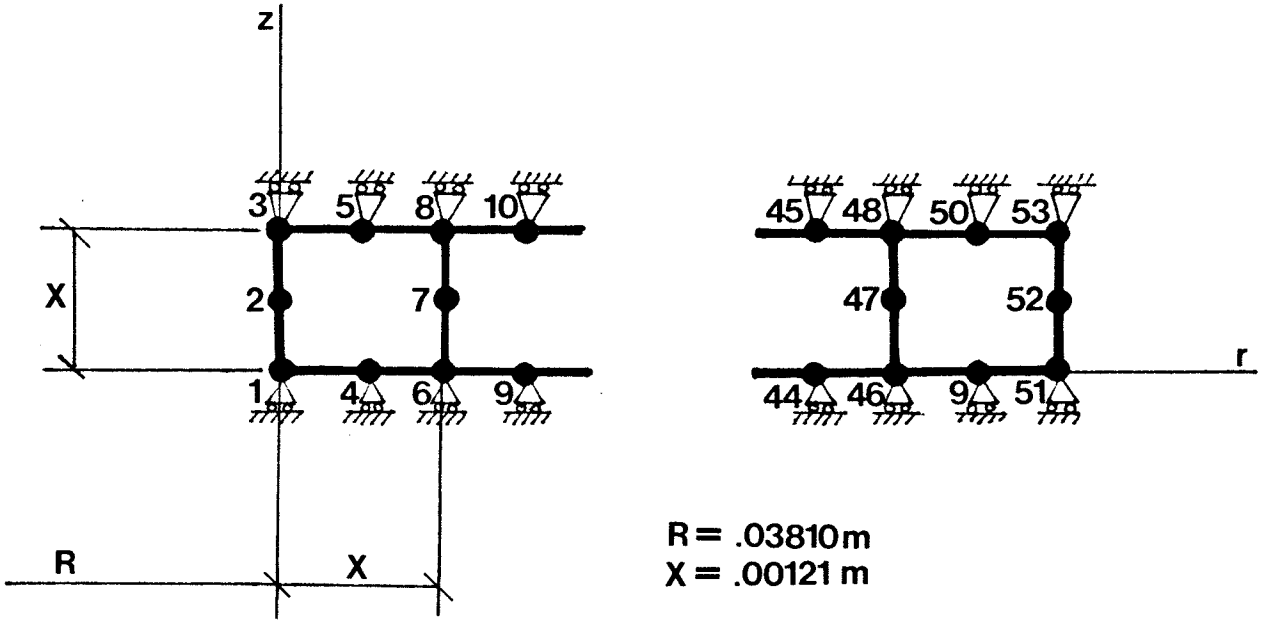

FIGURE 9: FE Model used in the Thermal Shock on the Tube Case Study.

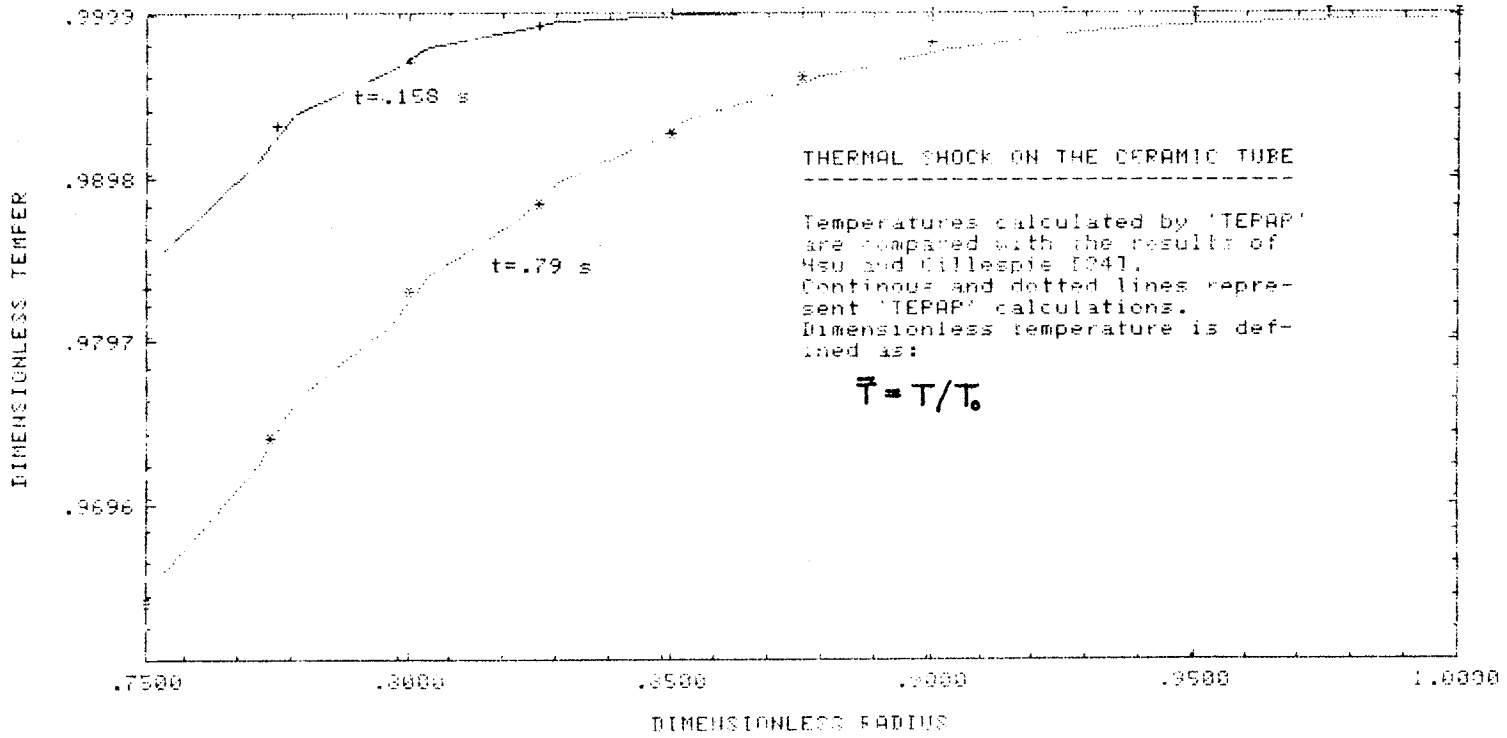

FIGURE 10: Temperatures Predicted for the Thermal Shock on the Ceramic Tube Case Study.

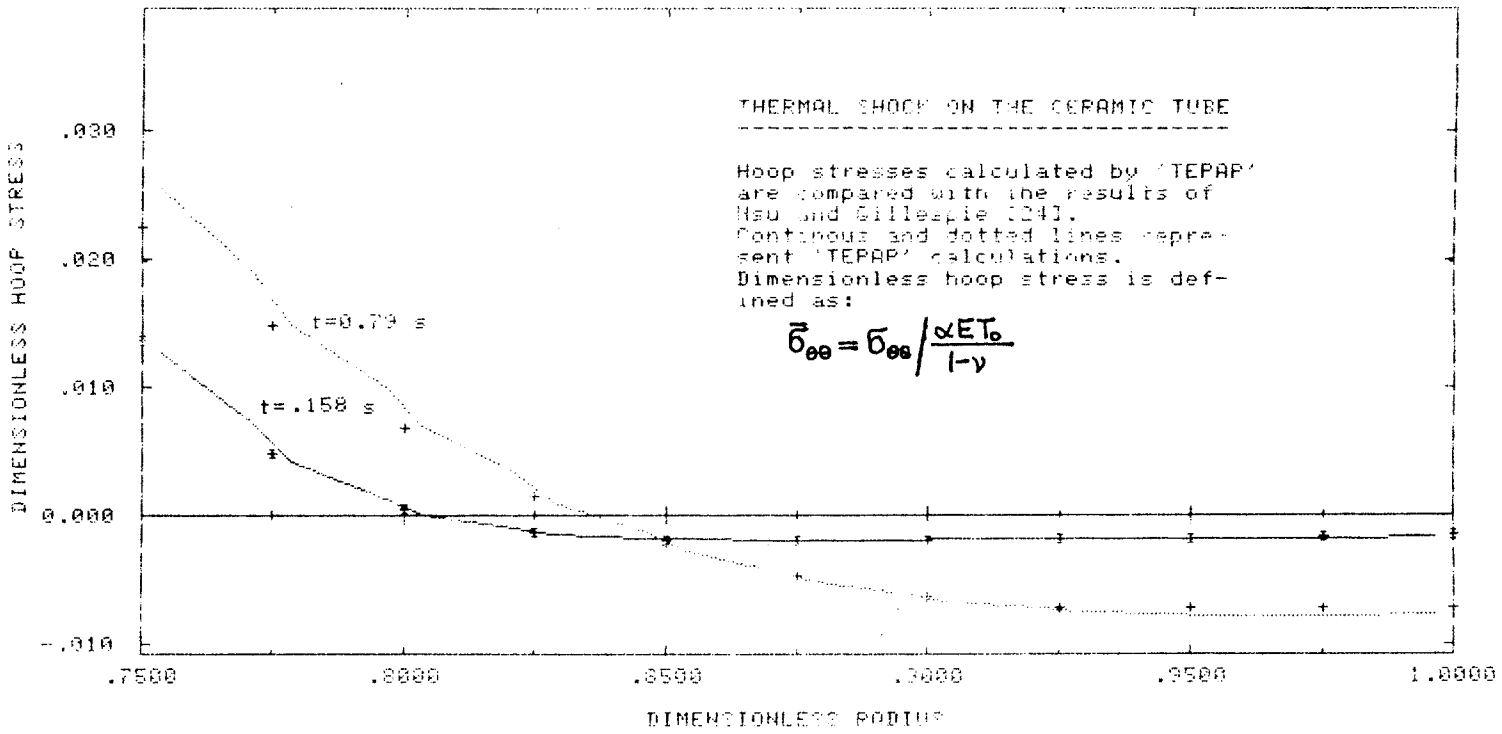

FIGURE 11: Tangential Stress Predictions for the Thermal Shock on the Ceramic Tube Case Study.

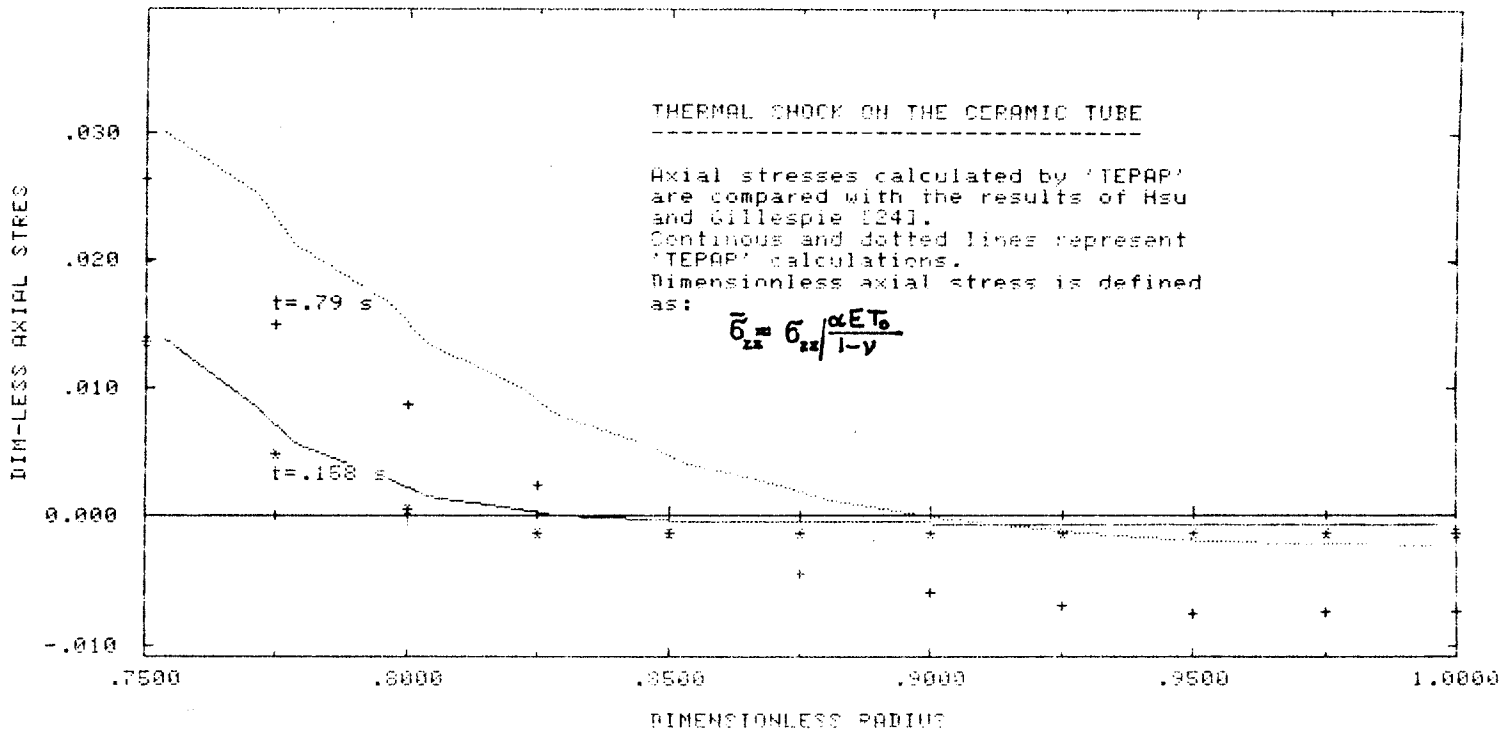

FIGURE 12: Axial Stress Predictions for the Thermal Shock on the Ceramic Tube Case Study.

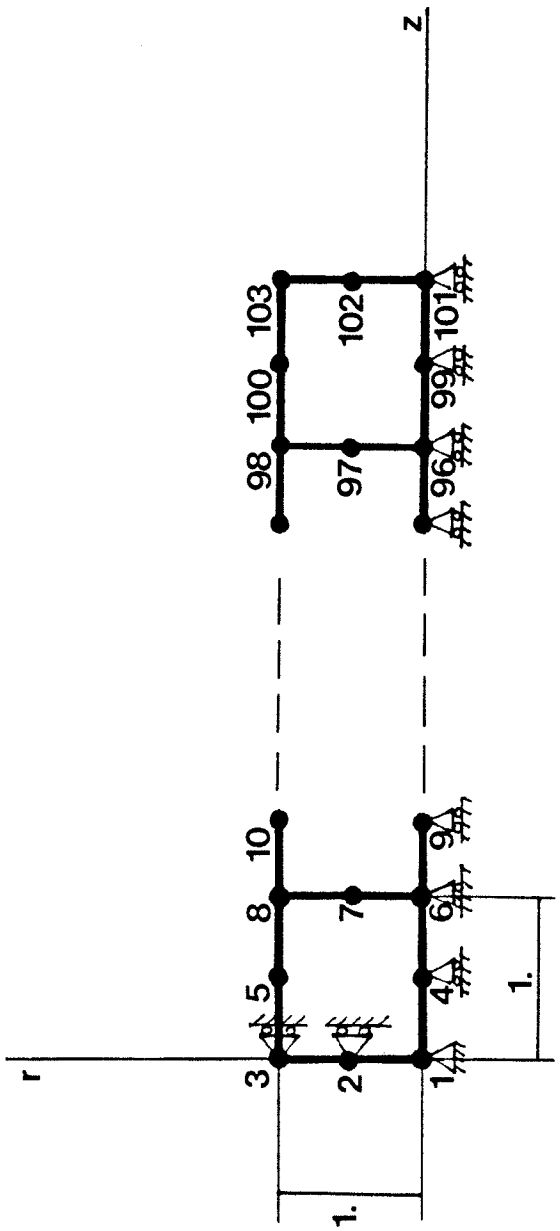

FIGURE 13: FE Model used in the Second Danilovskaya's Problem Case Study.

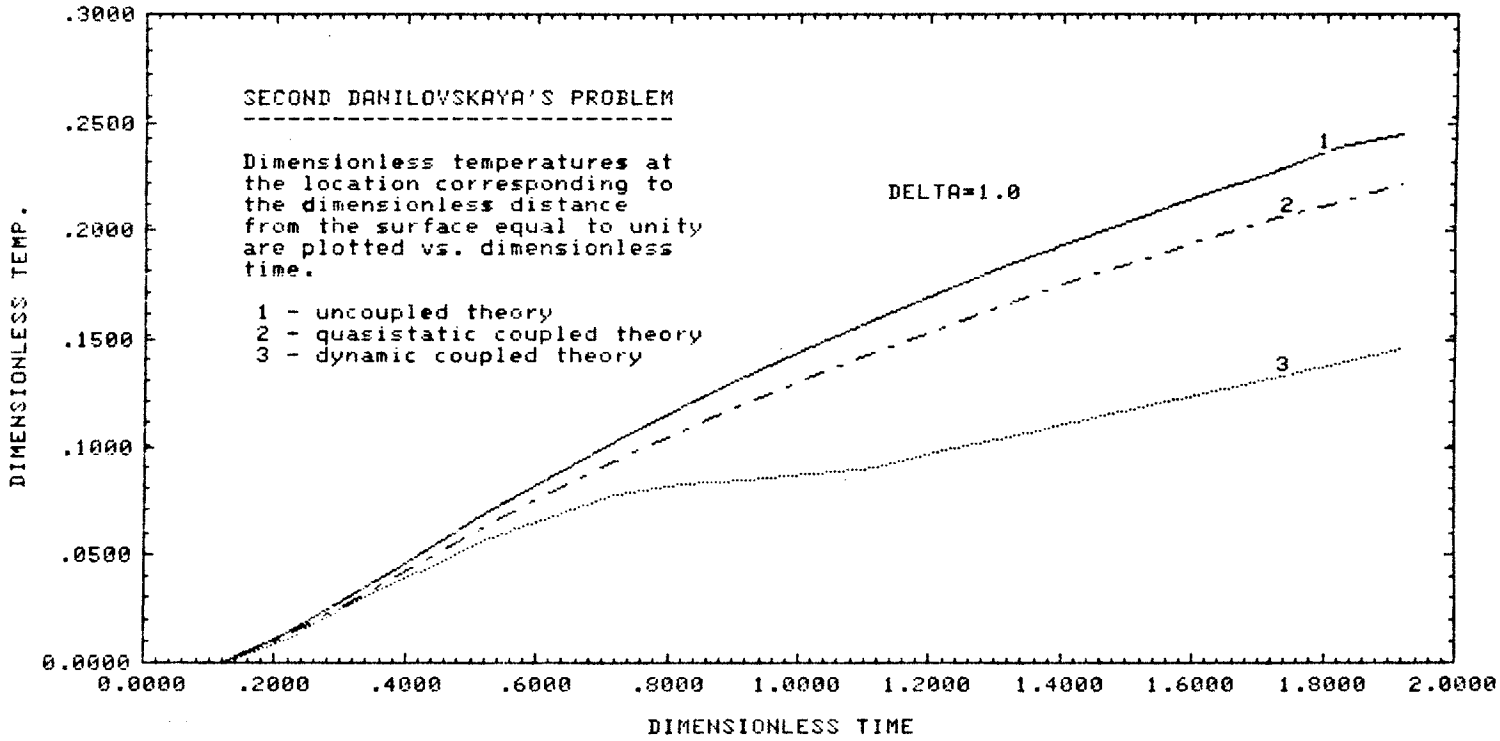

FIGURE 14: Temperature Predictions for the Second Danilovskaya's Problem Case Study with $\delta = 1$.

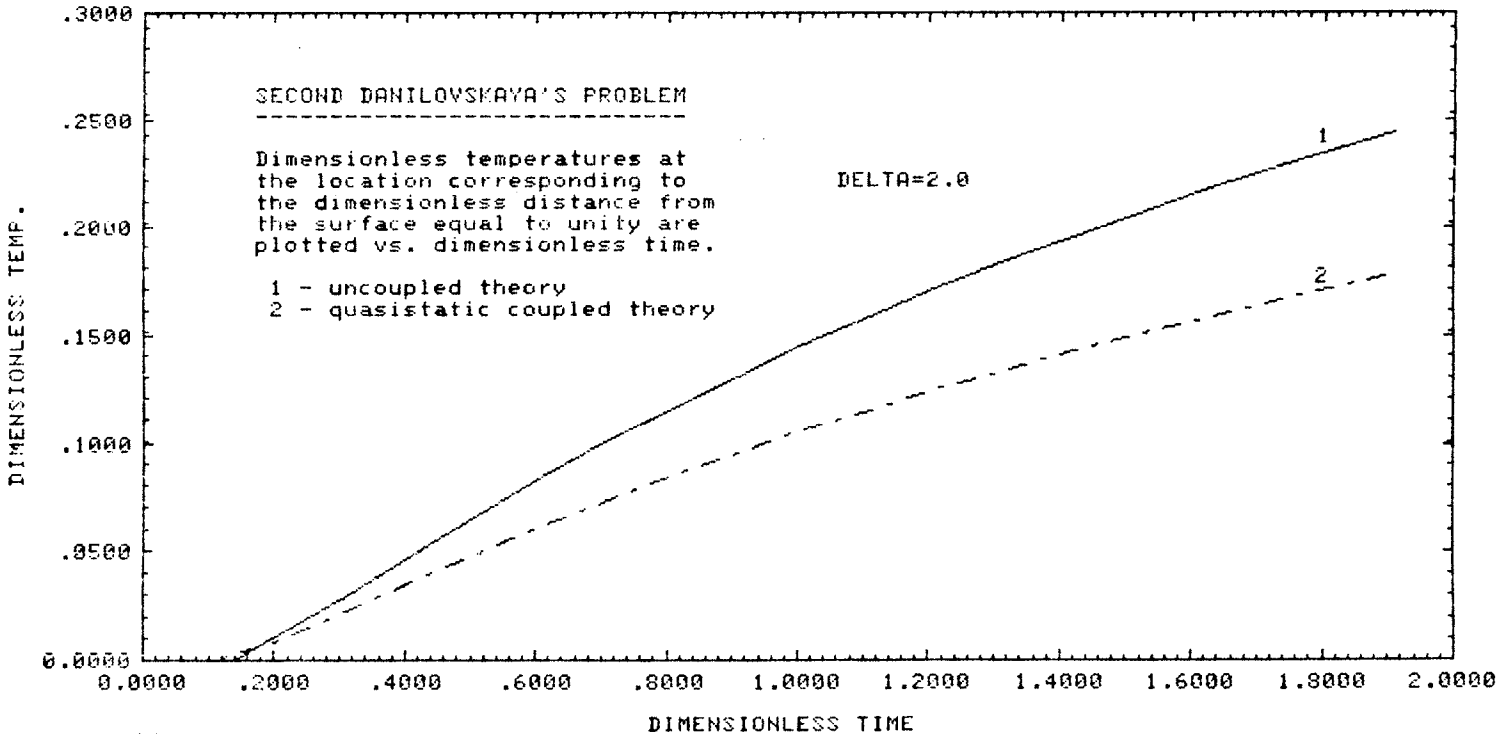

FIGURE 15: Temperature Predictions for the Second Danilovskaya's Problem Case Study with δ=2.

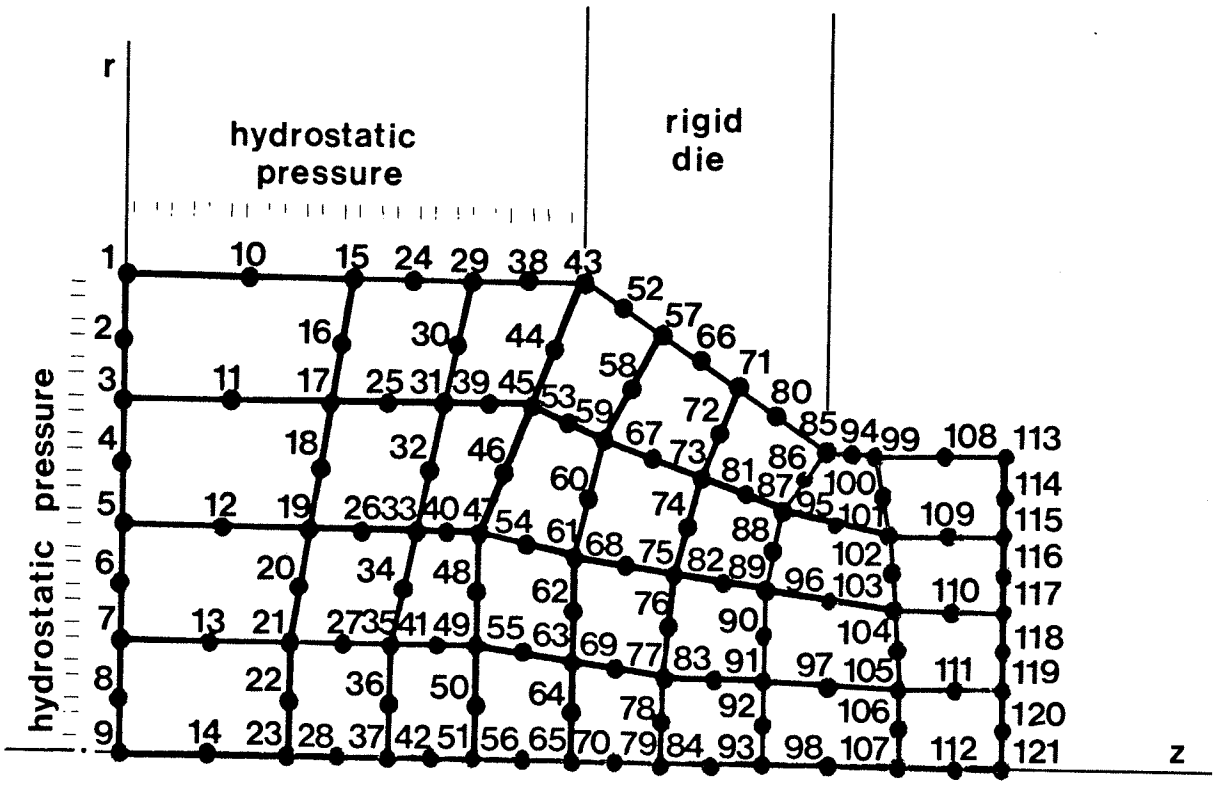

FIGURE 16: FE Model used in the Axisymmetric Extrusion Case Study.

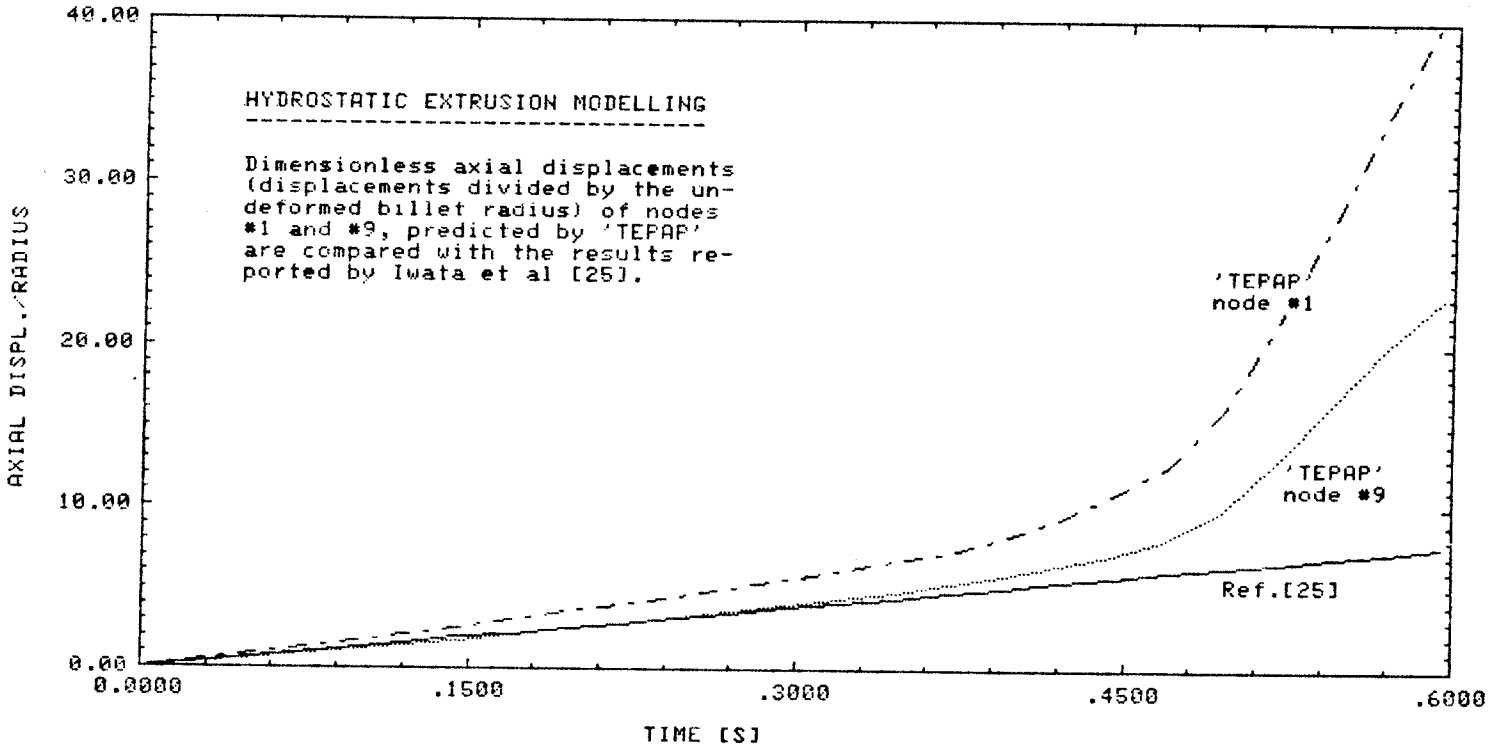

FIGURE 17: Applied Pressure - Dimensionless Billet Displacement Predictions for the Axisymmetric Extrusion Case Study.

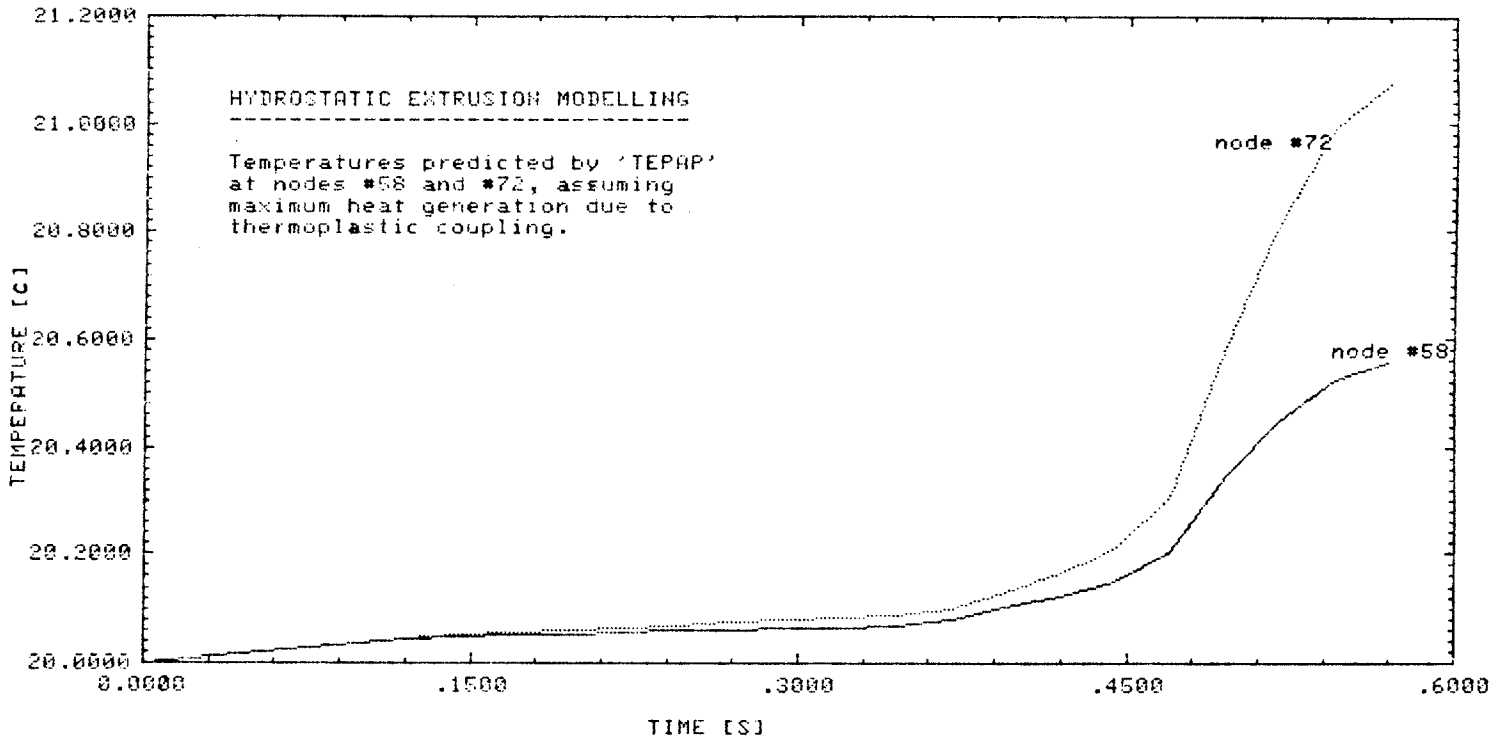

FIGURE 18: Temperature Histories for the Axisymmetric Extrusion Case Study.